CREEP-FATIGUE ANALYSIS FOR REMAINING LIFE ASSESSMENT OF STEAM TURBINE BLADE USING NUMERICAL SIMULATION AND EXPERIMENTAL TESTING

A Thesis

Submitted in partial fulfillment of the requirement for the

DOCTOR OF PHILOSOPHY

In

MECHANICAL ENGINEERING

By

POOJA RANI

(Roll No--2K17/PhD/ME/58)

Under the supervision of

Professor Atul Kumr Agrawal

Mechanical, Production & Industrial

and Automobile Engineering Department

DELHI TECHNOLOGICAL UNIVERSITY

(Formerly Delhi College of Engineering)

Main Bawana Road, Shahabad Daulatpur, Delhi - 110042, India

DELHI TECHNOLOGICAL UNIVERSITY

(Formerly Delhi College of Engineering)

Shahbad Daulatpur, Bawana Road,

Delhi-110042

DECLARATION

I, Pooja Rani, hereby declare that the thesis titled "**Creep-Fatigue Analysis for Remaining Life Assessment of Steam Turbine Blade Using Numerical Simulation and Experimental Testing**" which is submitted by me to the Department of Mechanical Engineering, Delhi Technological University, Delhi in partial fulfillment of the requirement for the award of the degree of Doctor of Philosophy, is original work carried out as a doctoral student and, to the best of my knowledge, it contains no material previously published or written by another person. This work has not previously formed the basis for the award of any Degree, Diploma Associateship, Fellowship or other similar title or recognition.

Place: Delhi **POOJA RANI**

Date: 24.04.2024

DELHI TECHNOLOGICAL UNIVERSITY

(Formerly Delhi College of Engineering)

Shahbad Daulatpur, Bawana Road,

Delhi-110042

CERTIFICATE

This is to certify that the thesis entitled **" Creep-Fatigue Analysis for Remaining Life Assessment of Steam Turbine Blade Using Numerical Simulation and Experimental Testing "** being submitted by **POOJA RANI** to the Delhi Technological University, Delhi for the award of the degree of **Doctor of Philosophy** is a bonafide record of original research work carried out by her. She has worked under my guidance and supervision and has fulfilled the requirements for the submission of this thesis, which has reached the requisite standard.

The results contained in this thesis have not been submitted, in part or full, to any other University or Institute for the award of any degree or diploma

(**Dr. Atul Kumar Agrawal**)

Professor

Mechanical, Production & Industrial

And Automobile Engineering Department,

Delhi Technological University

Delhi-110042

INDIA

Acknowledgement

I would like to express my deepest gratitude to my supervisor, Prof. Atul Kumar Agrawal, for his invaluable guidance, support, and encouragement throughout the journey of completing this doctoral thesis. His expertise, mentorship, and unwavering dedication has been instrumental in shaping the direction and quality of this research.

I extend my sincere appreciation to the Department of Mechanical Engineering at Delhi Technological University for providing me with the necessary resources and conducive environment for pursuing my research work. I would also like to extend my gratitude to Prof. B. B. Arora, Head, Mechanical Engineering Department, Prof. S.K. Garg, Former Head, Mechanical Engineering Department, Prof. Vijay Gautam, DTU Delhi, (Late) Prof. Vikas Rastogi, DTU Delhi, Prof. R C Singh, DTU Delhi. I am also indebted to the members of my doctoral committee, Prof. P.M.V Subbarao, IIT Delhi, Prof. Mohammed Suhaib, Jamia Millia Islamia New Delhi, Prof. Raj Kumar Singh, DTU Delhi, Prof. A.S. Rao, DTU Delhi for their insightful feedback, constructive criticism, and valuable suggestions, which have greatly enriched the content and scholarly rigor of this thesis. I would like to thank the technical staff members, Mr. Narender Bisht and Mr. Lakhan for helping me during lab engagements.

I would like to express my sincere appreciation to Dr. M. K. Sharma, Technical Director at AEQUITAS VERITAS INDUSTRIAL SERVICES (AVIS) laboratory, for his invaluable assistance and for providing the necessary laboratory facilities and data for conducting experiments. Dr. Sharma's expertise, guidance, and support have been instrumental in the successful completion of this research project. I am deeply thankful to Mr. D. C. Nirmal, Senior DGM at STE-BHEL Bhopal, and Mr. Manoj Yadav, Manager at COE-BHEL Bhopal, Mr. Sorabh Khurana, Dy. Mgr. at HLE-BHEL Bhopal for their invaluable technical advice and insights regarding steam turbines. Their expertise and guidance have greatly enriched the research process and contributed to the depth of this thesis.

I am immensely grateful to my friends and colleagues Nitin, Abdul, Yamika, Gaurav, Kiran, Simmi, Pawan, Anuj Sharma, for their support, encouragement, and camaraderie throughout this journey. Your friendship and solidarity have made the challenges more manageable and

the victories sweeter. A special thanks to Renu Didi and Kismat Didi for their support and kindness during my stay in the hostel.

I am immensely grateful to my family for their unwavering love, encouragement, and understanding throughout this challenging academic journey. Their patience, support, and sacrifices have been a constant source of motivation and strength. I am deeply indebted to my grandparents, Late Sh. Prabhati Ram Dhania and Late Smt. Patasi Devi, Capt. Zorawar Singh Dahiya, Smt. Gindori Devi for their endless blessings and encouragement. To my beloved parents, Mr. Kailash Dhania and Mrs. Sumitra Devi, your unconditional love, unwavering belief in my abilities, and endless sacrifices have been my pillars of strength. This achievement is as much yours as it is mine. To my elder brother, Sunil Dhania, for being my source of inspiration, and constant source of support. To my younger sister, Jyoti Dhania, thank you for your unwavering support, understanding, and encouragement. I gratefully acknowledge my cousin brother, Amit, for all his support throughout the journey of completing this doctoral thesis. I would like thank my little cousin, Harshita, for her sweet smile, infectious laughter, boundless energy, curiosity, and unconditional affection throughout the duration of my doctoral thesis journey. Her presence, as a beacon of joy and innocence, brought warmth and inspiration to my daily life. I extend my thanks to my In-laws for their presence and support in my life.

To my husband, Anup Singh, your unwavering love, support, and understanding have been my source of strength. His belief in my abilities, even during the most challenging times, has been a source of inspiration and motivation. Thank you for being my rock and for standing by me through thick and thin.

Last but not least, to my son, Appu, born in the final days of my doctorate, you are my greatest blessing and the light of my life. Your arrival has brought immense joy and inspiration, reminding me of the importance of perseverance and resilience.

Lastly, I would like to acknowledge the countless individuals, institutions, and resources that have contributed to this research in various ways, directly or indirectly. Your collective efforts have been indispensable in the completion of this doctoral thesis.

Thank you all for being an integral part of this remarkable journey.

To my beloved parents

You have always believed in me, inspired me to pursue my dreams, and stood by me through every challenge and triumph. This thesis is a testament to your endless sacrifices, guidance, and belief in my abilities. This thesis is dedicated to you with all my heart and deepest gratitude.

Abstract

Due to the rapid growth of the global economy and the rising need for electric energy, there is an urgent requirement to enhance the power output and efficiency of steam turbines. Blades, which serve as the crucial element of a steam turbine, have a direct impact on the efficiency and safety of the equipment. The phenomenon of water droplet erosion (WDE) is a significant factor in the working conditions of turbine blades, and it has a detrimental impact on the lifespan of the blades. Because of the intricate nature of turbine blade operating conditions, which encompass blade vibration, material erosion, and liquid-solid interaction, properly forecasting their useful lifespans using theoretical calculations is challenging. The final stage blades of steam turbines consistently operate inside the wet steam region and are susceptible to the influence of WDE (Water Droplet Erosion) or wet steam erosion, which has two negative effects. Firstly, it increases the losses and decreases the efficiency of the turbine stage. Secondly, it can induce blade breakage, posing a risk to the safety of the equipment. Currently, the utilisation of ultralong blades and the expansion of working conditions in new steam turbines have presented significant challenges to the resilience of blade materials against water droplet erosion (WDE). To guarantee the secure functioning of the steam turbine, it is necessary to halt the equipment for maintenance as per schedule. Observing the worn surface of the blade poses a challenge in determining the blade's potential for continuing use. Due to the economic implications and concerns over operational safety, it is challenging to ascertain the necessity of replacing the deteriorated blades. Simultaneously, due to the blades operating at high speeds, temperatures, pressures, and within a confined environment, it is not feasible to visually examine the surface characteristics and wear debris accumulation of the blades when they are in normal operation. Hence, it is crucial to ascertain the remaining useful life (RUL) of the blades based on the erosion morphology of the blades during maintenance. Based on the literature survey, it is evident that there is limited study on the WDE life of turbine blades, and a comprehensive approach for predicting the WDE life has not yet been established. Previously, researchers predominantly relied on initiation crack life as the measure of useful blade life. However, in real engineering applications, the blade may still be utilised despite the presence of a WDE fault on its surface, as long as it does not pose a significant risk to the equipment's

safety. This is done in order to reduce costs. Therefore, the fault diagnosis of the remaining useful life (RUL) of the blade is a more significant metric compared to the initiation crack life of the material.

Theoretical calculations are conducted to assess the creep-fatigue damage by considering the degraded material characteristics. The failure probability is then determined by calculating the damage using a deterministic model and accounting for the dispersion in material property data. Material testing is conducted to detect both surface and volumetric cracks, as well as to assess micro-structural damage. This is achieved through the use of replica or microscopic tests. Crack presence testing is conducted on all available surfaces of the component, whereas microstructure damage and volumetric crack tests are specifically carried out at the most significant sites determined through theoretical calculations. Damage calculations serve the purpose of identifying essential regions for testing and providing crucial information regarding the following aspects: - The dominant damage mechanism at a certain location. - The extent of damage for the most unfavourable material properties. - The rate at which damage accumulates. This information is valuable for determining suggestions regarding component repair, inspection intervals, or modification of operating conditions. The significance of both creep and fatigue damage in the overall damage is crucial in terms of failure probability. The failure probability is influenced by the contribution of creep and fatigue damage for a given total damage.

Keywords: *low-pressure Steam turbine blade, damage causes, erosion pitting, NDT, X20Cr13 stainless steel, AISI 420, Finite Element Analysis, Temperature and pressure distribution, Fatigue life estimation, Fractography, Erosion pits, Scanning Electron Microscopy (SEM), energy-dispersive X-ray (EDX), Remaining life, fatigue life, fatigue damage, creep damage, probabilistic simulation, deterministic damage calculation, fracture mechanics*

Research Publications from the Thesis

Published/Accepted research papers in referred international journals of repute in the concerned area.

1. Rani, Pooja, and Atul K. Agrawal. "Failure analysis of a low-pressure stage steam turbine blade." *Nondestructive Testing and Evaluation* (2022): 1-15. DOI: 10.1080/10589759.2022.2156503 (Published)
2. Rani, Pooja, and Atul K. Agrawal. " SEM and EDX analysis of erosion products formed on steam turbine blade." *Materials at High Temperatures* (2023), DOI: 10.1080/09603409.2023.2264058 (Published)
3. Rani, Pooja, and Atul K. Agrawal. "Fatigue Life Evaluation of a low-pressure stage steam turbine blade." *Journal of Vibration Engineering & Technologies (JVET) (2023)*, DOI: https://doi.org/10.1007/s42417-023-01173-3 (Published)
4. Rani, Pooja, and Atul K. Agrawal. "Lifetime assessment of a low-pressure steam turbine blade." *Journal of Vibration Engineering & Technologies (JVET) (2024), DOI: 10.1007/s42417-024-01412-1(Published)*
5. Rani, Pooja, and Atul K. Agrawal. " Failure Analysis of Steam Turbine Blades: A Comprehensive Review." *Tribology International, Manuscript No.-TRIBINT-D-24-02933 (Communicated)*

Paper presented in International Conferences:

1. Rani, Pooja, and Atul Kumar Agrawal. "Static Analysis of a Low-Pressure Stage Blade of a Steam Turbine Using ANSYS." *3rd Biennial International Conference on Future Learning Aspects of Mechanical Engineering (FLAME- 2022)", Singapore: Springer Nature Singapore. DOI:.1007/978-981-99-3033-3_29*
2. Rani, Pooja, and Atul Kumar Agrawal. "Natural Frequency Evaluation of Low-Pressure Stage Blade of a 210 MW Steam Turbine." *International Conference on Materials Science and Engineering (ICMSE 2022)" IOP Conference Series: Materials Science and Engineering, Volume 1248. DOI: 10.1088/1757-899X/1248/1/012032*

Table of Contents

List of Figures

Chapter 1: Introduction

Chapter 2: Study of the Causes of Failure of Low-Pressure Turbine Blades

Chapter 3: Investigation of Failure of Seventh Stage Low Pressure Steam Turbine Blade and Framework for Life Assessment

Chapter 4: Metallographic analysis of erosion products formed on Seventh Stage Low Pressure Steam Turbine Blade

Chapter 5: Computational Framework for Life Assessment of Seventh Stage Low Pressure Steam Turbine Blade

Chapter 6: Conclusions and Future scope

List of Tables

Chapter 1: Introduction

Chapter 2: Study of the Causes of Failure of Low-Pressure Turbine Blades

Chapter 3: Investigation of Failure of Seventh Stage Low Pressure Steam Turbine Blade and Framework for Life Assessment

Chapter 4: Metallographic analysis of erosion products formed on Seventh Stage Low Pressure Steam Turbine Blade

Chapter 5: Computational Framework for Life Assessment of Low Pressure Seventh Stage Steam Turbine Blade

List of Abbreviations

2-D	Two Dimensional
BHN	Brinell Hardness No.
CFD	Computational Fluid Dynamics
DPT	Dye Penetration Test
EDAX	Energy-Dispersive X-ray Analysis
FEA	Finite Element Analysis
FSI	Fluid-Structure Interaction
HP	High Pressure
IP	Intermediate Pressure
LCF	Low Cycle Fatigue
LP	Low Pressure
LSB	Last Stage Blades
NDT	Non-Destructive Test
RANS	Reynolds-Averaged Navier-Stokes Equations
RLA	Remaining Life Assessment
SEM	Scanning Electron Microscope
SIF	Stress Intensity Factor
SWT	Smith Watson Topper
WDE	Water Droplet Erosion

List of Symbols

b	Fatigue strength exponent
c	Fatigue ductility exponent
C	Specific heat
E	Elastic Modulus
K'	Cyclic strength coefficient
n	Number of cycles
n'	Cyclic strain hardening exponent
N_f	Number of cycles to failure
P	Pressure
σ	Stress
σ'_f	Fatigue strength coefficient
σ_a	Von-Mises stress amplitude
σ_y	Cyclic yield stress
T	Temperature
ε	Strain
ε_a	Strain amplitude
ε_x	Characteristic creep strain
ε'_f	Fatigue ductility coefficient
ΔK_I	Stress intensity factor range
ṁ	Mass flow rate

CHAPTER 1

INTRODUCTION

1.1 Introduction and motivation

In India, the energy sector is one of the most important infrastructure components affecting economic growth. Over the past three decades, the demand for energy in India has increased by an average of 3.6% per year. India ranks fifth in electricity generating capacity and sixth in energy consumption, accounting for approximately 3.4% of global energy consumption [1]. Figure 1.1 and 1.2 show the fuel wise energy contribution in India in year 2018 and 2023.

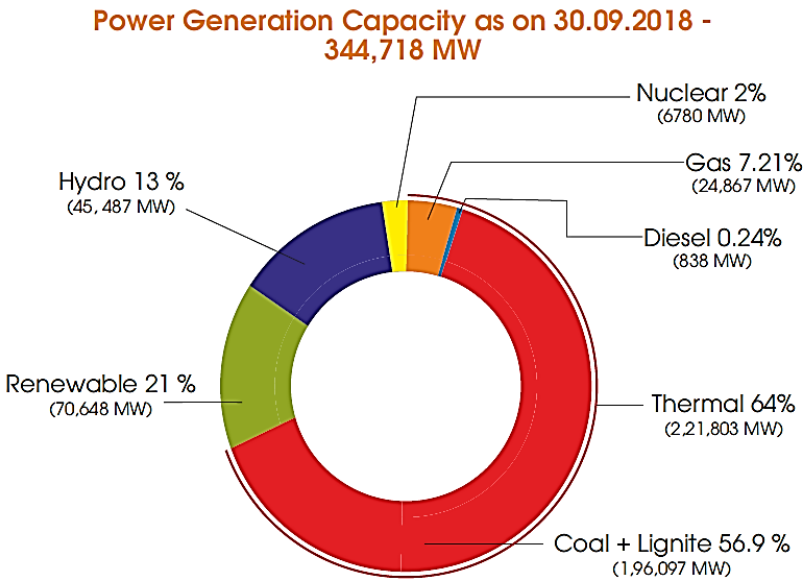

Figure 1.1 Percentage segregation of all India installed power generation capacity (source: HLEC report [2])

Approximately 65% of India's and 80% of the world's electricity comes from thermal power generation. With annual increases in thermal capacity expansion and ever-increasing power usage, this trend is expected to continue [3], [4]. Being the backbone of power generation, thermal plants have had a desperate need for increased efficiency, increased energy output, and decreased costs [1], [5].

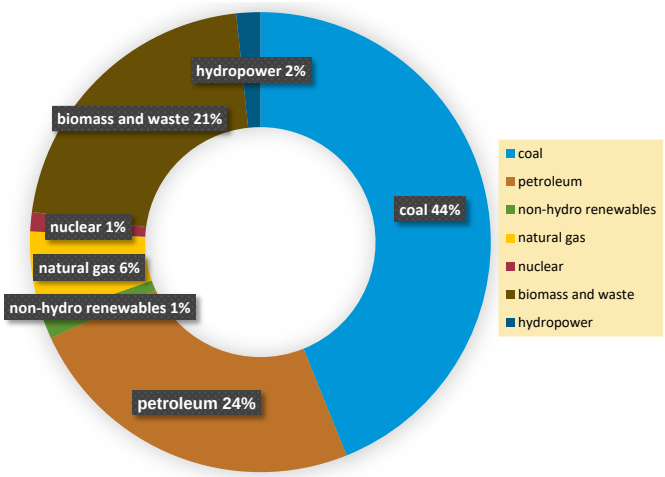

Figure 1.2 Installed power generation capacity (fuel wise) as on 31.05.2023 (source: International Energy Agency, World Energy Outlook 2022)

In thermal power plants, water is heated to steam using the heat energy produced by the combustion of solid fuel (often coal). Steam at high pressure and temperature is utilised to turn a turbine, which in turn powers an electrical generator. The generator transforms the turbine impeller's kinetic energy into electrical energy. The engineer’s biggest concern these days is turbine blade maintenance and failure. A blade failure represents a critical concern for power plant managers and owners, particularly when it occurs in the Last Stage. Such failures pose substantial risks to both human safety and equipment integrity, potentially resulting in catastrophic outcomes. The secondary consequences, including the downtime required to restore the unit to service after such failures, further exacerbate the situation. So, assessment of life of existing machinery is important to avoid any catastrophic failure and as well as reduce cost by avoiding early rejection of components.

The misinterpretation of remaining life assessment as "life extension" is common, but it's crucial to recognize that this analysis doesn't actually prolong component lifespans. Its primary function is to gauge the remaining useful lifetime, relying on metallurgical inspections and theoretical calculations, particularly in fracture mechanics. In addition to its primary function, remaining life assessment technology serves several ancillary purposes. It assists in establishing optimal inspection schedules, maintenance plans, and operational procedures. It's important not to assume that conducting a remaining life assessment for a 20-year extension means waiting 20 years without interim monitoring. Regular checks are necessary to validate the initial approach. Consequently, remaining life assessment should be seen as an ongoing task, rather than a one-time activity [6].

As a new field of study to address the rising demand and consumption of electricity, many scientists and engineers have shown a considerable interest in the analysis of turbine blade failure. The goal of specialists in turbomachinery is to investigate the fundamental reasons behind the failure of different turbines' blades and provide corrective measures to prevent such failures and reduce the need for forced downtime. In this chapter, the contribution of the thesis is also highlighted along with a brief assessment of the literature.

Steam turbine blades play a pivotal role as critical components within power generation plants, enduring rigorous mechanical and thermal stresses during operation. Creep and fatigue are primary mechanisms leading to material degradation and potential failure of these blades over time. This thesis presents a comprehensive investigation into the creep-fatigue behaviour of steam turbine blades, aiming to develop a framework for remaining life assessment. The approach integrates numerical simulation techniques with experimental testing to accurately predict the remaining life of turbine blades under various operating conditions. Through this research, insights into the interaction between creep and fatigue phenomena are gained, enabling more effective maintenance strategies and enhancing the reliability of steam turbine systems.

1.2 Cyclic operation of steam turbines

Starting up, steady state, load shift, shutdown, and natural cooling are the usual phases of a steam turbine's operational cycle. Different stages of operation are depicted schematically in Figure 1.3. The runup phase of a turbine involves the transition from the turning gear to the rated speed (0-1) and the gradual increase in steam parameters from their initial settings. Following the synchronisation of the units (1), turbine loading (1-2) begins, and the steam temperature and pressure continue to rise until they reach their nominal values. Now that initialization is complete, the process can operate at constant parameters in the steady-state (2-3) phase. Changes in load (3–4, 5–6) at varying rates are possible during steady-state operation, as are changes in steam temperature and pressure. When all of the process parameters decrease during shutdown (phase 7-8) and natural cooling (phase 9), the operating cycle is completed [7], [8].

Three primary categories of start-ups:

- Cold start-up
- Warm start-up
- Hot start-up

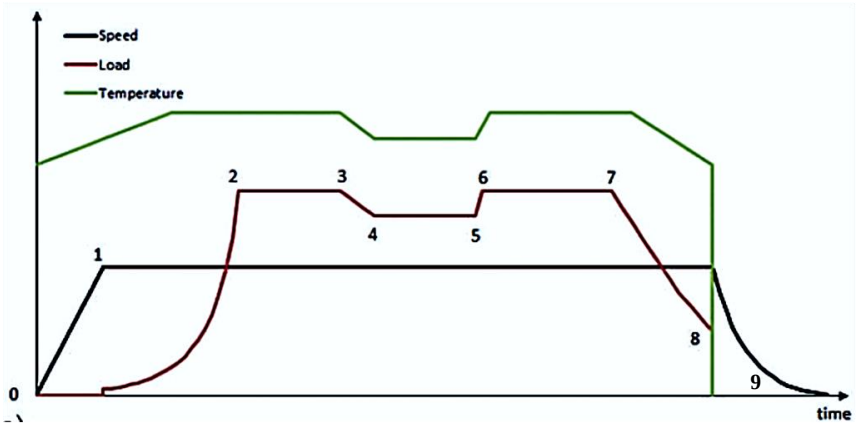

Figure 1.3 Process parameters for a typical steam turbine operating cycle [8]

1.2.1 Importance of Blades in Steam Turbines

The key to the efficient operation of any turbomachinery is the structural integrity of all rotating components, which is dependent on the parts of the machine's ability to withstand the constant and alternating loads exerted on them. Turbomachinery and other types of rotating equipment have a particularly difficult challenge because of the magnitude of the cyclical loads they must bear [9].

The steam turbine's blades are subjected to extreme static and dynamic loads over the course of its lifetime. To prevent blade failure, analysis must be performed regularly [3]. A steam turbine can have tens of thousands of blades, with each row of blades potentially having its own unique dynamic features. High tensile strength and high fatigue strength are desirable qualities in a turbine blade material. The best blade material also has great ductility, is resistant to corrosion and erosion, and can withstand high temperatures [9]. Figure 1.4 depicts a typical blade profile, showing the low-pressure (suction) and high-pressure sides, as well as the position of the leading and trailing edges [10].

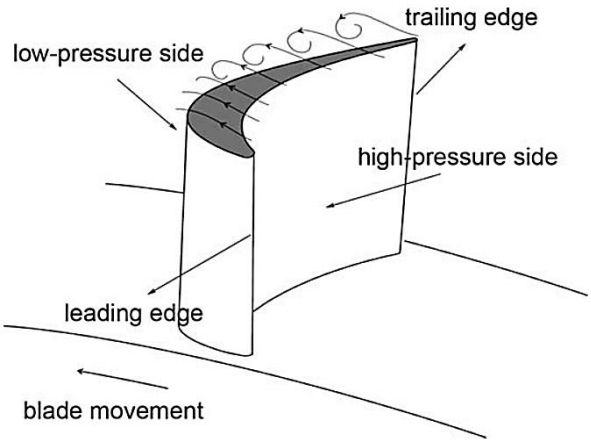

Figure 1.4 Standard profile of a blade, showing leading and trailing edges as well as the suction and pressure faces [10]

There are typically three stages to the blade operation: start up, steady operation, and shutdown. As demonstrated in Figure 1.5 with blue lines, the blade experiences low cycle fatigue (LCF)loadings during the start and stop phase due to the wildly fluctuating centrifugal loads and static steam bending loads. In Figure 1.5's red lines, we can see that the dynamic forces exerted on the blades during high-speed steady operation are caused by steam flow turbulence and have a small steady amplitude but high frequency, leading to high cycle fatigue (HCF) loadings [11].

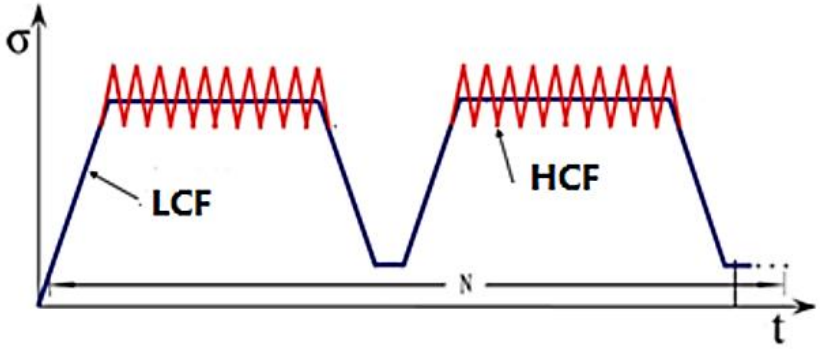

Figure 1.5 cyclic loads in steam turbine Blade [11]

Blades can be divided into two categories according to how they are used in the turbine modules: LP, which has large blades that bend due to impulse changes and high static pressure, and HP and IP, which have high temperatures and small blades that should withstand minor centrifugal forces [3]. Figure 1.6 shows the different pressure regions of turbine rotor. Figure 1.7 illustrates the breakdown of typical losses in a recent large-scale steam turbine, specifically detailing the relative fractions of each loss compared to low-pressure blade loss.

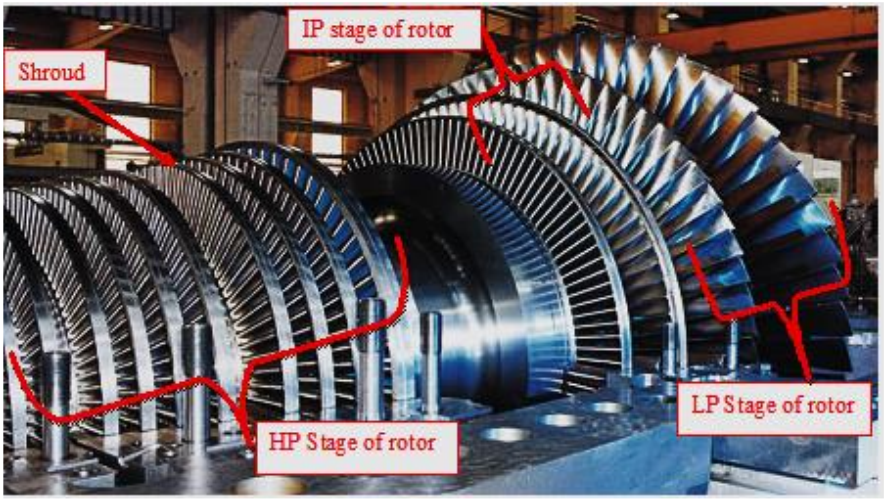

Figure 1.6 different pressure regions (high pressure, intermediate pressure, low pressure) [3]

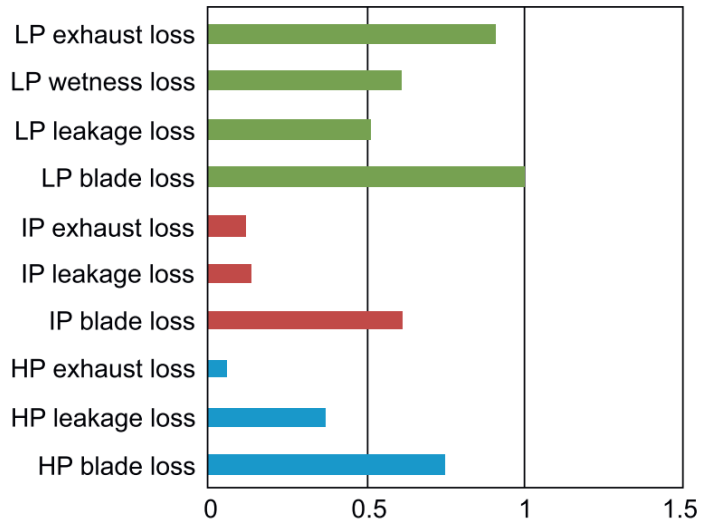

Figure 1.7 The breakdown of typical losses in a recent large-scale steam turbine, relative to the low-pressure blade loss [12]

Blades in both the High Pressure (HP) and Intermediate Pressure (IP) sections require static tensile strength and toughness to withstand the centrifugal forces generated by high rotational velocity and pressure loading, respectively, thereby preventing sudden failure in cracked components. Additionally, HP and IP blades need resistance to creep rupture to mitigate the risk of failure at elevated temperatures and prevent blade encroachment on the turbine casing. They also require oxidation resistance to avoid material loss and potential local temperature elevation, as these turbines operate at sufficiently high temperatures. Furthermore, they necessitate resistance to local corrosion to prevent deterioration in specific areas. While LP blades require resistance to stress corrosion cracking due to exposure to chemically

aggressive environments, they also need to withstand corrosion fatigue, given the propensity for steam condensation leading to the deposition of impurities and localized high salt concentrations, potentially causing corrosion pits and initiating fatigue failure. Both HP/IP and LP blades require resistance to low cycle fatigue (LCF) and high cycle fatigue (HCF) stresses, crucial during start-up and shut-down phases and susceptible to external initiation such as foreign object damage or changes in vibrational characteristics. Moreover, erosion resistance is essential for both types of blades to withstand potential solid particle presence in steam. Additionally, both types of blades must possess weldability to meet manufacturing requirements. However, LP blades may not require resistance to Type IV cracking, which can occur in weld heat-affected zones under creep conditions [13].

1.3 Literature review

A plethora of information may be accessed via academic journals, electronic databases, and books, providing detailed explanations of different factors leading to steam turbine blade failures and proposing effective strategies to prevent such incidents. The literature review is structured into four distinct sections. The first section encompasses research papers and articles that delve into Studies on fatigue failure of turbine blades. The second section offers exhaustive details sourced from research papers, articles, and other archival literature concerning creep failures in turbine blades. In the third section, research papers, articles, and books are examined concerning fracture of turbine blades. The fourth section outlines all archival literature explored on the modal analysis of turbine blades. Within this framework, subsequent subsections discuss literature pertinent to metallurgical defects detected in turbine blades. The subsequent subsection focuses on literature pertaining to fatigue failure studies of turbine blades.

1.3.1 Studies on fatigue failure of turbine blade:

Fatigue failures occur under cyclic loading and encompass various stressors such as vibration stresses on blades, alternating bending loads on shafts, and fluctuating thermal stresses during start-stop cycles.

Fatigue fracture can only occur under three specific conditions: (a) a sufficiently large maximum tensile stress, (b) a highly variable or fluctuating applied stress, and (c) a large number of stress cycles [14].

Fatigue can be categorized into two types: low cycle fatigue (LCF) and high cycle fatigue (HCF). Traditionally, LCF failure is classified as occurring below 10^4 cycles, while HCF occurs above this threshold. A crucial distinction between HCF and LCF lies in the

distribution of fatigue life: in HCF, most of the life is spent in crack initiation, whereas in LCF, the majority of the life is spent in crack propagation as cracks tend to initiate within a small percentage of the fatigue life. HCF typically occurs under lower stress, while LCF typically occurs under higher stress [6].

Before the development of Linear Elastic Fracture Mechanics (LEFM)-based approaches such as the Paris Law (1963), the role of cyclic loading in causing failures was recognized, with notable work by A. Wohler (1860) who conducted rotating bend tests on various alloys. Empirical methods, including two design approaches—the stress-life method and the strain-life method—have been developed to address fatigue failure [15].

Stress-Life Approach:

When plotting $\log(\sigma_a)$ (where σ_a represents stress amplitude) versus $\log(2N_f)$ (where $2N_f$ represents the number of reversals to failure, with one cycle equaling two reversals), a common observation is a linear relationship. This relationship is typically observed under conditions involving primarily elastic deformation.

The stress-life approach described above is applicable in scenarios where the component experiences predominantly elastic deformation, leading to a long lifetime expectation. However, in situations characterized by high stresses, elevated temperatures, or stress concentrations such as notches, where significant plastic deformation occurs, this approach is not suitable [16][17].

Strain Life Approach:

Rather than the stress amplitude σ_a, the loading is characterized by the plastic strain amplitude. Under these conditions, a plot is made of $\log(\Delta\varepsilon_p/2)$ (where $(\Delta\varepsilon_p/2$ represents plastic strain amplitude versus log $(2N_{f)}$ [15][16][17].

- Shun-Peng Zhu *et al.* [18] conducted an *evaluation* of the fatigue life and reliability of a turbine bladed disk under cyclic loadings, employing a combination of experimental testing and stochastic stress-s1train response modeling. Here are the key findings:
  - They developed and implemented a computational-experimental framework for the fatigue reliability assessment of bladed disks, which accounts for uncertainty stemming from experimental data, material properties, and loads. Two schemes for fatigue reliability analysis were outlined. The first scheme utilized probabilistic S-N curves, considering random variables related to the load spectrum and material properties. The second scheme involved stochastic Finite Element (FE) simulation coupled with sampling techniques, integrating the Chaboche constitutive model with the fatigue behavior modeling and life prediction.

- Full-scale overspeed tests of the bladed disk revealed that the stochastic FE-based scheme yielded more conservative predictions compared to the probabilistic S-N curves-based approach.

- Tulsidas d., *et al.* [19]assessed low cycle fatigue life of steam turbine blade using linear elastic finite element analysis (using Neuber's rule) and elastic-plastic Finite Element analysis (FEA). Strain amplitude approach was followed through Universal slope method and Coffin-Manson equation to determine the number of start-up and shut down cycles.
- Citarella R, *et al.* [20] adopted combined FEM-DBEM approach to study the assessment of damage accumulation and growth occurring on the leading edge of a turbine blade, with the crack propagation starting from part-through surface flaws. In particular, the stress analysis on the global model was performed by FEM whereas the crack propagation phase was simulated by DBEM (dual boundary element method).
- V.N. Shlyannikov *et al*. [21] estimated the turbine blades fatigue life by a approach which included numerical stress-strain analysis of real rotor components, experimental study of fatigue and fracture resistance material properties and determination of crack growth rate characteristics on the round bar specimens with the single edge notch. Both specimens with the initial surface state and specimens with high velocity air fuel (HVAF) coating were tested. Numerical analysis of stress state in specimens was performed under uniaxial loading.
- Mariusz Banaszkiewicz [22] performed numerical investigations of stresses and strains in the intermediate pressure steam turbine rotor to identify life-limiting locations and to evaluate fatigue life to crack initiation for typical operating conditions including cold, warm, and hot start-ups and shutdown. The study found that the accuracy of analytical stress-strain correction methods is influenced by the magnitude of strain amplitude. Strain amplitudes were calculated using three different methods: Neuber's rule, the Glinka-Molski rule, and finite element analysis with the Prager-Ziegler model. Neuber's rule tends to overpredict strain amplitudes, while the Glinka-Molski rule tends to underpredict them when compared to finite element analysis using the Prager-Ziegler model.

  Furthermore, it was observed that the region experiencing maximum stress varies among different start-up scenarios. Heat grooves were identified as the most critical areas in terms of thermal fatigue.
- Mariusz Banaszkiewicz *et al.* [23] performed a root cause analysis on the phenomenon of groove cracking in steam turbine rotor blades. The analysis encompassed metallographic examinations, material evaluations, and estimations of mechanical integrity. The subsequent deductions were made based on their research findings:

- Metallographic tests conducted in the inlet area of the Intermediate Pressure (IP) rotor did not reveal any signs of material deterioration. Nevertheless, the examination of the damaged grooves by metallographic analysis uncovered a microstructure that is characteristic of stress corrosion cracking (SCC).
- Stress corrosion cracking was identified as the root cause of the blade groove failures.
- In order to alleviate stress corrosion and decrease the rate at which corrosion fractures develop, it was necessary to decrease the yield stress of the material.

- A study by A.L. Tejeda *et al.* [24] investigated the fatigue behavior of the final stage L-1 blades of a steam turbine when subjected to cyclic loading. The findings revealed that the fatigue strength of the blades diminishes when resonance conditions occur, leading to accelerated cracking and eventual failure in a shorter duration. The study observed that natural frequencies decrease and displacement amplitudes increase as cracking progresses, and the propagation of cracks requires fewer cycles.
- Ronald N. Salzman [25] presented an approach to predict fatigue failure of power plant component which had been subjected to over 30 years of service. They concluded that accurate life prediction requires a detailed knowledge of the material fracture mechanics properties as well as a detailed knowledge of the component load history, including the sequence of events.
- Zdzislaw Mazur *et al.* [26] presented a comprehensive analysis of failures in low pressure blades of steam turbines caused by flow excitation and torsional vibrations resulting from abrupt changes in the grid. The analysis was based on several case studies. The examination of the fracture surface of the blades in the laboratory revealed that the cause of failure was high cycle fatigue (HCF). The examination of the blade that experienced failure involved metallurgical analytical techniques such as metallography, SEM (scanning electron microscopy) fractography, and chemical analysis. Centrifugal stress deformation and mode shapes of individual and coupled blade were calculated by using FEM. Fracture propagation analysis was carried out using metallurgical investigation findings and fracture mechanics (PARIS law). From all case studies they conclude that flow induced blade oscillations of the turbine can lead to blade fatigue failure.
- Bernd M. Schönbauer *et al.* [27] estimated the fatigue life of a steam turbine blade composed of 12% Cr steel under various stress ratios and test environments. They conducted their study

at a temperature of 90°C, employing the ultrasonic fatigue testing technique. The test environments included ambient air and two distinct aqueous solutions.

- An estimation of the fatigue life of a low-pressure steam turbine blade that is transiently loaded during start-up was done by M. Shakeel *et al.* [28] using a probabilistic model. The approach uses Finite Element Analysis (FEA) to model the stochasticity of structural damping, rotational speed, and elastic modulus of the blade material. The results of the Finite Element Analysis are used to create random values for the stress and fatigue cycles through the use of Monte Carlo simulation. After that, the probabilistic fatigue life is calculated using the Palmgren-Miner rule.

1.3.2 Studies on creep failure of turbine blade:

Creep refers to the phenomenon of gradual and permanent deformation in solid materials when subjected to prolonged exposure to stresses, typically below the material's yield strength. Figure 1.8 depicts a typical creep curve.

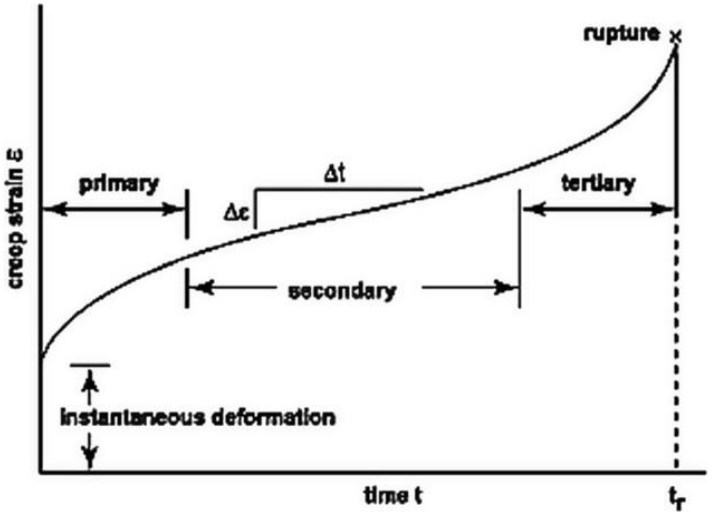

Figure 1.8 The typical form of a creep curve [29]

- S. M. Sanjay kumar *et al*. [30] forecasted the creep life of a basic impulse steam turbine blade, employing a Finite Element Method (FEM) for creep analysis. Their investigation of the creep phenomenon and subsequent prediction of the component's creep life allowed for an estimation of its design life. Creep, characterized by a rate-dependent material nonlinearity, entails continued deformation even under constant load, particularly prevalent in components subjected to high temperatures. Their analysis revealed that the creep life diminishes as stress values escalate. Consequently, reducing stress levels in the component can extend its creep life.

- Mariusz Banaszkiewicz [31] analyzed the creep behavior of rotating components using a characteristic strain model (CSM). Numerical creep analysis of the steam turbine rotor is performed by thoroughly analyzing the creep strain and stress fields within the rotor disc. The building of creep strain in the disc happened in a very nonuniform manner. Creep strains increased more rapidly and in greater amounts in locations with higher elastic stresses, such as the fillet radii, compared to regions with lower elastic stresses. Thus, areas with large stress concentrations may have reached their limit of creep ductility and be on the verge of experiencing creep crack initiation.
- Mariusz Banaszkiewicz [32] created a quick and accurate way to monitor the creep life of steam turbine rotors online. This was achieved by examining and validating a creep characteristic strain model with test data of 2%CrMoV rotor steel. Creep damage functions, derived from the model and based on the Robinson time fraction rule, are introduced to calculate creep damage at a constant temperature. A turbine rotor was subjected to finite element (FE) creep computations using the same creep model in order to validate the proposed method and provide reference damage values.
- Mariusz Banaszkiewicz [33] introduced a comprehensive approach for assessing the lifetime of a steam turbine in his work, which involves damage calculation, probabilistic analysis, and fracture mechanics considerations..
    - The calculation of creep-fatigue damage forms the foundation for assessing the current expenditure of the turbine's lifetime and for outlining further analytical steps.
    - Probabilistic analysis becomes necessary due to the inherent uncertainty associated with estimating lifetime expenditure, mainly stemming from variations in material properties.
    - Fracture mechanics considerations play a crucial role in determining extra safety margins for components that harbor cracks, enhancing the overall integrity of the system.

1.3.3 Studies on fracture failure of turbine blade:

Fracture is characterized by the separation or fragmentation of a solid body into two or more parts due to the application of stress. This process entails the complete disruption of the component's continuity. Fracture can occur under various conditions, including:

1) Under static load: Fracture can result from the application of a constant load, leading to either brittle or ductile failure.

2) Under fluctuating or cyclic load: Fatigue fracture occurs when a component is subjected to repeated loading and unloading cycles. This is the most common mode of failure for machine parts in service [34].

- J.A. Segura, *et al.* [35] conducted a failure diagnostic, determined the cause of blade fractures in the L-0 stage of the low-pressure section (LP) of a 300 MW steam turbine, and analyzed crack propagation.
    - Visual inspection of the 300 MW steam turbine revealed fractured blades in the last stage, L-0, which subsequently affected neighboring blades. There were three broken blades and several more with noticeable cracks. The blade joints suffered damage and fractures due to a combination of high-cycle fatigue and high vibrational loads.
    - A metallographic examination identified crack initiation from a cavity caused by particle erosion. Numerical calculations indicated that stub blade groups became disconnected due to vibration induced stresses during turbine shutdown and startup.
    - The original blade showed resonance characteristics, which caused the group to detach and started the crack to propagate. The number of cycles until the 300 MW steam turbine's final stage blades cracked was determined.
- Ernst Plesiutschnig, *et al.* [36] conducted an evaluation of crack propagating stresses utilizing Linear Elastic Fracture Mechanics (LEFM) and Finite Element Analysis (FEA), integrating experimental data and literature findings.

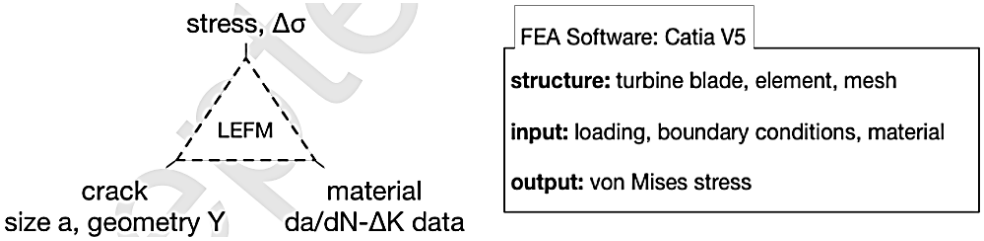

Figure 1.9 Input parameters for LEFM and output parameters of FEA

Parameters used by FEA and those used by LEFM as inputs are shown in Figure 1.9. Main Findings are:

- FEA projected a local mean stress σ_m exceeding 500 MPa at the turbine blade root edge in an un-notched condition, attributed to rotor speed.
- Changes in rotor speed, leading to the excitation of natural frequencies, were not identified as significant factors in crack propagation.

- Crack propagation was primarily attributed to centrifugal load and superimposed bending load induced by unsteady steam forces.
- Inspection intervals should consider the number of fluid flux variations.
- The lifespan of steam turbine blades was constrained by unsteady steam bending forces.
- The estimation of damaging loading conditions is derived from fatigue crack analysis.
- The cyclic bending stress and the time taken for crack size progression are estimated factors.

➢ N. S. Vyas *et al*. [37] introduced an analytical code designed for dynamic stress analysis and fatigue life prediction of blades. The key features of their approach include:

- Utilization of a combination method for life prediction, merging the local strain approach to forecast initiation life with the fracture mechanics approach to assess propagation life, thereby estimating the total fatigue life.
- Application of Neuber's rule to dynamic stresses to derive elasto-plastic strains, followed by iterative solutions for plastic stress using the material hysteresis curve.
- Incorporation of static stress effects in the analysis, with estimation of crack initiation life through the solution of the strain life equation.
- Utilization of crack growth formulations to analyze the propagation of initiated cracks, leading to eventual failure.

➢ Stuart Holdsworth [38] focused on the aspects of creep-fatigue failure diagnosis and found that it involves consideration of both associated material condition and the results of a mechanical analysis of prior operating history. An important step in any creep-fatigue assessment procedure is a determination of the state of stress and strain at the critical location in the component which can be determined by approximate analytical solutions or finite element analysis (FEA). The effectiveness and efficiency of the diagnosis of failures due to creep-fatigue loading are enhanced by a familiarity with the characteristics of the material of the failed component which can come from the routine post-test examination of laboratory specimens.

➢ Using scanning auger microscopy and potentiodynamic polarisation D Saidi *et al.* [39] described the microstructure and fracture mechanism of a steam turbine blade made of martensitic stainless steel. The researchers discovered that steam turbine blades go

through metallurgical changes when they're in service. One of these changes is the fracture mode, which changes from intergranular in new blades to trans-granular in used ones. This change is accompanied by the formation of new precipitates inside the grain and the beginning of micro-cracks caused by fatigue-damage accumulation.

1.3.4 Studies on Modal analysis of turbine blade:

- Akash Shukla *et al.* [40] conducted a comparative study of modal analysis of steam turbine blades using analytical, Finite Element Method (FEM), and Experimental Method. Here are the key points from their study:
  - Modal analysis of the last stage blade was initially performed using FEM techniques, followed by testing the blade in the NFT lab at BHEL Haridwar. Natural frequencies were calculated using both methods.
  - The study yielded the following conclusions:
    1) Dynamic behavior of the blade undergoes a definite change in the presence of cracks. This alteration can facilitate crack detection in blades without requiring dismantling from the rotor during overhaul.
    2) Combining FEM analysis with experimental analysis offers a comprehensive understanding of the dynamic behavior of complex structures like steam turbine blades, providing a broader perspective for analysis.
- The objective of the study by Akash Shukla *et al.* [41] was to investigate the differences in vibration response between free-standing blades with varying crack diameters at the root of fir trees. Here are the key points from their study:
  - The presence of cracks in the blade root leads to a loss of stiffness in its vicinity. This loss of stiffness causes a shift in natural frequencies and redistributes static & dynamic stresses in the root of blade, potentially leading to blade failure. The researchers examined the fluctuations in the natural frequency and mode forms of blades with varying crack widths.
  - According to the research, blade geometry cracks are indicated by changes in natural frequency. This provides insights into crack detection in blades. The authors proposed conducting natural frequency tests on blades during overhaul before actual removal for Magnetic Particle Inspection (MPI) and Ultrasonic Testing (UT) to detect cracks in their assembled condition. This approach aims to minimize downtime and prevent production losses in power plants.

- J.C. Pereira *et al.* [42] investigated the low cycle fatigue problem in low-pressure turbine by determining the natural frequencies and the associated modes of vibrations of a bladed disk through a case study using computational model and experimental measurements. They concluded that no resonance had occurred, so the low cycle fatigue was not the root-cause of the damage on the blades. That's why high cycle fatigue must be investigated in LP region.
- M Heidari *et al.* [3] examined a finite element model of steam turbine blades of varied thickness and length in three dimensions. The key findings from their study are:
  - All materials in the model were assumed to be linear, homogeneous, elastic, and isotropic. A widespread force of 5N was applied to the blades.
  - The study concluded that using shorter and thicker blades is advantageous for reducing stress and strain, potentially enhancing durability.
  - Understanding the stress and strain patterns in turbine blades offers valuable insights that can aid in estimating fatigue in these components.
  - Results indicated higher stress and strain concentrations at the base of the blades compared to the tips.

1.4 Findings from literature survey

From the literature review, it's evident that research has been conducted across various domains including turbine blade failures and many modeling methodologies. However, the findings from these evaluations exhibit certain limitations, some of them are highlighted below. The main aim of this study is to conduct a qualitative analysis of the blade of a 210 MW low pressure steam turbine after 1,52,241 hours of operation in order to identify the specific areas of damage and determine the underlying cause. Furthermore, the research aims to delve into the remaining life assessment of steam turbine blade ANSYS® and fracture mechanics technique. The major objective is to determine how much longer the steam turbine blade will last by establishing appropriate inspection, maintenance, and operating procedures.

1.4.1 Key Points:

- Experimental studies face limitations due to cost and component variability, such as different sizes of cracked blades. Therefore, validated Finite Element (FE) models offer a viable alternative for further studies on blade variations. These investigations should encompass considerations like blade looseness and uneven or partial support on blade roots, aiming to identify any less stiffened blades within grooves. Additionally,

extending FE analysis to incorporate the coupled static and dynamic responses of blades during operational conditions is recommended [41].

- The S-N-Mean stress model isn't perfect because it doesn't take into account the growth of plastic strain zones, especially when low cycle fatigue is present. This limitation results in the S-N approach providing a lower life expectancy compared to a combination approach that considers plastic zone development [43].
- For smooth specimens, the crack initiation life is usually estimated using total life techniques. However, inherent defects in engineering materials can lead to an overestimation of useful life using these methods. There is a paucity of research in this domain, indicating a need for further investigation and refinement of assessment techniques [43].
- Micrographs of fractured faces and potentiodynamic cyclic polarization curves provide evidence of microstructural evolution, which can aid in refining the lifespan assessment of turbine blades [43].
- An effective, structured life extension strategy should extend T/G operation beyond their designed lifetime. The life extension strategies should be comprehensive.
- The precision of local multiaxial High Cycle Fatigue (HCF) criteria predictions could be enhanced through fatigue tests conducted under multiaxial loading conditions.
- Experimental investigations, focusing on low failure probabilities, can help determine the most accurate probabilistic HCF model for fatigue prediction.
- A more comprehensive analysis of the material microstructure and fracture surfaces of specimens may offer deeper insights into the parameters crucial for fatigue crack initiation. Optimization of parameter identification should be tailored to the relevant loading conditions, with multi-axial experiments being incorporated.
- Incorporating stochastic variables representing geometric variations, such as blade thickness, in failure probability computations could improve accuracy.
- Fatigue tests aimed at characterizing fatigue behavior in the Very High Cycle Fatigue (VHCF) regime are essential, particularly for components subjected to high-frequency vibrations.
- Furthermore, it's vital to compare and validate numerical damage predictions against experimental results from both uni-axial and multi-axial loading scenarios. Additionally, the method's applicability should be assessed across various materials and

thermal cycles. Encouragingly, a strong correlation between predicted and measured lifetimes in uni-axial tests has been observed, bolstering confidence in the approach.

- Blend of classical and simulation approach can be successfully adopted for blade life estimation.
- Finite Element Method (FEM) studies offer a valuable tool for identifying less stiffened blades within grooves. Additionally, the analysis of a validated FEM model can be expanded to encompass the coupled static and dynamic response of blades under operating conditions.

1.4.2 Research Gaps

After a detailed and extensive literature survey in the area of turbine blade failure following research gaps are identified:

- There is a need to undertake detailed analysis of fluctuating loads on turbine blades during start up, shutdown and speed change events. Complex stress/strain history of blade due to unsteady steam pressure and blade vibrations needs to be considered for estimation of creep-fatigue damage.
- Evaluation of different in-elastic material models and creep-fatigue models for residual life prediction is needed.

1.4.3 Objectives of Present Research Work

After analyzing the research gaps, following objectives are set as research objectives for this proposed work-:

1. Calculations of stresses and strains for different transient events like cold, warm and hot startups, speed change event and shutdown.
2. Identification of critical locations on blade along with dominant damage mechanism.
3. Calculation of remaining life of turbine blade as a result of fatigue damage, creep damage and creep-fatigue interaction using operation and material data.
4. Formulation of methodology for a steam turbine blade life assessment based on deterministic damage calculation, probabilistic simulation and fracture mechanics considerations.
5. Recommendations regarding the component repair, inspection intervals or modification of operating conditions.

1.5 Contributions of the Thesis

In the present work, a real case seventh stage turbine blade of 210MW steam turbine has been investigated experimentally and computationally to assess metallurgical and mechanical defects in order to identify the root causes of turbine blade failure. The present dissertation work investigates the eroded surfaces of a 210 MW steam turbine blade. The purpose of this examination is to qualitatively examine the blade of a 210 MW low pressure steam turbine after 1,52, 241 hours of working to identify the critical locations of damage and the reason behind it. The turbine has been started up 379 times, which includes 118 hot starts, 205 warm starts, and 56 cold starts. So, we have performed fractography with a SEM (Scanning Electron Microscope) to determine the failure mode, metallographic examinations including inclusion rating to determine the micro-constituents responsible for the crack initiation, and EDX (Energy Dispersive X-Ray) to analyse the micro-chemical composition of the areas where the crack first appeared.

Focus of this research is remaining life assessment of the steam turbine blade. After determining the temperature and stress distribution by numerical simulation, life estimation calculations have been performed to provide a deterministic estimate of the blade damage. Calculations are made for the fatigue characteristics of material AISI 420 to determine the number of cycles at a nominal stress level before blade fatigue failure. The magnitude of a numerical model's constants is thus determined. Blade damage is also predicted using numerical models predicated based on Smith Watson Topper (SWT), strain life, Morrow mean stress theories by using ANSYS® software. For determining the Life consumption of steam turbine components, steady-state stresses (thermal and centrifugal) and transient stresses have been evaluated. Transient stress analysis has been carried out for cold start, warm start, and hot start. Based on this, the most highly stresses zones are identified. Finite element method temperature and stress evaluations with automatically generated input files including thermal and mechanical boundary conditions form the basis for lifetime estimations. The calculation of fatigue damage is based on transient temperature and stress fluctuations, whereas the calculation of damage due to creep is based on steady-state temperature and stress distributions.

1.6 Organization of the Thesis

This thesis has six chapters. The first chapter serves as a foundation. It summarizes the prior research in this area. There is also a presentation of the thesis's goals, research gaps, contribution, and structure. Chapter 2 provides an introduction to steam turbines, including how they are built and how they work. It also delves into the reasons behind turbine blade failure

and the methods that are employed to address them. Fractography of a real-life case of a 210 MW steam power plant's seventh-stage, low pressure steam turbine blade that was rejected is presented in the third chapter. In Chapter 4, the fatigue life of a steam turbine blade is evaluated computationally using the finite element programme ANSYS®. Chapter 5 details the calculations of fatigue and creep damage on a real-life, low pressure stage steam turbine blade that has been rejected due to erosion damage. The thesis is summarized and future research directions are laid out in sixth chapter.

CHAPTER 2

STUDY OF THE CAUSES OF FAILURE OF LOW-PRESSURE TURBINE BLADES

2.1 Introduction

This chapter provides an overview of fundamental principles pertaining to the operation of a steam turbine. This chapter provides a concise review of steam turbines, focusing on their construction, operational principles, and the materials used for turbine blades. The chapter additionally provides an overview of the composition and material properties of steam turbine blades. This knowledge will prove valuable in identifying the underlying factors contributing to failure in the proposed study on low pressure steam turbine blades. The subsequent chapter provides a detailed account of the methods employed in the investigation of turbine blade failure, as well as the sample preparation technique utilised for fractographic examination.

Steam turbines are mechanical devices used to convert thermal energy contained in pressurized steam into mechanical work, which is then used to generate electricity or drive various types of machinery. The contemporary version of it was invented by Sir Charles Parsons in 1884 [44]. They are widely used in power plants, industrial facilities, and marine propulsion systems due to their efficiency, reliability, and versatility.

Initially, high-pressure steam enters the turbine at the HP stage, where it expands and transfers its energy to the turbine blades, causing the rotor to rotate. The steam then progresses through the IP stage, further expanding and releasing additional energy before entering the LP stage. Here, the steam completes its expansion, extracting the remaining energy and imparting momentum to the turbine blades. Throughout this process, the steam undergoes a gradual decrease in pressure and temperature, maximizing the utilization of thermal energy [8]. A typical steam flow path is shown schematically in figure 2.1

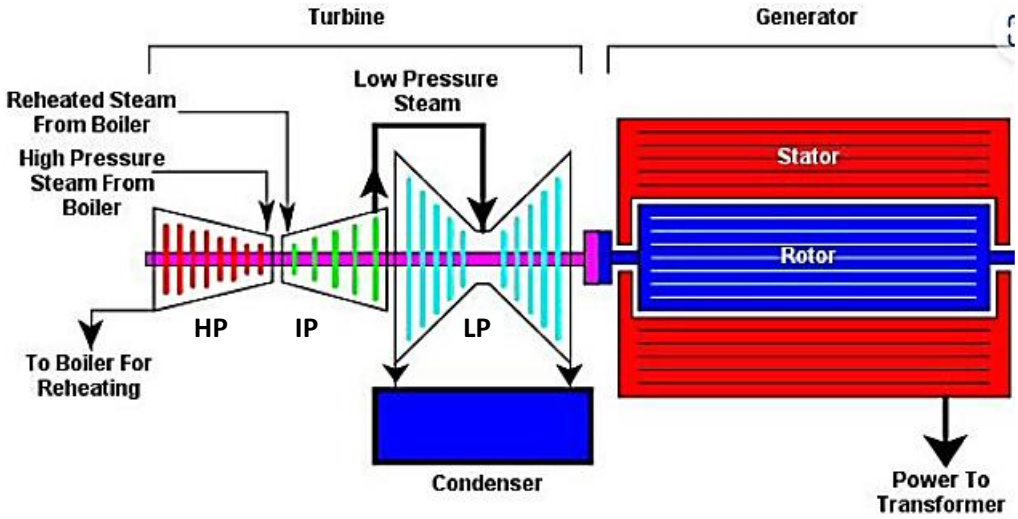

Figure 2.1 Flow of Steam in a turbine

Steam turbines may be classified into different categories depending on their construction, working pressures, size and many other parameters. But there are two basic types of steam turbines [45]:

Impulse turbines: The impulse turbine consists of a series of rotating blades that are interspersed with stationary nozzles. In an impulse turbine, the steam undergoes expansion in stationary nozzles and maintains a consistent pressure as it flows over the blades. The Curtis turbine, Rateau turbine, and Brown-Curtis turbine are all examples of impulse type turbines [46][45].

Reaction turbines: Rotating blades, or nozzles, and stationary nozzles make up the reaction turbine. The steam is expanded in both stationary and mobile nozzles within the reaction turbine. What this means is that as steam passes over the blades, it expands at a constant rate. The key difference is in the way the steam is expanded when it goes through the turbine [47].

Turbine Blades

The blades of turbine are the most crucial components of the turbine. These are the main parts that convert the working fluid's pressure energy into kinetic energy. Turbine blades can be classified into two fundamental categories [45]:

- **Rotating blades**
- **Stationary blades**

Steam turbines utilise fixed blades, known as nozzles, to facilitate the expansion of steam. During this process, the pressure potential energy of the steam is transformed into kinetic energy. When high-velocity steam from stationary nozzles strikes moving blades, it expands

(for reaction-type blades) and changes direction. The alteration in its trajectory & the increase in velocity of steam (Considering blades designed for reactive forces) exert a force. "The resulting impulse drives the blades forward, leading to the rotation of the rotor." [45][48]. Properly designed blades are the key to a turbine's efficiency and dependability. As a result, it is critical for all turbine engineers to understand the significance and fundamentals of steam turbine blade design [45].

Modern steam turbines often combine both impulse & reaction in a single unit, with the degree of reaction and impulse varying across blades. The rotor blades are typically designed with different characteristics at the root and tip, resulting in an impulse blade-like design at the root and a reaction blade-like design at the tip [44][45].

Figure 2.2 Modern steam turbine blade

The history, design, and operation of steam turbine blade are covered in the following section.

2.1.1 Historical and Technological Development of steam turbine blade

The present design level establishes a 30-year service life for this category of machinery. This often means that infinite life is required in design, which may be more than what is needed for a particular installation.

Starting with research into spring-mass systems and progressing to the creation of a single cantilever beam, blade band [49], and bladed disc, blade design has changed over time. Adjustments were made to include new techniques as turbine design progressed and manufacturers gained experience. Campbell (1925) found that axial vibration caused blade failure (bursting) when studying disc failure.

Blades had to get taller to handle the increased power, therefore they had to be linked by a metal band either at the very tip or midway in the middle of the blade. Kroon (1934) outlined a technique for judging how well such architecture dampens the design's dynamic reaction to steam forces. Blades for use in high-pressure and high-temperature environments were described by Allen (1940).

Banded constructions feature more frequencies and mode shapes than single blades, as revealed by the investigation conducted by Weaver and Prohl (1956). The numerical method

and the equations for estimating the frequencies, mode shapes, and dynamic response of the banded blades were detailed by Prohl (1956) in a companion study. Key assumptions were made to simplify the research and make the results manageable, as detailed below.

- A row of similar blades was uniformly spaced and presumed to run parallel to each other.
- The axial and tangential directions of the rotor were considered to be parallel to the principal axes of the blades' cross sections.
- It was presumed that the cross section's shear centre and centre of gravity coincided [49].

The advent of FEA did away with the need to assume a banded construction analysis for pinpointing the right frequency and dynamic response. It was a turning point in the analytical development of blade vibration and the reliability decision-making process [49]. The next step in technology was the bladed disc system, in which the blades were coupled via the disc and the rigidity of the disc had to be taken into account. The incorporation of geometric changes between blades and the subsequent analysis of discs comprising groups of blades represented the next step forward in the study of the dynamic response of blades. The packeted bladed disc was the subject of research by Singh (1982, 1988, and 1989).

Given that every design choice carries some degree of uncertainty, a probabilistic approach has been implemented to enable the estimation of such uncertainty. Despite the fact that further research and testing is required, blade design and reliability have come a long way in recent decades [9].

2.1.2 Working environment of low-pressure steam turbine blade

The basic principle behind steam turbines involves the expansion of high-pressure steam through a series of stationary and rotating blades, known as stages, which are arranged in a turbine casing. As the steam flows over the blades, it imparts momentum to them, causing the rotor to rotate. This rotational motion is then used to drive a generator or other mechanical equipment. One set of stationary blades is connected to the casing and one set of rotating blades is connected to the shaft.

To maximize turbine efficiency the steam is expanded, generating work, in a number of stages. These stages are characterized by how the energy is extracted from them and are known as either impulse or reaction turbines shown in figure 2.3. Most steam turbines use a mixture of the reaction and impulse. Typically, higher pressure sections are impulse type and lower pressure stages are reaction type [50].

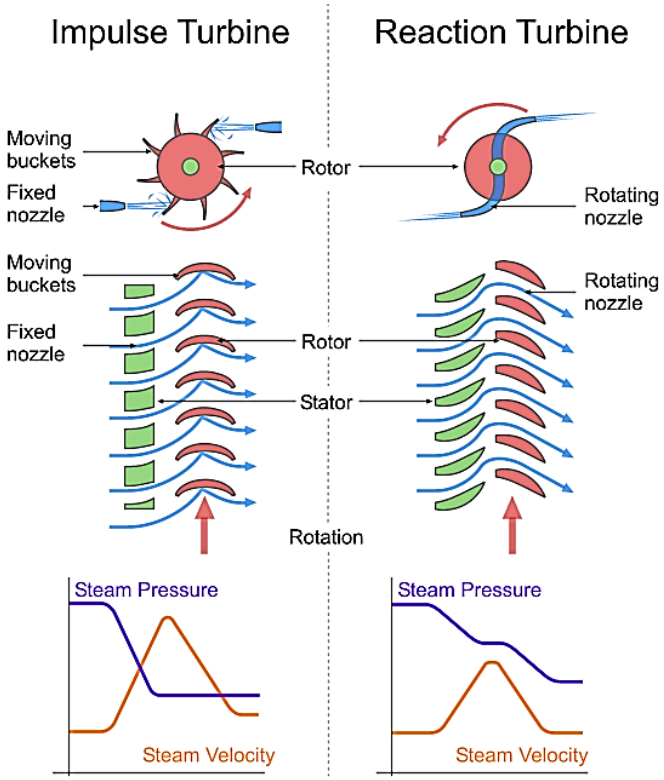

Figure 2.3 Schematic diagram outlining the difference between an impulse and a reaction turbine[45]

The LP Turbine, or low-pressure turbine, typically consists of a double-flow reaction turbine with approximately 5-8 stages. The turbine features shrouded blades and the last 3 stages have free-standing blades. LP turbines generate around 60-70% of the total power output of the power plant unit [45][51]. The low-pressure section is designed in such a way that its diameter increases from inlet to outlet.

Low-pressure steam turbine blades encounter the operational challenge of handling two-phase fluid conditions. The presence of a high concentration of water droplets can lead to rapid impingement and erosion of the blades when condensed water is forcefully directed onto them. To mitigate this issue, measures such as installing condensate drains in the steam piping leading to the turbine are implemented [5]. Additionally, engineers face the task of designing blades for the last stage of the LP turbine, which must be exceptionally long due to the high specific volume of steam. Consequently, these blades are subjected to significant centrifugal forces during operation, as turbine stages can rotate at thousands of revolutions per minute (RPM), typically around 3000 RPM. This combination of centrifugal and fluid forces poses risks of fracture, yielding, or creep failures in turbine blades [45].

Next subsection will present the overview of turbine blade material and its importance

2.1.3 Importance of Blades in Steam Turbines and Material of steam turbine blade

The steam turbine's blades are subjected to extreme static and dynamic loads over the course of its lifetime. To prevent blade failure, analysis must be performed regularly [3]. A steam turbine can have tens of thousands of blades, with each row of blades potentially having its own unique dynamic features. Turbine blade materials should have high tensile and fatigue strengths [49]. The best blade material also has great ductility, is resistant to corrosion and erosion, and can withstand high temperatures [9]. Figure 2.4 depicts a typical blade profile, showing the low-pressure (suction) and high-pressure sides, as well as the position of the leading and trailing edges [10].

Blades can be divided into two categories according to how they are used in the turbine modules: LP, which has large blades that bend due to impulse changes and high static pressure, and HP and IP, which have high temperatures and small blades that should withstand minor centrifugal forces [3]. Blade materials property requirements for high-pressure and low-pressure steam turbines are listed in table 2.1.

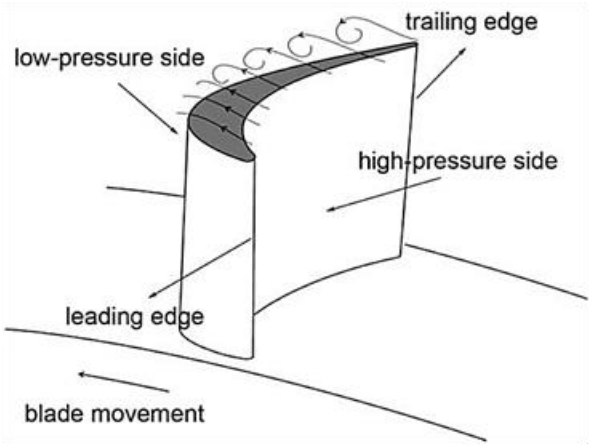

Figure 2.4 Standard profile of a blade, showing leading and trailing edges as well as the suction and pressure faces [10]

When choosing a blade material, high stress and erosion should be considered [12]. Last stage blades which are up to about 40 inches in height have been made of 12Cr martensitic stainless steel for many years for 3600-rpm designs because of its excellent properties like high toughness and resistance to corrosion [12]. Present study is focused on low pressure steam turbine blade made of martensitic stainless steel (X20Cr13). The Chemical composition and Mechanical properties of X20Cr13 steel are presented in table 2.2 and 2.3.

Table 2.1

Blade material requirements for high-pressure and low-pressure steam turbines [13]

Requirement	HP/IP Blades	LP Blades	Justification
Static tensile Strength	Y	Y	Because blades are subjected to Centrifugal (high rotational velocity) and pressure loading.
Toughness	Y	Y	To avoid sudden failure in cracked components.
Creep rupture Strength	Y	N	HP and IP function at elevated temperatures. Minimizes the risk of creep rupture and prevent the blades from coming into contact with the turbine casing [52].
Oxidation Resistance	Y	N	Avoid material loss and possible raised local temperatures [53], HP and IP turbines operate at sufficient temperature.
Local corrosion Resistance	Y	Y	Avoid possible local corrosion.
Corrosion fatigue Strength	N	Y	Steam begins to condense as it reaches the LP turbine. This results in deposition of impurities and localized regions of high salt concentration. If condenser leakage results in HCl formation, the pH of water droplets is lowered. This combination can result in corrosion pits forming [54] and acting as start points for corrosion fatigue [55][56].
Stress corrosion Cracking resistance	N	Y	LP turbine blades are susceptible [54][56] since they are under stress in a chemically aggressive environment.
LCF and HCF resistance	Y	Y	LCF stresses of thermal and mechanical origin during start up and shut down are especially critical because of two shift [57] and flexible operation HCF may become a problem due to external initiation such as from foreign object damage or changes in vibrational characteristics
Erosion resistance	Y	Y	Solid particles may be present in steam [57].
Weldability	Y	Y	Manufacturing requirement.
Type IV cracking resistance	Y	N	Failure can occur in a weld heat affected zone under creep conditions [58][13].

Material Properties

The Chemical composition and Mechanical & thermal properties of X20Cr13 steel are presented in table 2.2 and table 2.3 [59].

Table 2.2

Chemical composition (wt.%).

C	Cr	Si	Mn	P	S	Ni
0.17-0.22	12.50-14.0	0.10-0.60	0.30-0.80	≤0.03	≤0.02	0.30-0.80

Table 2.3

Mechanical and thermal properties

Characteristic	Magnitude
Density, ρ (kg/m^3)	7750
Elastic Module, E (GPa)	193
Elongation, EI (%)	8.0 to 15
Reduction area, Min (%)	50
Brinell Hardness, HB	280
Tensile strength, S_{ut} (MPa)	800-950
Fatigue strength (MPa)	220-670
Proof stress (MPa)	≥ 650
Cp (Specific Heat)	478.71 J/(kg K)
Thermal Conductivity	24.606 W/(m K)
Coefficient of thermal expansion	10 μm/m-K

2.2 Root Causes of low-pressure steam turbine blade Failure

The blades of a steam turbine are among its most vital parts. A steam turbine might have hundreds of blades or perhaps thousands. Static stress, primarily caused by steam bending and centrifugal stresses, is one of the reasons of blade deterioration. There are a number of causes of blade wear, some of which are mentioned here [49].

- Centrifugal stress
- Steady stress
- Stress due to resonant vibration
- Impact stress

- Alternating stress
- Creep damage
- Corrosion fatigue
- Low cycle fatigue
- Thermal fatigue
- Stress corrosion
- Stress due to steam forces
- Environmental effect

An industrial survey for blade failures shows that blade failure caused a significant loss of unit availability between 1970 and 1981. This report claimed significant revenue losses from blade repair and power production owing to unit downtime. Based on the statistics, utilities, manufacturers, and EPRI (Electric Power Research Institute) should work together to develop adaptable technology to increase LP, IP, and HP blade reliability [60].

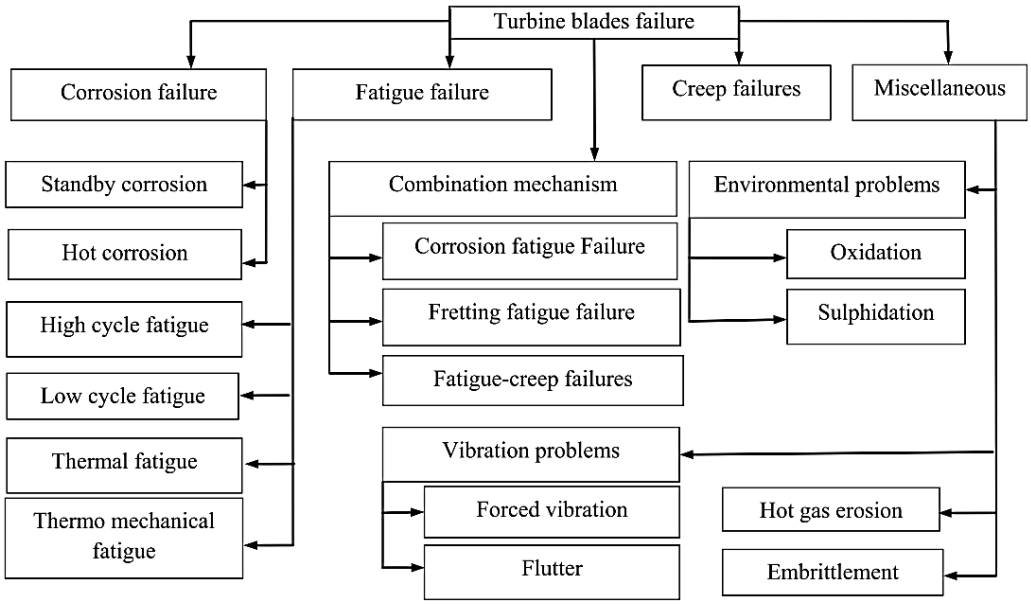

Figure 2.5 Turbine blade failure reasons[29]

As part of project RP 1266-24 (Reinhart, 1987), the Electric Power Research Institute found that 72% of turbine blade failures in power plants occur in low-pressure (LP) turbines, with half of those failures occurring in the last two blade stages. Roots and blade trailing edges usually fail. Cracks caused 79% of LP turbine blade failures, according to Project RP 1266-24. Cracking can occur for various reasons [61]. The following tree structure in Figure 2.5 shows turbine blade failure causes that significantly affect blade life.

2.3 Losses in turbine blades

Steam turbine blade efficiency is a critical aspect of turbine performance, directly impacting power generation efficiency and overall system reliability. Efficiency in steam turbine blades refers to the ability of the blades to extract maximum energy from the steam flow and convert it into mechanical work. However, various factors contribute to efficiency losses in turbine blades, including aerodynamic losses, mechanical losses due to friction and leakage, and thermodynamic losses associated with steam wetness and incomplete expansion. These losses result in reduced energy extraction and lower overall turbine efficiency. Minimizing efficiency losses requires careful design optimization, operational adjustments, and maintenance practices aimed at mitigating factors such as blade erosion, steam wetness, and flow irregularities. Wetness loss in steam turbines refers to the decrease in efficiency caused by the presence of moisture or liquid water droplets in the steam flow. Wetness loss can lead to various adverse effects, including erosion and damage to low pressure stage turbine blades. Erosion is one of the primary reasons for low pressure turbine blade failure. By addressing these losses, turbine operators can enhance blade efficiency, optimize power generation, and improve the overall performance of steam turbine systems.

2.4 Need for reliability evaluation of steam turbine blades

Reliability assessment of mechanical components is a multidisciplinary task and has a great importance in blade design of a steam turbine because the blades have large impact on the overall reliability of the steam turbine. Although more research and testing are required, tremendous progress has been made in this area over the past few decades. Better evaluation of the challenges, leading to more precise and optimal designs, is possible with the help of today's state-of-the-art technology and tools [61]. As a result, "Remaining Life Assessment" of steam turbines is becoming increasingly desirable to ensure the reliability of turbine components.

In reality, RLA won't make the parts last longer. Only by metallurgical analysis and theoretical (fracture mechanics) calculations can the remaining useful lifetime be estimated. Remaining life assessment tools have several additional applications beyond this primary goal. It's useful for establishing reliable routines for inspections, repairs, and operations. Thus, it should be acknowledged that developing methods for estimating remaining life has a greater lasting significance and a wider aim than only prolonging plant life. For contemporary rotors, for instance, assessments from fracture mechanics calculations have allowed inspection intervals to be increased from six to ten years, resulting in significant cost savings [6].

2.5 Methodology for investigating turbine blade failure

The failure analysis performed on the fractured/rejected blade involves the examination of blade surfaces, such as pits, erosion, oxidation, and other relevant factors. Additionally, the analysis includes the fractography of the crack or fractured surfaces, as well as the analysis of metallography. For keeping track of a turbine blade's condition, all of these techniques are highly important.

2.5.1 Fractography

Fractography is the study of fracture surfaces to understand the mechanisms and causes of material failure. Fractography is the examination of fracture surfaces to establish the connection between the microstructure and the mechanisms of crack formation and spread, and ultimately, the underlying reason for the fracture [62]. The objective is to analyse and describe the characteristics of the fracture surface, such as its topography, morphology, and colour [63]. These properties are directly influenced by the structure of the material and its reaction to stress and the spread of cracks. It involves analysing the features and characteristics of fractured surfaces using microscopy techniques, particularly scanning electron microscopy (SEM). Fractography can be employed to identify the following:

- Failure mechanism of rejected parts
- Material defects
- Environmental interaction
- Nature of stresses
- Fracture origin
- Direction of crack propagation

The subsequent subsections provide a comprehensive explanation of the procedures involved in fractographic analysis.

2.5.1.1 Surface Preservation

Because of their fragility, fracture surfaces are vulnerable to mechanical and chemical environmental deterioration, which can affect microstructural characteristics. As a result, during the entire analytical process, fracture specimens need to be handled with extreme caution. Damage to the fracture surface can happen mechanically or chemically during or after the fracture event.

The chemical damage observed on the fracture surface is caused by the ambient conditions during the fracture event. If the environment surrounding the effected zone is corrosive to the underlying metal, the resulting fracture surface that comes into contact with

the environment will be chemically degraded. The fracture surface often experiences mechanical damage as a consequence of the loading conditions during the fracture event. If the loading condition is such that the mating fracture surfaces come into contact, the surfaces will sustain mechanical damage.

An effective method for preserving a fracture involves using a gentle flow of dry compressed air to remove moisture, followed by storing it in a desiccator, a vacuum storage tank, or a sealed plastic bag with a desiccant. Nevertheless, the act of separating the fracture in this manner is frequently impractical. Hence, it is imperative to employ a corrosion-preventive surface coating to impede the process of oxidation and corrosion on the fracture surface. The surface coating must be non-reactive with both the base metal and the surrounding environment. The surface coating must be fully and effortlessly eliminated without causing any harm to the fracture.

2.5.1.2 Sectioning of fracture

Often, in order to investigate the defect, it is required to either remove the fractured section from the entire part or decrease the specimen to a size that is manageable. The inspection equipment, such as the scanning electron microscope and the electron microprobe analyser, include specimen chambers that impose restrictions on the size of the specimens. It is important to perform all cutting procedures in a manner that avoids any damage or alteration to the fracture faces and their surrounding areas. This includes ensuring that the fracture surface remains dry wherever feasible. Flame cutting is the prevalent technique used for removing big sections of specimens.

2.5.1.3 Cleaning of fracture surface

Fracture surfaces that are exposed to different environments typically have undesired surface debris, corrosion or oxidation products, and accumulated artefacts that need to be eliminated prior to conducting fractography (Dahlberg *et al.* 1974). The predominant methods utilised for cleansing fracture surfaces include:

- Either dry air blasting or gentle cleaning with a soft organic-fiber brush can be used.
- Organic-solvent cleaning refers to the process of using solvents derived from organic compounds to clean surfaces or remove contaminants.
- Water-based detergent cleaning
- Cathodic cleaning refers to the process of using an electrical current to remove contaminants from a surface.
- Chemical etch cleaning

2.5.1.4 Visual examination

In order to assess the physical dimensions, structural integrity, and shape defects of the blade, visual testing is employed [64]. Additionally, it possesses the capability to identify flaws and other pertinent details on the surface of the blade. Visual examination offers numerous advantages. The principal under consideration is a sample. The operation is straightforward and unaffected by the material, structure, shape, or size. The inspection outcome is characterised by its simplicity, speed, reliability, sensitivity, and reproducibility. Little flaws on the surface of the blade could go unnoticed during inspection because of the limitations of human vision and the resolution of the equipment.

2.5.1.5 Dye penetration test (DPT)

The liquid permeation method is employed for the purpose of examining surface-breaking flaws present on the surface of the blade. The solution that has been penetrated exhibits high permeability. Due to the wetting action and capillary action, the penetrated solution will penetrate the surface-breaking defects on the blade surface when brushed on the tested area. Subsequently, the solution that has permeated is carefully removed, followed by the uniform application of a developer possessing a high sorption capacity. The penetrated solution that remains in the defect is adsorbed to the blade surface due to capillary action, revealing the precise location and geometry of the faults. The premise of inspection in the liquid permeation method is straightforward. The level of sensitivity in the inspection is relatively high. Nevertheless, the liquid permeation approach has a clearly restricted examination range. The methodology exclusively examines surface-breaking faults and places significant emphasis on surface roughness and clarity.

2.5.1.6 Electron fractography

Fractography is an essential technique in the analysis of failures. Failure analysis is to establish a correlation between the appearance of a failure and its underlying cause. Scanning electron microscopy is effectively employed to detect local material anomalies that serve as initiators of fatigue cracks. Scanning electron microscopy can provide a clear indication of the likely cause of failure by examining certain fractographic characteristics, along with information on the material and the loading conditions. Fractography is widely regarded as an excellent method for studying the failure analysis of turbine blades. So, SEM is a versatile imaging technique that provides detailed information about the surface morphology, microstructure, and composition of samples at high resolution, making it an indispensable tool for scientific research, industrial applications, and materials analysis.

The subsequent significant technique is metallography, which is explained in the following subsection.

2.5.2 Metallography

Metallography is a branch of materials science and microscopy that focuses on the study of the microstructure of metals and alloys. It involves preparing metal samples, examining them under a microscope, and analysing their microstructural features. Metallography provides valuable insights into the properties, behaviour, and performance of metals and alloys, aiding in various fields such as materials engineering, metallurgy, and failure analysis.

Metallography employs a range of techniques and instruments, including optical microscopy, scanning electron microscopy (SEM), transmission electron microscopy (TEM), electron backscatter diffraction (EBSD), X-ray diffraction (XRD), and image analysis software. Each technique offers unique capabilities for examining microstructures at different length scales and resolutions. Metallography helps characterize the properties, behavior, and performance of materials, providing insights into factors such as grain size, grain boundaries, phases, inclusions, and defects.

Fractography focuses on the analysis of fracture surfaces to understand failure mechanisms, while metallography focuses on the examination of the microstructure of materials to characterize their properties and behaviour. Together, these techniques provide valuable insights into the structure-property relationships of materials and contribute to advancements in materials science and engineering.

2.5.2.1 Sample preparation for optical metallography and scanning electron microscopy (SEM)

Sample preparation for optical metallography and scanning electron microscopy (SEM) involves several steps to obtain high-quality specimens suitable for examination under these microscopy techniques [65].

- **Sectioning** (**the portion to be examined)**
- **Mounting (if sample is too small)**
- **Grinding**
- **Polishing**
- **Etching**
- **Cleaning and Drying**

1) Sectioning

Obtain a representative sample from the material of interest, ensuring that it contains the region of interest for analysis, such as the area of failure or specific microstructural features. Use

precision cutting techniques, such as abrasive sawing or wire EDM (Electrical Discharge Machining), to section the sample to the desired size and shape. Ensure that the cutting process minimizes deformation and damage to the sample.

2) Mounting

Mount the sectioned sample in a suitable material to provide support during subsequent preparation steps and facilitate handling during analysis. Choose a mounting material with properties that match the sample, such as epoxy resin or acrylic, to minimize the risk of introducing artifacts or altering the microstructure. Additionally, it is possible to mount and polish many specimens from a single component simultaneously. It is not advisable to put dissimilar metals together in the same mount.

3) Grinding

Grind the mounted sample using successively finer abrasives to remove surface imperfections, scratches, and cutting damage. This step aims to achieve a smooth, flat surface for microscopic examination.

Emery papers with grit sizes of 60, 120, 220, 320, 400, and 600 are frequently employed in a series of six stages. The sample should be translated in both forward and backward directions over the paper until the entire surface is uniformly marked with scratches in a single direction. Subsequently, the paper is rinsed with flowing water to eliminate any impurities linked to the quality of the paper utilised. Next, it is ground on a finer paper such that the scratches it creates are perpendicular to the ones the preceding paper generated. This process is repeated through the range of papers available. After the specimen has been ground on the last paper, it is usually beneficial to rotate it through and grind it again under less force. The time needed for the polishing stage, which comes next, can be shortened with this method.

4) Polishing

Polish the sample using diamond pastes or suspensions to further refine the surface and produce a mirror-like finish. Proper polishing is essential for revealing fine microstructural details during microscopy. Polishing is a multifaceted process that requires careful consideration of various elements, including the quality and appropriateness of the cloth, the abrasive used, the pressure applied while polishing, as well as the speed and duration of the process. The final polishing outcome is influenced by these elements and the surface finish achieved at each preceding stage.

Once the sample has been ground, it undergoes either manual or electrolytic polishing to get a completely flat and smooth surface like a mirror. This process involves the removal of any small scratches that may have occurred during the grinding stage. When polishing by hand,

the flat surface is held on moving wheels coated in cloth and sprinkled with abrasive suspension (Al2O3). Three sequential polishing processes are performed using 20μm and 10μm Al2O3 particle dispersion and 5μm diamond paste. Anodic dissolution in an electrolyte cell is the method used for electrolytic polishing. The cell comprises a vessel containing electrolyte with a stainless steel or platinum cathode submerged within it. The sample is positioned as the anode within the cell, while a direct current (D.C.) supply is connected to both the cathode and anode. The process of selectively dissolving the raised areas of grinding scratches leads to the formation of a highly polished surface like a mirror.

5) Etching

Apply a suitable chemical etchant to the polished surface to selectively reveal the microstructure of the sample. Etching highlights grain boundaries, phases, and other microstructural features by preferentially attacking different constituents of the material. Choose an appropriate etchant based on the material composition and the microstructural features of interest. Common etchants include Nital, Picral, and Keller's reagent for ferrous alloys.

The optical microscope allows for the observation of features like as pores, pits, cracks, inclusions, and relief development caused by variations in hardness in the polished sample. However, other microstructural characteristics such as the size of the grains, segregation, and the form, size, phases distribution, inclusions, and grain boundaries can be observed on a polished surface using a technique known as etching. The primary etching methods employed in metallographic sample preparation are:

- Chemical etching
- Electrolytic etching
- Heat tinting

(a) Chemical Etching

This etching procedure entails submerging the sample in an etchant or applying an etchant to the surface by swabbing. The choice of the most suitable etchant and the duration of immersion are crucial factors in sample preparation. For tests with low magnification, it is preferable to have deeper etches, but for greater magnification examinations, shallower etches are desired.

(b) Electrolytic Etching

Electrolytic etching and electrolytic polishing are essentially identical processes, with the only difference being that electrolytic etching employs lower voltages and current densities. The majority of electrolytic etching techniques employ direct current electrolysis. In this procedure,

the specimen serves as the anode, while the cathode is made of a very insoluble substance that is also conductive, such as platinum, graphite, or stainless steel.

(c) Heat tinting

Heat tinting, also known as thermal etching, refers to the oxidation process of a sample in a furnace. This causes surface characteristics to oxidise at varying rates, revealing diverse characteristics.

6) Cleaning and Drying

Thoroughly clean the etched sample using a sequence of solvents (e.g., acetone, ethanol) to remove any residual etchant, polishing debris, or contamination. Dry the cleaned sample using gentle airflow or a non-reactive drying agent to prevent damage or oxidation. Proper drying is essential to preserve the integrity of the microstructure before analysis.

2.6 Summary of chapter

This chapter provides a detailed analysis of the construction and operational principles of a steam turbine. The manufacturing techniques for steam turbine blades and the primary reasons for the failure of low-pressure steam turbine blades have been thoroughly examined and analysed. A comprehensive explanation of the procedure employed to determine the root cause of the turbine blade's failure has been provided. The techniques employed were fractography and metallography. The process of preparing a sample for metallographic investigations has been thoroughly detailed, covering all the necessary phases. These tools facilitate the identification of the primary reason for turbine blade failure, whether it is attributed to material flaws, maintenance issues, or environmental conditions within the turbine casing. This study will utilise an experimental technique to evaluate the causes of failure of a low-pressure stage steam turbine blade. Equipment, data, or supplies for this study was provided by AVIS LABORATORY, VADODARA, INDIA. The upcoming chapter will focus on the thorough analysis of low pressure seventh stage steam turbine blade failures, as well as the measures taken to address the reasons of these failures.

CHAPTER 3

INVESTIGATION OF FAILURE OF SEVENTH STAGE LOW PRESSURE STEAM TURBINE BLADE AND FRAMEWORK FOR LIFE ASSESSMENT

3.1 Introduction

This chapter focuses on the diverse causes of turbine blade failure. An in-depth analysis was conducted on a failed steam turbine blade, as a case study. Experimental examination of a failed blade is hailed as the primary contribution of this case study. The research encompasses visual examinations, dye penetration testing, study of material composition, hardness testing, tensile testing and microstructure analysis. The chapter provides a detailed examination of the experimental study done and presents various strategies for preventing failures.

Steam turbines are very significant and crucial components of thermal power plants, as they characterize the entire unit's lifetime and efficiency, and thus the entire power plant. As a result, steam turbine reliability is critical [66]. Steam turbine blades are a critical component and play a critical role in the turbine's reliability. If turbine blades fail, it will lead to more failures and significant financial losses. So, detailed research into the causes of turbine blade failure is critical in order to improve turbine system reliability [67] [68].

A major concern for power plant operators is the fatigue failure of steam turbine blades that can be caused by corrosion pits. This failure can lead to catastrophic damage. Blades at low pressure, where condensation forms early, are more likely to fatigue and fail in steam turbines due to pitting corrosion [27]. The low pressure (LP) turbine blades have a higher failure rate than high pressure (HP) and intermediate pressure (IP) turbine blades, according to statistics. Generally, LP blades are expected to last 30 years, although there are several incidents of blades failing prematurely in practice [69]. A low-pressure blade failure occurred prematurely at a 110 MW fossil fuel power plant. The fracture occurred at the profile region near the root, and the causes were investigated using various techniques. And it was found that Corrosion fatigue was the reason for failure. But there was no evidence of blade material deterioration [70]. Visual inspection, microstructure analysis, chemical analysis, microhardness, and tensile testing were used to investigate an untimely demise of steam turbine

rotor blades. The low-pressure side of the blade's lower trailing edge had erosion caused by foreign particles and water droplet erosion on the upper leading edge [71].

Erosion is a loss of material due to mechanical interaction between the surface and liquids or particles. The liquids/particles when accelerated in steam or process gas can impact components resulting in the removal of small amounts of material. Eventually pits and microcracks form at the surface. When cyclic stresses are present the pits and microcracks will create stress concentrations from which fatigue cracks can initiate. Erosion is particularly problematic for steam turbine blades. Steam turbines operate at higher temperatures and with a more closed gas path compared to centrifugal compressors. Solid particle erosion can occur on steam turbine blades due to the exfoliation of scales from piping during transient conditions. As the latter stages of a steam turbine increase in wetness the blades become susceptible to liquid droplet erosion [72].

Due to improper filler attachment, microcracks in the brazing metal and high cyclic fatigue were identified by fractographic observations as the main cause of the blade's failure in a 17th stage steam turbine blade. The fatigue crack was observed to have originated and extended next to the lacing hole, starting from the brazing interface connecting the rod and the blade [73]. This chapter discusses the experimental analysis and presents techniques to prevent failures.

The following section will outline the multiple causes of steam turbine blade failure, mainly in LP stage.

3.2 Major Reasons of turbine blade failure

There can be various mechanisms involved responsible for the failure of blades in a turbine. Numerous reasons contribute to the blade's eventual failure, including as wear and tear, creep, oxidation, erosion, corrosion, and surface deterioration brought on by hot operations [74]. Together with the resulting damage and common failure modes, these processes are listed in table 3.1. Regular inspection and assessment of the steam blading condition is crucial for the reliable and available operation of steam turbines. Neglecting to diagnose or address any of the failure mechanisms listed in table 3.1 might result in failure.

LP turbine blades are prone to premature failure, and corrosion, erosion, fatigue and their interactions are the principal causes [75]. Many researchers have done work in this area to find the root cause of failure of turbine components. They carried out the failure analysis in form of chemical composition, microstructural degradation and mechanical tests. A low-pressure steam turbine blade failed after 13,200 service hours because of environment-assisted fatigue fracture [67]. In a 210 MW plant, Corrosion fatigue initiated from pits was the reason

for blade‘s failure in LP steam turbine [76]. Foreign particle erosion-corrosion was the reason for fatigue failure of a steam turbine blade after 72,000 hours of working [77]. Damage to a steam turbine blade occurred after approximately 165,000 hours of operation. Fatigue was found to be the primary cause of failure, followed by erosion and the development of notches [78].

Table 3.1

Steam Turbine Blading Failure Mechanisms [79]

Sr. No.	**Failure Mechanism**	**Resultant Damage**	**Cause(s) of Failure**
1.	Corrosion	Extensive pitting of airfoils, shrouds, covers, blade root surfaces	Chemical attack from corrosive elements in the steam provided to the turbine
2.	Creep	Airfoils, shrouds, Covers permanently deformed	Deformed parts subjected to steam temperatures in excess of design limits
3.	Erosion-solid particle or liquid impingement	Thinning of airfoils, shrouds, covers, blade roots	1) Solid particle erosion from very fine debris and scale in the steam provided in the turbine 2) Water droplet erosion from steam which is transitioning from vapor to liquid phase in the flow path
4.	Fatigue– high cycle or low cycle	Cracks in airfoils, shrouds, covers, blade roots	1) Parts operated at a vibratory natural frequency 2) Loss of part dampening (cover, tie wire, etc.) 3) Exceeded part fatigue life design limit 4) Excited by water induction incident – water flashes to steam in the flow path
5.	Foreign/ Domestic Object Damage/ Mechanical Damage	Impact damage (dents, dings, etc.) to any part of the blading	Damage from large debris in steam supplied to the turbine (foreign) or damage from debris generated from an internal turbine failure (domestic) which causes downstream impact damage to components
6.	Stress Corrosion Cracking (SCC)	Cracks in highly stressed areas of the blading	Specialized type of cracking caused by the combined presence of corrosive elements and high stresses in highly loaded locations
7.	Thermal Fatigue	Cracks in airfoils, shrouds, covers, and blade roots	Parts subjected to rapidly changing temperature gradients where thick sections are subjected to high alternating tensile and compressive stresses during heat-ups and cooldowns or when a water induction incident occurs where the inducted cool water quenches hot parts

3.3 Case study investigating the cause of Low pressure seventh stage steam turbine blade failure

The challenging operating environment of steam turbine blades, characterized by high temperatures and fluctuating loads, frequently leads to their damage. For a steam turbine, the ability to identify the damage mechanism or reasons for turbine blade failure is critical. In most instances of blade failures, metallurgical analyses alone often fail to conclusively identify the underlying mechanisms. Therefore, in the current research, a mechanical analysis is conducted in tandem with the metallurgical analysis to provide a comprehensive understanding of blade failure. To assess the damage, non-destructive testing (NDT) is employed. This examination aims to qualitatively assess a rejected low-pressure stage blade of a 210 MW steam turbine after 152,241 hours of operation to pinpoint critical areas of damage and ascertain their causes. The examination includes visual inspection, chemical analysis, dye penetration testing, and metallurgical testing. Additionally, mechanical properties are assessed through hardness and tensile testing. The material of the examined blade is martensitic stainless steel X20Cr13. Toughness, excellent corrosion resistance and high strength are the essential qualities of martensitic stainless steels. This study contains a thorough investigation to see if it was a material issue or some other reason behind the failure. The investigation uncovered that blade failure was expedited by water droplet erosion, particularly targeting the edges of the blades. These erosion pits, functioning as stress concentrators, have the potential to initiate crack propagation if left unaddressed, posing a risk of catastrophic system failure. Therefore, conducting this type of failure analysis is strongly recommended to enhance reliability and prevent such failures in the future.

The detailed experimental procedure is outlined in next subsection.

3.3.1 Experimental procedure

This work presents an experimental case study of a low-pressure stage blade after 379 start-ups of the power plant. Generally, the blades are recommended to check after 100000 hours of operation. This blade has completed over 100000 hours of operation. This LP blade has been in use for more than 1,52,241 hours, according to the information available. Since commissioning, there have been an estimated total of 379 turbine starts till dec. 2017. The details are as follows:

No. of Cold starts: 56, No. of Warm starts: 205, No. of Hot starts: 118

Total No. of starts: 379

During inspection after 1,52,241 hours service, dent marks and pits are observed on the surface of the LP stage-7 blade. In order to assess the material's state of health and the dominant damage mechanism to decide on its further operation, detailed analysis results, such as visual examination, chemical analysis, dye penetration testing, metallographic study and mechanical testing, are presented. A pictorial view of the studied blade is shown in Figure 3.1.

Figure 3.1. Pictorial view of a steam turbine blade

Pits observed on the blade are due to erosion caused by water droplets. The steam received from the (high-pressure) HP turbine is low-quality steam, and further, the steam continuously expands in low-pressure turbine. So, when condensed water is sprayed against the blades, they can be quickly impinged and eroded by the high volume of water droplets [80]. Droplet impact erosion results in blade material loss, making a significant change to the aerodynamically optimal blade geometry and causing a significant flow disruption. This negatively impacts the machine's performance, eventually necessitating turbine blade replacement [81].

The thinnest region of the aerofoil are the trailing edges, where material removal could modify the stress level. Erosion damage caused by water droplets at high-speed swirling from tip to the base of the aerofoil scarring the trailing edge may form macroscopic notches and ‘worm holes’ at the base of these scars. These notches act as stress concentrators, and in a high stress region become detrimental to integrity of blade. If unattended, the notches act as crack initiators developing into propagating cracks. In combination with dynamic stresses this could quickly develop to a blade failure. So, this type of failure analysis plays a very important role in improving the reliability of turbine systems and also prevents such failure incidents in future. Damage to steam turbine blades can occur at any step of the design, production, or operation. To avoid a major accident and significant economic losses, it is necessary to inspect the blades periodically during planned outages and repair or replace damaged or deformed blades as soon as they are found to be faulty [64]. Non-destructive evaluation (NDE) is becoming increasingly important in assuring pre-service quality and monitoring in-service degradation to avoid

premature component or structure failure. After visual inspection, Dye Penetration Testing (DPT) was carried out on Steam Turbine Blade according to ASTM E165 [82] to find out the presence of any defect or any crack-like defect over the surface and subsurface. The chemical analysis was carried out on LP blade by Spectro analysis according to ASTM E-A448M [83] to determine the chemical composition of the blade material. Metallurgical testing was performed for microstructural study on LP blade by polishing and chemical etching. The grain size was measured after surface preparation and etching with Kalling II solution as per ASM handbook for metallography and microstructure [84]. Mechanical tests such as hardness, tensile strength, and proof stress were performed on tube samples. The sample was tested in accordance with ASTM-370 [85]. All the tests for present analysis were performed at AVIS (Aequitas Veritas Industrial Services) laboratory in Vadodara, Gujrat.

3.3.2 Visual examination

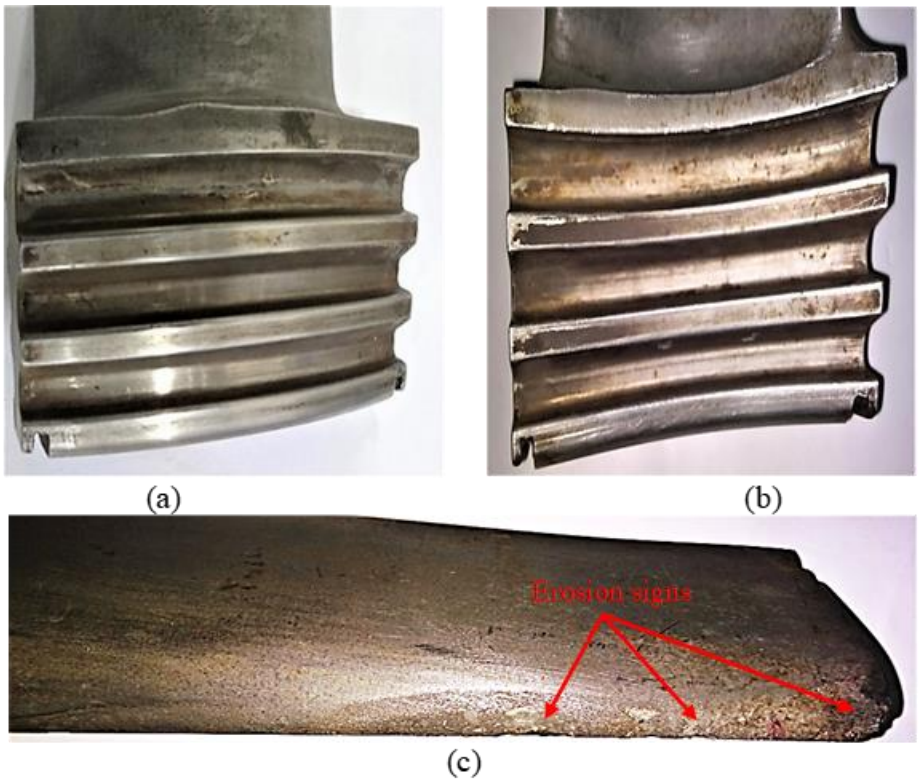

Figure 3.2. Blade root (a) back (b) front view with some dent marks (c) Erosion signs on blade's edges

A visual assessment was carried out to look for any markings or pitting on the blade surface that would indicate erosion or mechanical failure. Some dents marks were observed on the profile and root of the blade. According to visual checks, the erosion pits occurred on the

edges of the turbine blade, which can increase the stress concentration. However, significant erosion damage was discovered on Blade's edge parts, which is shown in Figure 3.2. On the surface, there was no sign of a crack or any other fault.

3.3.3 Dye penetration test (DPT)

In dye penetration testing, the developer either bleeds penetrant out from defects onto the surface, resulting in a visible signal known as bleed-out, or pulls dye penetrant-containing flaws back to the surface, resulting in a red mark on a white backdrop, as shown in Figure 3.3. Any bleed-out area on the surface can reveal the location, orientation, and type of faults present.

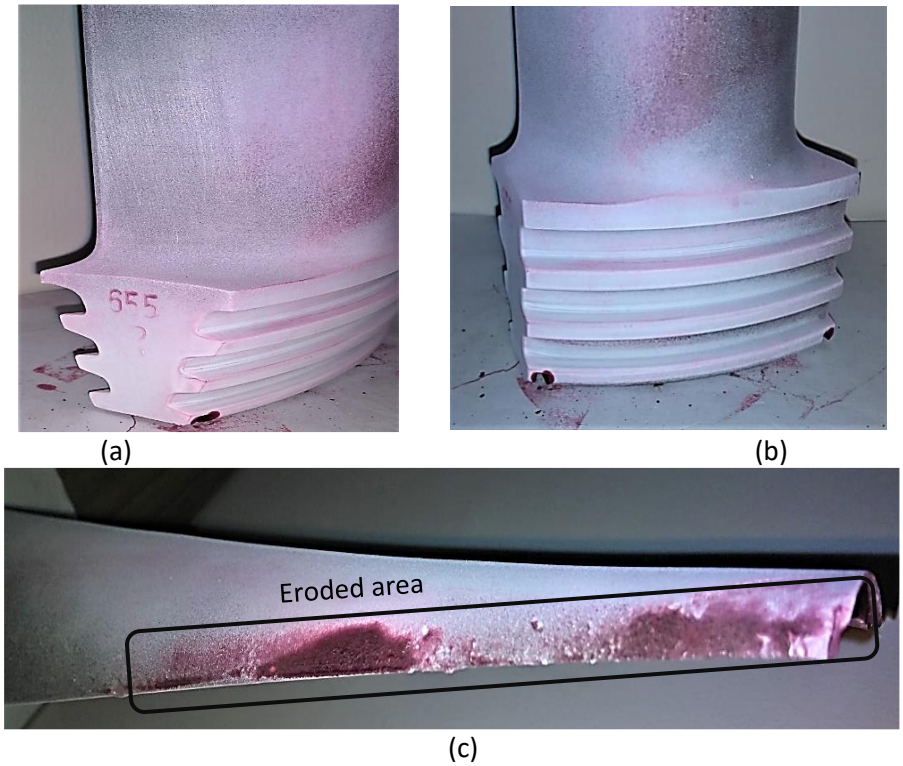

Figure 3.3 Blade root (a) side view (b) front view with no sign of a crack
(c) Erosion pits on blade’s trailing edge

It can be seen that there is no defect or crack found on the blade root and only erosion pits were present on the edges of the blade. The erosion pits are formed due to striking of fine moist droplets formed by condensation of steam. Because of the loss of aerodynamic efficiency caused by leading-edge erosion, annual energy production drops dramatically [86]. Table 3.2 shows the detailed results of dye penetration testing.

Table 3.2

Dye penetration test results

Details of parts	Qty./No. tested	Finding
Steam turbine blade-front	1 no.	No defect/crack was observed on the surface.
Steam turbine blade-back	1 no.	No defect/crack was observed on the surface.
Steam turbine blade-LHS	1 no.	No defect/crack was observed except erosion on edges.
Steam turbine blade-RHS	1 no.	No defect/crack was observed except erosion on edges.
Remarks: No crack observed except pitting damage corrosion.		

3.3.4 Chemical analysis

The chemical composition of the blade material was found to be as shown in table 3.3. And it was found to be consistent with AISI 420 grade martensitic stainless steel.

Table 3.3

Chemical Analysis Results

Element	C	Cr	Si	Mn	P	S	Ni
Observed value in %	0.20	13.3	0.43	0.62	0.029	0.019	0.58
Standard AISI 420	0.17-0.22	12.50-14.0	0.10-0.60	0.30-0.80	≤0.03	≤0.02	0.30-0.80

Values are quoted in wt%

3.3.5 Metallurgical testing

The damaged blade was also subjected to microstructural examinations. Standard metallographic sample preparation was followed by optical microscopy for this objective. Microstructures show uniform and homogeneous structures in the matrix. The hardened and tempered martensitic structure can be seen in the micrographs. Figure 3.4 shows the microstructure of the blade consisting of tempered martensitic and delta ferrite phases in the matrix.

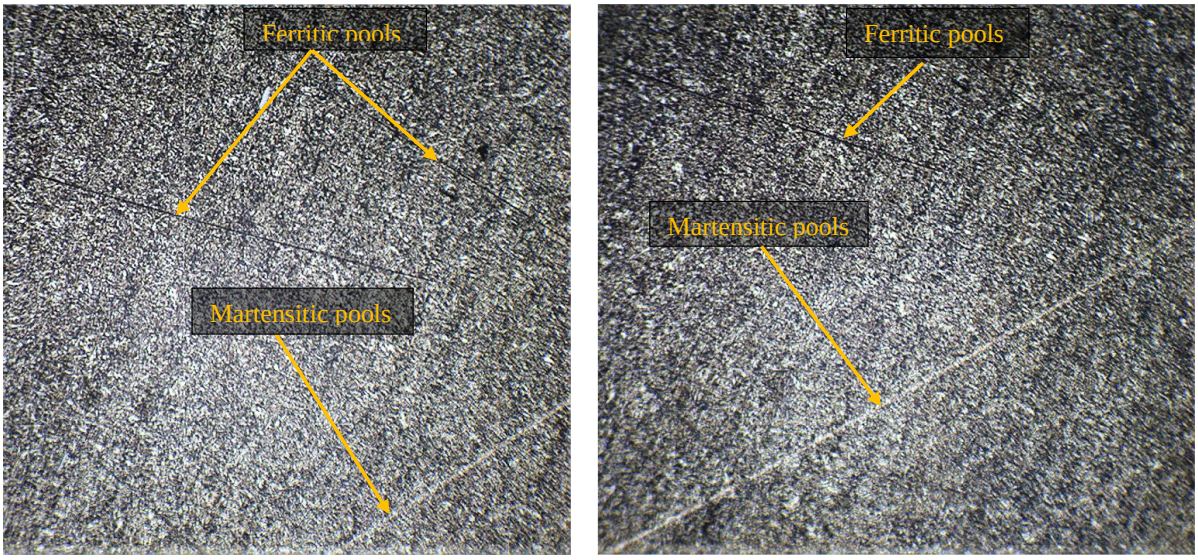

Figure 3.4 Tempered martensite and ferritic pools can be seen in the microstructure (100x).

Figure 3.5 illustrates the microstructures of the sample containing Very fine tempered martensite and ferritic pools areas in the matrix.

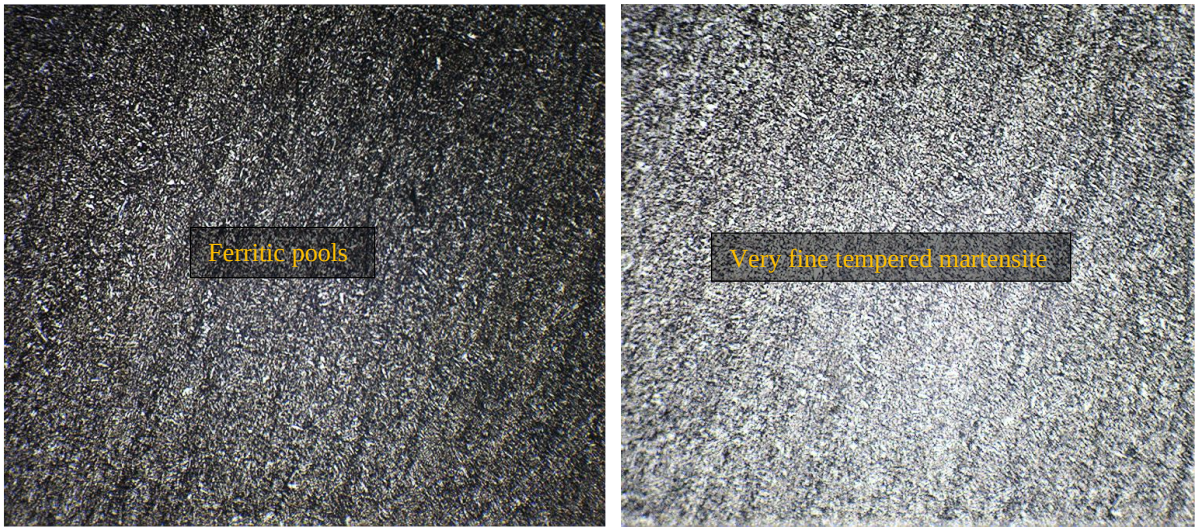

Figure 3.5 Optical micrographs at 100x of the root of damaged blade showing Very fine tempered martensite and ferritic pools.

Optical micrographs of blade root and airfoil region clearly demonstrate uniformly distributed hardened and tempered martensite. There was no indication of microstructural degradation in the airfoil and root regions of the damaged blade, which is in compliance with the X20Cr13 specification (AISI 420).

The eroded portion is further studied to know the changes in microstructure of blade due to erosion pits and the microstructure shows bainitic structure and retained austenite as shown in Figure 3.6. Delta ferritic pools has also been observed on the top eroded portion of blade. The bright white phase shows the presence of ferritic pools in microstructure shown in

Figure 3.7. The grain boundary carbides were also observed as shown in Figure 3.8 was also observed. These grain boundaries will provide a path to crack propagation resulting in a faster rate of failure.

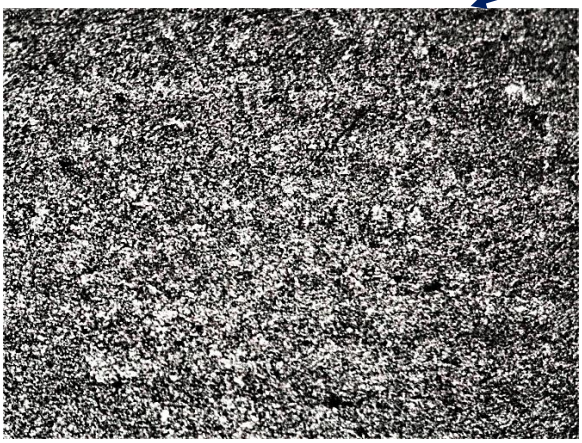

Figure 3.6 Microstructure shows bainitic and structure retained austenite (40x)

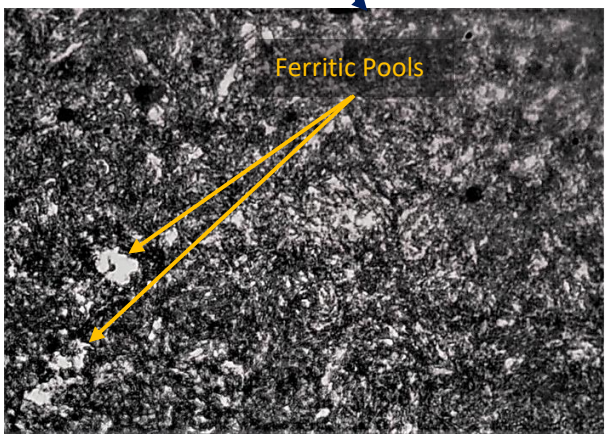

Figure 3.7 Microstructure shows delta ferrite pool (100x)

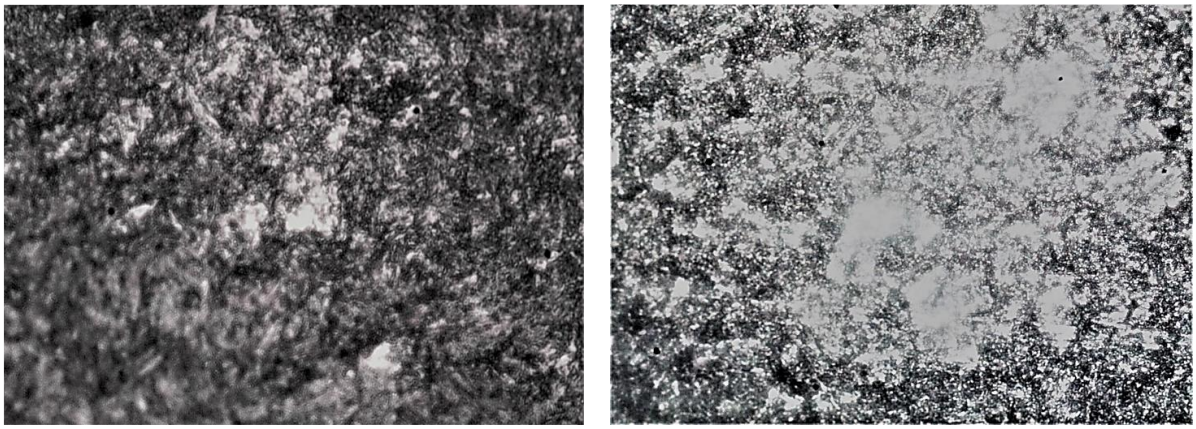

(a) (b)

Figure 3.8 Microstructure showing grain boundary carbides (a) 200x (b) 400x

For the analysis of failure behaviour of the material surfaces, It was necessary to ascertain the grain sizes of the blades under consideration; hence grain size was measured after surface preparation and etching with Kalling II solution, as per the ASM handbook for metallography and microstructure [87]. Though grain boundaries are not identified in this

structure, the grain size of this blade material was measured to be grain size number-10 as per ASTM, as shown in Figure 3.9.

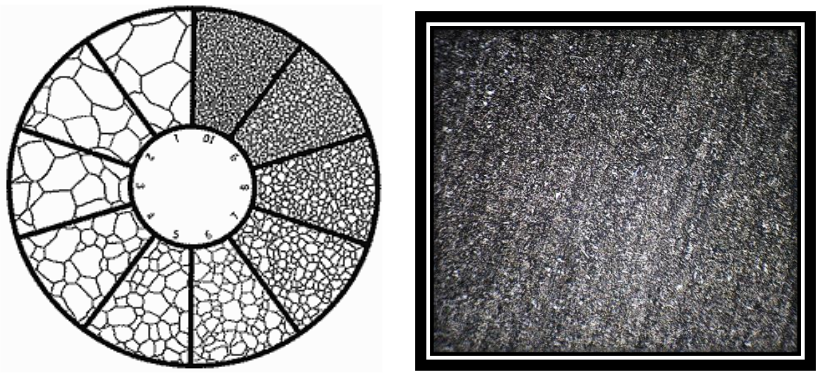

ASTM Grain Size No. Blade Grain Size Measured- 10

Figure 3.9 Grain size in accordance with ASTM

3.3.6 Mechanical testing

To determine the change in material properties, the mechanical properties of the fractured blade were also investigated by measuring the material's hardness and subjecting the material specimen to a tensile test.

3.3.6.1 Hardness testing

The hardness test was carried out on a tube sample. Brinell hardness measurements were performed on blade materials using a universal hardness tester shown in Figure 3.10(a). The hardness values of the blade are found to be in the standard range, indicating that they had been properly tempered. Table 3.4 shows the observed values for hardness at different positions of turbine blade profile and root shown in Figure 3.10(b). Figure 3.11 shows a comparison of hardness at different locations of LP blade with the standard hardness required for LP turbine blade.

(a) (b)

Figure. 3.10 (a) Hardness testing machine (b) blade profile and root hardness locations

Table 3.4.

Hardness Testing results

Sr. No.	Steam Turbine Blade (BHN)		
	Blade Root –Front Side	**Blade Root – Back Side**	**Blade Profile**
1	258	260	261
2	269	257	255
3	250	264	265
4	237	268	252
5	261	258	258
6	262	260	260

The average hardness value for blade root front side, blade root back side and blade profile are 256, 259 and 261 respectively.

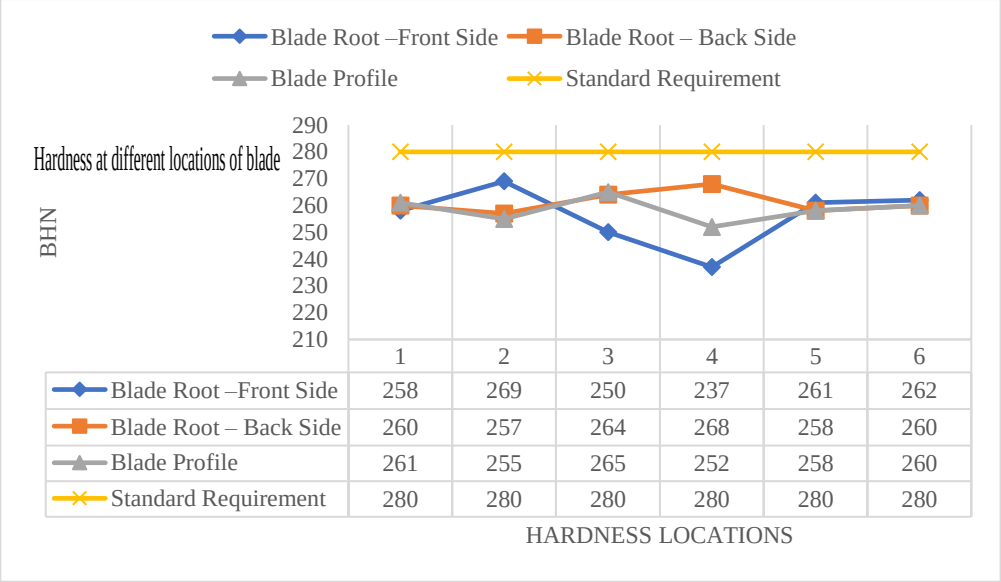

Figure 3.11 Hardness at different locations of blade.

The hardness results were compared with standard requirements, i.e., 280 BHN, and the obtained values are a little lower. So, we can say that no appreciable decrease in hardness or creep initiation was observed in blade root and blade profile areas.

But it was observed that the value of hardness dropped significantly from 500 BHN to 261 BHN near the tip of turbine blade (approx. 200 mm. from the tip) where the hardness was increased initially by flame hardening. The hardening was done to improve the erosion resistance of the blade tip where pitting occurs due to moisture content of steam.

Flame Hardening: Flame hardening is used to give the blades more durability against this erosion. An improper application of this procedure can make the blade material, X20Cr13, more vulnerable to stress corrosion cracking. Stress corrosion cracking requires the presence of sufficiently high tensile stresses. The amount of total surface stress at the flame-hardened leading edge of the blade is mostly influenced by the residual stresses that remain after the process. Stress corrosion cracking is to be expected after a given amount of time in service if there are high tensile residual stresses. So, it is very important to estimate the residual stresses to prevent structural failure in industrial turbines. For improved resistance to water droplet erosion, Siemens invented x-ray diffraction residual stress control of the flame hardened edge in the 1980s. The XRD method measures strain by utilizing the d-spacing between crystallographic planes. The d-spacing of a material will change depending on the direction of stress: it will widen when the material is under tension and narrow when it is under compression. A change in the angular position of the XRD peak caused by the presence of residual stresses can be directly detected by the instrument. Using X-ray or micromagnetic

testing tools, the crucial residual surface stresses can be precisely identified [88]–[93]. Pineault *et al.* discussed how XRD can be used to characterize residual stresses in a component or assembly in order to prevent, minimize, or get rid of the impact of residual stress to premature failures, and then evaluate corrective measures that alter the residual-stress condition of a component [92]. Later on, magnetic Barkhausen noise residual stress measurement supplanted the X-ray method. Using a noise-like signal produced by applying a magnetic field to a ferromagnetic sample, the Barkhausen noise analysis method measures residual stress. Domains, collections of magnetic dipoles that can be thought of as little magnets, are found in ferromagnetic materials. Heinrich Barkhausen originally noticed that domain walls move back and forth under alternating magnetic fields in 1919 [94].

3.3.6.2 Tensile testing

The tensile test was performed on the steam turbine blade specimen with specification detailed in table 3.5.

Table 3.5.

Tensile Testing specimen and loading details

Diameter (mm)	Area (mm^2)	Initial Gauge Length (mm)	Yield Load (kN)	Tensile load (kN)	Final Gauge Length (mm)
12.54	123.44	50.0	83.94	108.38	59.0

Table 3.6 summarizes the important tensile property data obtained by tensile testing of the specimens prepared from blade material. It can be argued that the blade did not significantly lose strength values while it was in use, disproving the idea that a decline in mechanical qualities caused the blade to fail. It can be seen from the table that X20Cr13 of the rejected blade material qualifies the requirement of mechanical properties.

Table 3.6

Tensile Testing results

Sr No.	Details	Yield Strength (MPa)	Elongation %	Tensile Strength (MPa)
1.	Required	≥ 600 MPa	≥ 15 Min.	800-950
2.	Obtained	680	18	878

Summarizing the test results, it can be seen that all of the determined parameters, like chemical composition, tensile strength, hardness and yield strength, meet the standard requirements for the given material.

3.4 Comments on the Failure Analysis of Seventh Stage Low Pressure Steam Turbine Blade

- Damage mechanisms affecting components within complex machines are typically difficult to detect and diagnose, especially if they are difficult to reach, examine, and are in constant use, jeopardizing system reliability and performance.
- The blades shall be free from faults due to forging, cracks, tearing, material defects, elongated non-metallic inclusions, seams etc. Any blade containing such defects shall be rejected for further use.
- The failed blade's material was discovered to have the same chemical composition and hardness as standard martensitic stainless-steel grade AISI 420. There was no sign of microstructural deterioration. As a result, the blade material is found to be in compliance with the standard specifications, indicating that material is not a factor in this failure.
- Distribution and pattern of erosion pits on the edges of final stage low pressure blade in steam turbine shows that quenching cannot eliminate the erosion of surface completely.
- Erosion scars and pits seen on blade surface can lead to crack initiation and growth due to stress concentration.
- Modern turbine blade's last two low pressure (LP) stages are expected to operate in a wet steam medium in steam turbines. Condensation during steam expansion typically produces fine mist droplets which causes water droplet erosion damage to blade.
- This study analyzed stainless steel ex-service steam turbine blade. (Water droplet erosion) WDE on different portions of the blade was identified.
- No crack or any other defect like appearance was noticed on the surface in visual inspection of a turbine blade. However, considerable erosion damage was observed on edge sections of the blade.
- It was determined that the blade material was not faulty based on chemical analysis and mechanical testing.
- The turbine blade under inquiry did not fail due to a material flaw, according to the dye penetration testing and microstructure study.
- The defective sections were carefully analyzed in order to determine the causes of failure, and it was found that water droplet erosion was the cause of blade damage. Identifying the deteriorating mode in advance allows us to replace and repair turbine

parts at the best possible moment, reducing the need for unneeded replacement and preventing unscheduled outages.

- The airfoil's edges are scarred by water droplets can be a reason of microscopic notches generation on the surface [78]. As stress concentrators, these notches compromise the integrity of the blade at areas of high stress. If left ignored, the notches serve as crack initiators that eventually lead to spreading cracks. This could soon progress to a blade failure if combined with dynamic loads. Each of the facets of a failure inquiry contributes to figuring out what went wrong and how to prevent such incidents in the future. Failure analysis is thus crucial for enhancing turbine system reliability and avoiding similar failure incidences.

3.5 Corrective measures to counter Water droplet erosion

Water droplet erosion is a significant concern for low-pressure steam turbine blades, particularly in areas where condensed water droplets impinge on the blade surfaces. Preventive measures to mitigate water droplet erosion in low-pressure steam turbine blades include:

a) **Surface Coatings**

Apply erosion-resistant coatings to the blade surfaces to protect against water droplet impingement. These coatings can include thermal spray coatings, such as chromium carbide or tungsten carbide, which offer high hardness and wear resistance.

b) **Surface Roughness Optimization**

Optimize the surface roughness of the blade to minimize the impact of water droplets. Smoother surfaces can reduce the likelihood of droplet impingement and erosion. However, a certain level of surface roughness may be necessary to promote boundary layer stability and prevent laminar separation.

c) **Improved Blade Design**

Design turbine blades with features to minimize water droplet impingement, such as aerodynamic shaping and deflectors to redirect droplets away from critical surfaces. Incorporating surface contours and features that promote droplet shedding can also help reduce erosion.

d) **Operating Conditions Optimization**

Optimize turbine operating conditions, such as steam quality and flow velocity, to minimize the formation of water droplets and their impact on blade surfaces. Adjustments to steam parameters can help mitigate conditions conducive to water droplet erosion.

e) **Steam Quality Improvement**

Improve steam quality by reducing moisture content and entrained water droplets in the steam flow. Proper steam conditioning and separation systems can help remove excess moisture before it reaches the turbine blades, reducing the risk of erosion.

f) **Water Management Systems**

Implement effective water management systems to control the distribution and flow of condensed water within the turbine system. Proper drainage and collection systems can prevent the accumulation of water on blade surfaces and minimize erosion.

g) **Regular Inspection and Maintenance**

Implement regular inspection and maintenance programs to monitor blade condition and detect signs of erosion or damage early. Periodic cleaning of blade surfaces and removal of accumulated deposits can help prevent erosion and maintain blade integrity.

h) **Material Selection**

Select erosion-resistant materials for turbine blade construction, such as high-strength alloys with enhanced corrosion and erosion resistance. Proper material selection can minimize the susceptibility of blades to water droplet erosion.

3.6 Summary of the chapter

In order to address a blading issue, the current research involves doing a mechanical analysis alongside a metallurgical analysis to thoroughly analyse the failure of the blades. In order to assess the extent of the damage, non-destructive testing (NDT) was conducted. The objective of this investigation is to conduct a qualitative analysis of the blade of a 210 MW low pressure steam turbine after 1,52,241 hours of operation in order to identify the specific areas of damage and determine the underlying cause. This evaluation encompasses visual inspection, chemical analysis, dye penetration testing, and metallurgical testing. Furthermore, the mechanical properties were assessed through the utilisation of hardness and tensile testing. The blade under examination is composed of martensitic stainless steel X20Cr13. Martensitic stainless steels possess crucial characteristics such as toughness, exceptional resistance to corrosion, and high strength. This study conducts a comprehensive examination to determine whether the failure was caused by a material issue or some other factor. The results indicated that the erosion caused by water droplets led to an increased rate of blade failure, with a particular focus on the edges of the blade. The erosion pits function as areas of concentrated stress and have the ability

to propagate cracks if not addressed, can lead to catastrophic failure. Therefore, in order to enhance reliability and prevent such failures from occurring again, it is strongly advised to conduct this type of failure analysis.

The next chapter will discuss the metallographic analysis of erosion products formed on Low Pressure Steam Turbine Blade.

CHAPTER 4

METALLOGRAPHIC ANALYSIS OF EROSION PRODUCTS FORMED ON SEVENTH STAGE LOW PRESSURE STEAM TURBINE BLADE

4.1 Introduction

The typical lifespan of the LP blades in a steam turbine assembly is 30 years, however in fact, several occurrences of early blade failure are seen. A study found that the reasons for around 40% of the failures were unknown [95]. Failure rates can be lowered by giving careful attention to all the factors that affect the effectiveness of the blade. For this reason, familiarity with the metallurgy material of the blade material, operating pressures, and operating environment is essential [69].

Mohd Sarim Khan *et al.* [96] analysed the microstructure of the material to determine the mechanisms of crack initiation and propagation. It was discovered that chromium carbide becomes oxidised to chromium oxide in certain spots. Steam erosion of these chromium oxides leaves a porous area. The results showed that water droplet erosion can accelerate fatigue crack growth in X20Cr13 and that the microstructure of the material plays a critical role in determining its resistance to erosion-induced fatigue failure. Xiaotong Guo *et al.* [97] studied the microstructure of the failed gas turbine blade in detail and compared it to that of thermally stressed samples. According to the findings, the majority of the blade components had been functioning normally before the failure. Unfortunately, there was severe overheating at the airfoil tip of the leading edge, and the temperature was about 200 °C higher than the typical service temperature. Due to the high temperatures, the substrate began to melt and the blade was damaged. The service temperature affects the microstructural development of grain boundaries, and carbides. Bhagi *et al.* [76] investigated the fracture of a low-pressure (LP) steam turbine blade of a 110 MW thermal power plant in Punjab, India. SEM fractography and micro-structural characterization were part of their investigation in order to determine the origin of the fracture. There was evidence of silicate and sodium oxides on the fracture surface. This is the root cause of the corrosion pitting that ultimately leads to corrosion fatigue. Because of a crack in the vane of the fourth stage blade in the low-pressure turbine, the investigation was carried out by Hyojin Kim [98] to determine its origin and progression. The blade

microstructure and EDS examination revealed corrosion pits near the leading edge which acts as crack initiator. Goutam Das *et al.* [99] presented the case of an LP (low-pressure) turbine blade failure. Phases rich in silicon were found all around the surface of the blade in fractography. Chloride was identified in several pits or grooves on the edges of the blade. These were the cause of the crevice corrosion. Ca and K, both of which were discovered on the blade, were likely to be the carriers of Cl. It was an intergranular form of failure. It is possible that corrosion fatigue played a role in the final breakdown. Ananda Rao *et al.* [100] discussed the failure of a turbine blade of a 60 MW thermal power plant. The creation of cracks of substantial size was facilitated by the presence of corrosive species like chlorine in the form of chlorides, which allowed localised corrosion assault in the form of pits. The mode of failure of the turbine blade is corrosion fatigue. It was confirmed by fractographic investigation that distinctive failure features such as beach marks and pits were present as well as the deposition of deposits containing substantial levels of chloride and silica. The tempering temperature affects the hardness and microstructure of the 13Cr martensitic stainless steels. The hardness can be increased by raising the tempering temperature to a maximum of 500°C. The resulting microstructure is tempered martensite rich in M23C6 carbides. Hardness can also be increased by the presence of carbides [101][102]. Many other turbine blade failures were also reported and fractographic investigation was an important tool used to find the reason behind every failure [103]–[109]. Low-pressure turbine failure has been reported to be more common than failure of intermediate- and high-pressure turbines [36], [75], [116]–[122], [98], [110], [111], [111]–[115].

Proper maintenance, effective functioning, and frequent repairs cost millions over the lifetime of each steam turbine. Blade failures, ranging from premature cracking to the in-service catastrophic breakdown of the components, pose the biggest risk to the scheduled maintenance and reliable operation of these massive pieces of equipment. Sister units using the same blade need an accurate and prompt diagnosis of the problem in order to deal with it in the short term and plan for the future [123]. Insight into the long-term behaviour of ruptures can be gained through fractography, which discloses the precise modes of failure and, by extension, the origin or source of the defect. It also facilitates comprehension of which sort of microstructural imperfection is most severe and promotes understanding [62], [124]. The earlier investigations outlined a range of possible failure causes, including overheating at the blade leading edge, local melting, influence of alloy microstructure, and corrosion-related mechanisms like corrosion fatigue, pitting, and crevice corrosion. Different operating conditions, such as temperature levels, were explored in earlier studies to elucidate their impact on failure modes.

Electrical utilities typically utilize various characterization methods, such as metallography, SEM/EDS analysis, X-ray diffraction, and finite element analysis, to understand the failure mechanisms, identify root causes, and develop mitigation strategies.

The blade studied here was manufactured from X20Cr13, a martensitic stainless steel, which has a tensile strength of 878 MPa, a yield strength of 680 MPa, and an 18% elongation after being quench hardened and tempered. This final-stage blade has been in operation for 152241 hours. The turbine has been started up 379 times, which includes 118 hot starts, 205 warm starts, and 56 cold starts. So, fractography was performed with a SEM (Scanning Electron Microscope) to determine the failure mode. Metallographic examinations including inclusion rating were also conducted to determine the micro-constituents that can be responsible for the crack initiation, and EDX (Energy Dispersive X-Ray) to analyse the micro-chemical composition of the possible areas where the crack first is likely to have appeared. Because of a drop in pressure on the exhaust side of the steam turbine, condensation formed, and water droplets impinging on the blades caused severe erosion. Condensed water droplets react with chromium carbide in the martensitic matrix to form chrome oxides, and high-velocity steam impinging on these oxides erodes them, creating a rough surface. The roughened blade surfaces can contribute to the development of fatigue cracks at potentially weaker locations and, ultimately, to the final fracture. It necessitates the SEM and EDAX analysis of turbine blades in order to avoid such fractures in the future by studying the mechanism behind such failures.

4.2 Experimental Details

Metallographic analysis serves as a valuable method for identifying metals and alloys, assessing the proper processing of alloys, examining various phases within a material, detecting and characterising imperfections like voids or impurities, and investigating areas of damage or degradation in failure analysis. Microscopy is the most commonly employed method in such examinations. Both optical microscopy and scanning electron microscopy (SEM) equipped with an X-ray energy dispersive spectrometer (EDS) can be valuable tools for metallographic examination.

A failed blade from the L-7 row of the LP stage was taken from the unit in order to determine the root of the problem. The operating temperature of this stage of turbine was about 102.4°C. Erosion pits are observed, on the edges (as shown in Fig. 4.1). Elemental composition was determined using energy dispersive X-ray analysis of fracture surfaces (EDAX). Microscopical specimens were prepared by cutting and polishing blades according to normal metallographic procedures and by etching them. The microstructure and fracture surface

morphology of a steam turbine blade were analysed using an optical microscope and a scanning electron microscope (SEM). SEM and EDX are valuable tools for investigating eroded steam turbine blades. By providing detailed information about the nature and extent of the erosion, as well as the elemental composition of the surface, these techniques can help to identify the underlying causes of the erosion and inform strategies for preventing or mitigating further damage.

A sample is mounted for polishing the mirror surface and etching for microstructure evaluation and one sample is cut for SEM and EDX analysis as shown in figure 4.1.

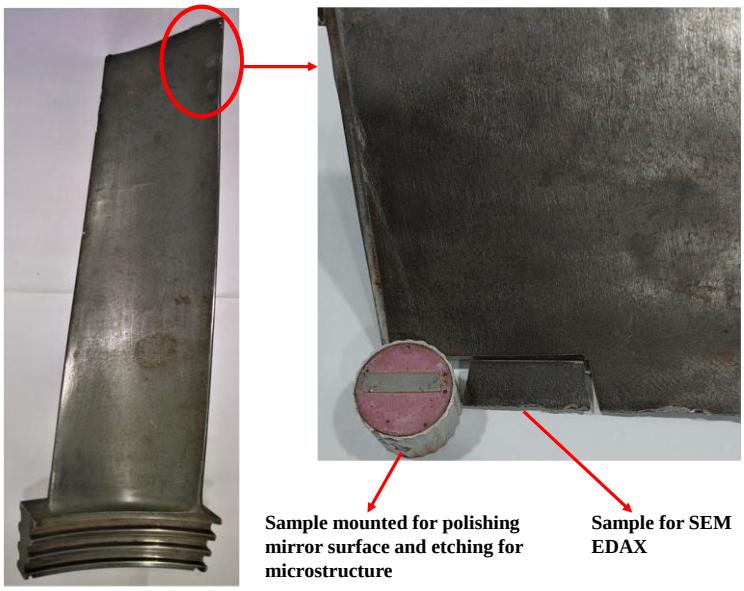

Figure 4.1 General view of the examined section of the blade

4.3 Metallographic Analysis

Erosion was detected on the leading edge of the seventh-stage blade, as discussed by non-destructive testing in previous chapter. The reason and mechanism of the blade rejection were investigated by analysing its material composition, measuring its hardness, and examining its microstructure [125]. Many fractographic characteristics, such as fatigue striations, intergranular cracking, micro void coalescence, trans-granular cleavage, and secondary cracking, can be recognised by SEM [62]. So, the blade has been further examined by undergoing fractographic analysis.

The steam turbine blade undergoes a thorough inspection for surface damage as discussed in chapter 3. Visual inspections revealed [125] that the erosion pits were located along the turbine blade's edges, where they could potentially enhance the concentration of stress. However, as illustrated in Figure 4.2, severe erosion damage was found on the edge of the blade. No crack or other flaw was visible from the outside as discussed in chapter 3.

Figure 4.2. The edge of the turbine blade shows several pits/grooves

4.3.1 Microstructure

After visual inspection, the microstructure of the failing blade was studied in detail and compared to that of the original samples. Figure 4.3 shows a micrograph of a polished metallographic specimen cut from the blade airfoil region, illustrating a homogeneous microstructure composed of hardened and tempered martensitic grains. The airfoil of the failing blade showed no signs of microstructural degradation and was in line with the X20Cr13 specification (AISI 420).

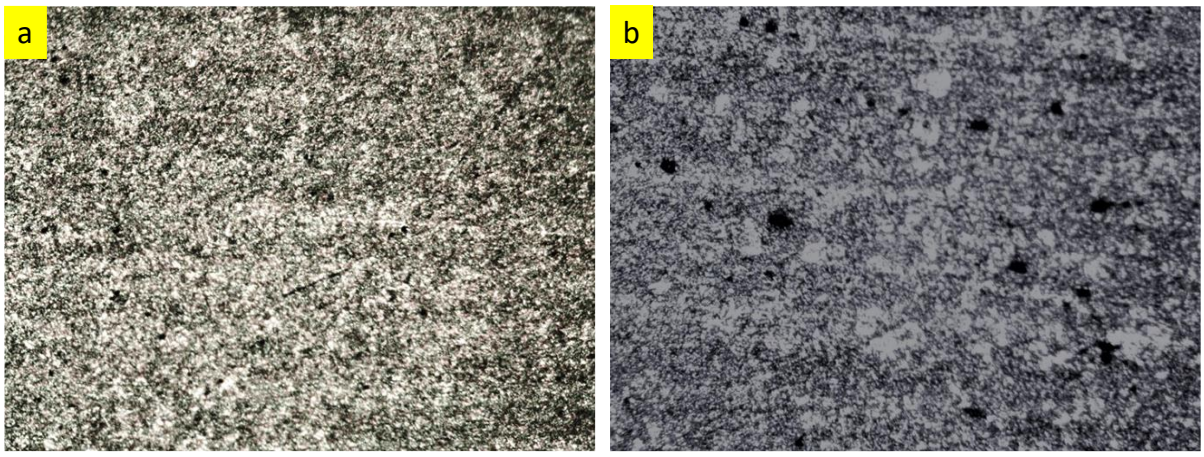

Figure 4.3. Microstructure (100X) shows a) bainitic structure and retained austenite. b) Delta ferrite pool (Bright white phase) and grain boundary carbide are also observed.

The presence and distribution of delta ferrite pools can affect the mechanical and corrosion properties of austenitic stainless steels. The formation of delta ferrite can improve the hot workability and ductility of the material but can also reduce its resistance to corrosion and intergranular cracking. The size of grain boundary carbides can vary from a few nanometres to several microns, depending on the type and amount of carbide-forming elements in the material.

Grain boundary carbides are important microstructural features that can significantly influence the mechanical properties of a material, including its strength, toughness, and resistance to wear and fatigue. Proper control and optimization of grain boundary carbides is essential for ensuring the desired mechanical performance of the material in specific applications.

4.3.2 Scanning electron microscopy (SEM) & Energy-dispersive X-ray (EDAX) analysis

An essential piece of equipment for fractographic research is the scanning electron microscope (SEM). The topographical features of fracture surfaces can only be seen using SEM due to its superior resolution and depth of field compared to optical microscopes [62]. Further SEM analysis was performed to investigate the failure mode of the blade more precisely. The purpose of this study is to identify the process through which the material was lost. Scanning electron microscopy (SEM) with an energy-dispersive X-ray analysis (EDAX) was used to evaluate the eroded surface of the blade in order to trace its origin. The eroded section was sliced from the blade for fractography analysis. Figure 4.4 is an overall view of the eroded surface of the blade. In order to analyse, the eroded surface has been divided into six distinct sections labelled "1", "2", "3", "4", "5" and "6".

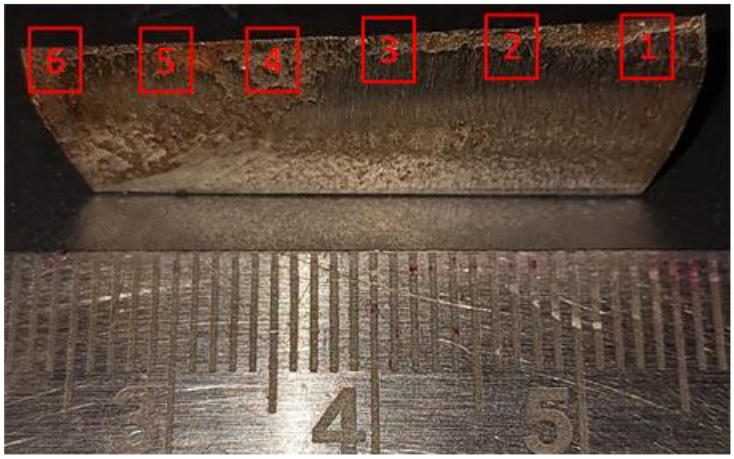

Figure 4.4 General view of the sample cut for SEM analysis from eroded surface of the blade.

4.3.2.1 SEM Analysis

When a steam turbine blade becomes eroded, it can be due to a variety of factors such as erosion from steam flow, particle impingement, or corrosion. By examining the surface of the eroded blade using SEM, one can determine the nature and extent of the erosion, such as the size and shape of the pits and cracks, and whether they are due to mechanical wear or chemical corrosion. A large number of pits are observed around the edge of the turbine blade, as shown

in SEM figures 4.55(a-b), 4.6(a-b), and 4.7(a-b). Moreover, in enlarged SEM images, white phases could be recognised, which shows the presence of foreign particles in erosion pits.

Fatigue striations are characteristic features that appear on the surface of a material that has undergone fatigue failure as shown in figure 4.5(a). These striations form perpendicular to the direction of the applied stress and are caused by the repeated loading and unloading of the material. Beach marks and ratchet marks are also visible. In SEM fractographs, erosion pits appear as circular depressions or craters on the surface of the material. Foreign particles shown in figure 4.5(b) are present at the edge of pits indicating that they were responsible for the erosion.

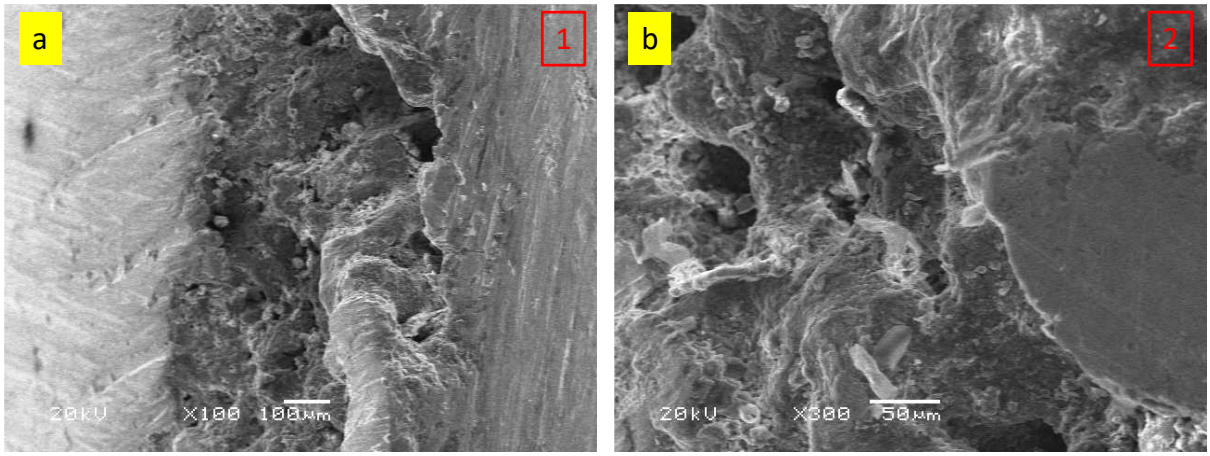

Figure 4.5 SEM fractographs of the eroded surface showing a) characteristic fatigue striations b) erosion pits with foreign particles at fractured edges.

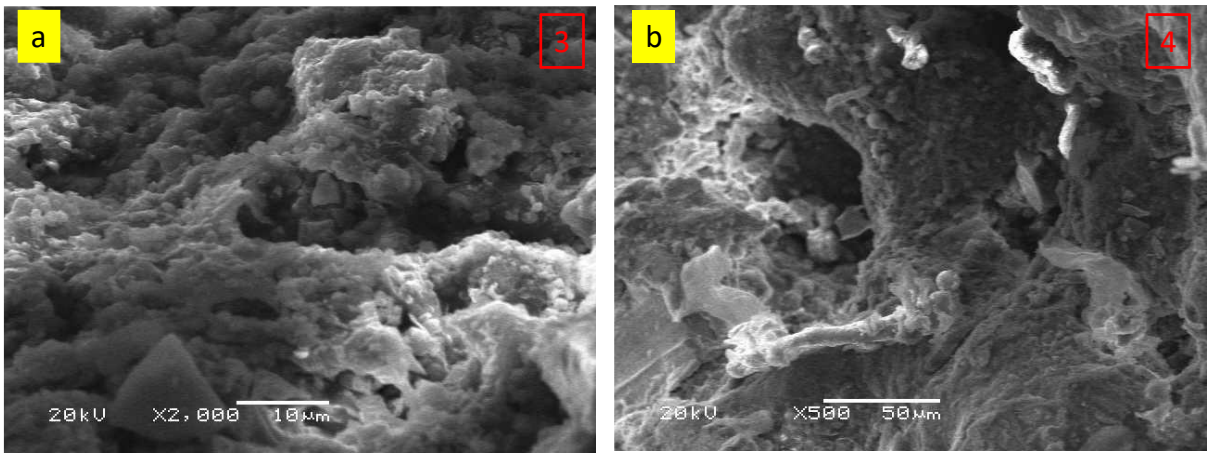

Figure 4.6 Fractographs showing a) micro void coalescence b) the presence of foreign particles in erosion pits.

Micro voids (shown in figure 4.6(a)) are formed when the material separates at the fracture surface. During plastic movement, these cavities enlarge and join to form larger ones. When the failure progresses, these voids begin to detach at the fracture surface and experience substantial necking, giving the material a distinctive dimpled structure. This phenomenon is

often associated with ductile fracture modes. Figure 4.6(b) clearly shows the presence of foreign particles in erosion pits at a higher magnification (500x). If the foreign particles are hard and abrasive, they can cause severe erosion and wear on the surface of the material, leading to premature failure.

These particles can also induce stress concentrations in the material, leading to crack initiation and propagation. In addition, the presence of foreign particles can also influence the corrosion resistance of a material.

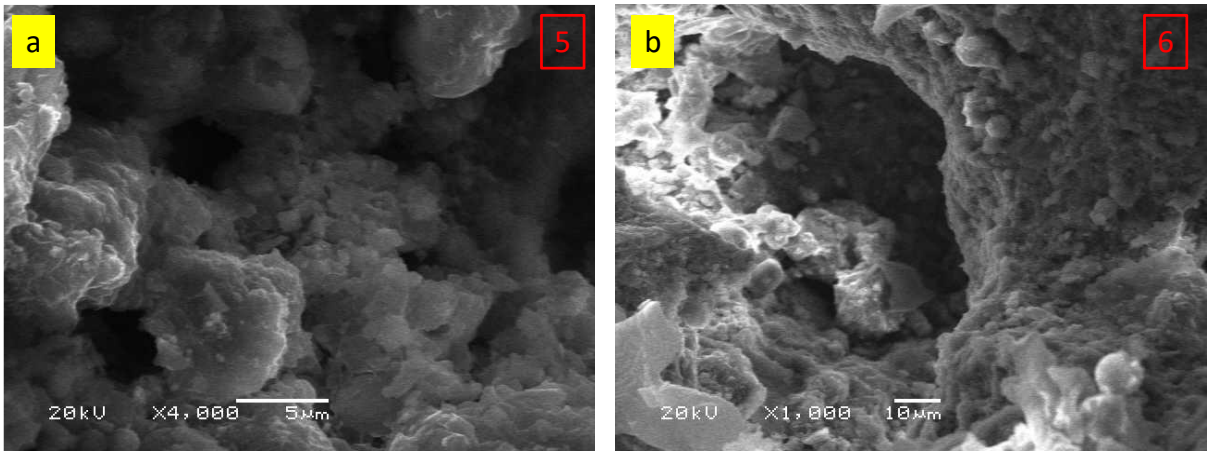

Figure 4.7 Fractographs of the fractured blade (a) indicating the presence of a substantial amount of Si (Silicon) in the grooves at 4000x b) Fractographs of the pit (region '6') at an enlarged scale1000x

The Si-containing particles or inclusions (shown in figure 4.7(a)) can act as stress concentrators, leading to crack initiation and propagation. The Si-containing particles may also contribute to the formation of microvoids, which can coalesce and lead to macroscopic fractures. The presence of a substantial amount of Si in the grooves indicates that suggests that Si inclusions played a role in the failure.

4.3.2.2 EDAX Analysis

Analysis of the composition of the pit and comparing it with the composition of the surrounding material, can help to identify the source of the erosion, such as whether it was caused by chemical corrosion or mechanical wear.

EDS spectrum identifies the Silicon (Si) rich oxides with other alloying elements of iron (Fe), sodium (Na), and manganese (Mn) as shown in figure 4.8(a,b). A trace of chlorine (Cl) is also noted. These eroding stages show maxima for chromium, oxygen, and carbon in EDX analysis (Figure 9). Silica and sodium are the main erosion-promoting components. Silica is a common contaminant in steam that can cause erosion in turbine blades. It can form hard deposits on the surface of the blade, which can cause abrasive wear and pitting. Sodium is

another impurity in steam that can cause erosion in turbine blades. It can react with the surface of the blade, leading to the formation of corrosive compounds that can cause material loss and pitting.

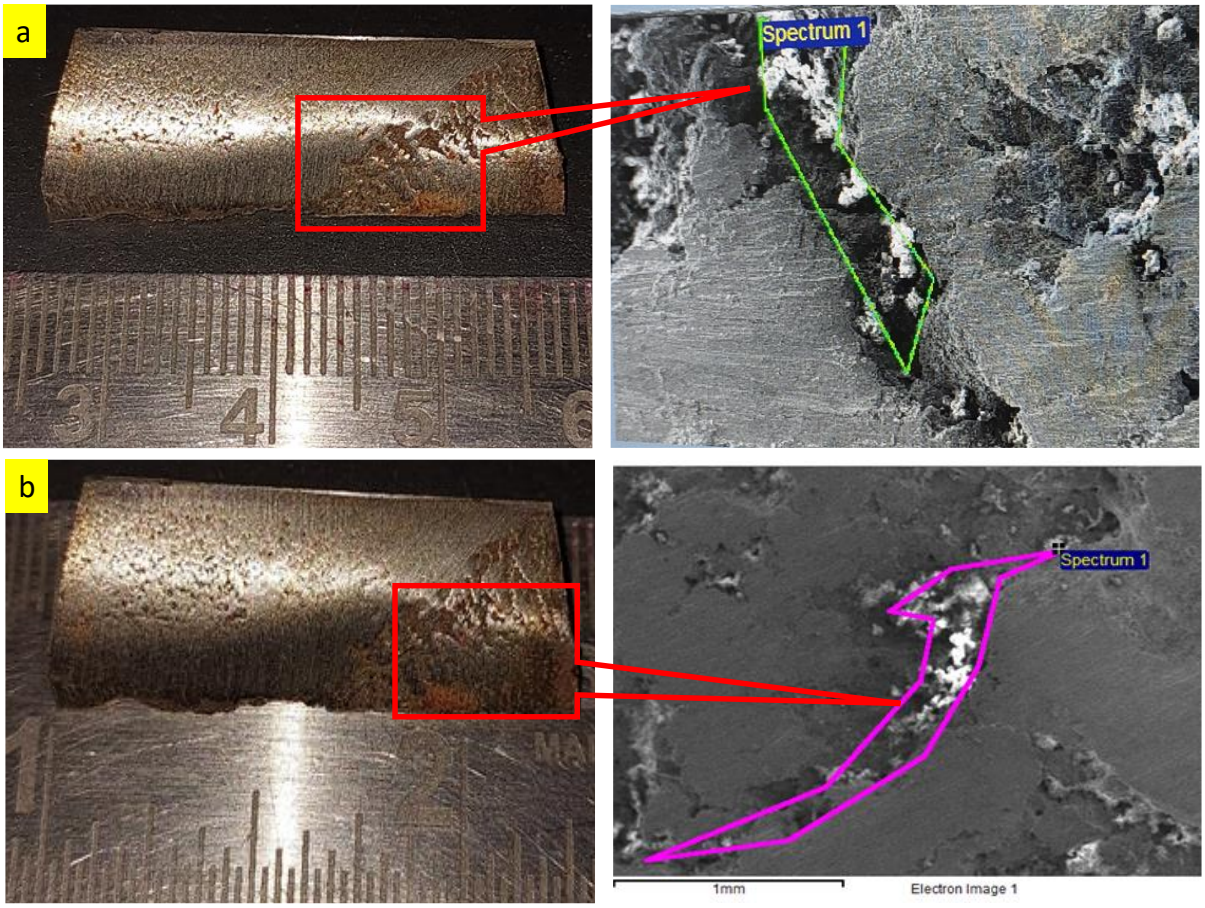

Figure 4.8 a) Evidence of Si was found using SEM-EDX. b) The EDS spectrum identifies the Silicon (Si) rich oxides with other alloying elements of Iron (Fe), Sodium (Na) and Manganese (Mn).

The effect of these erosion-promoting components on the microstructure of a turbine blade depends on the specific material used in the blade and the operating conditions of the turbine. In general, these components can cause various forms of material degradation, including:

1. Formation of hard, brittle phases: The impurities can form hard, brittle phases in the microstructure of the material, which can reduce ductility and increase susceptibility to cracking.
2. Formation of corrosion products: The impurities can react with the surface of the blade, leading to the formation of corrosive compounds that can cause material loss and pitting.

3. Formation of deposits: The impurities can deposit on the surface of the blade, leading to the formation of hard deposits that can cause abrasive wear and pitting.

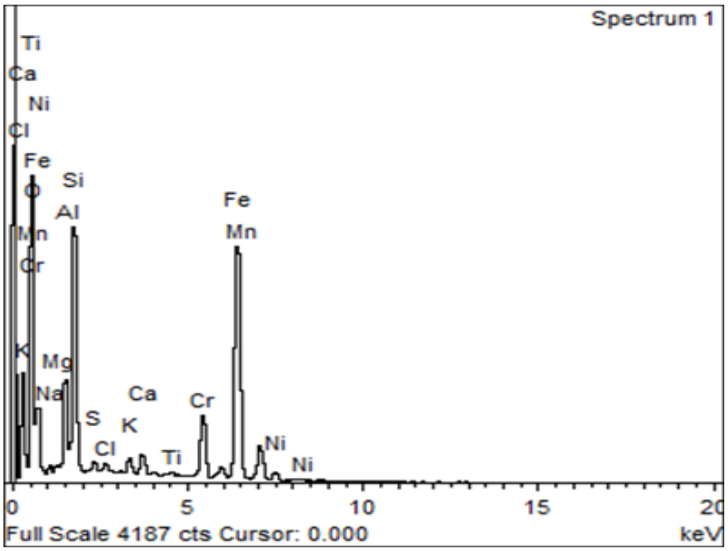

Figure 4.9 The EDX analysis of the most eroded phases shows chlorine, titanium, iron chromium, and oxygen peaks.

The damaged blade had a sizable amount of Si (silicon), along with O (oxygen), K (potassium), Al (aluminium), Na (sodium), and S (sulphur), as determined by EDS analysis (Figure 4.9). These non-metallic inclusions at a damaged surface are indicative of long-term exposure to the atmosphere or the reaction of blades with steam. Erosion and corrosion fatigue may have been the primary cause of blade failure, as suggested by fractographic analysis and EDS analysis of the fractured blade's selected areas shown by red marks in figures 4.8(a) and 4.8(b).

At elevated temperatures, the presence of Na, K, S, and Cl could lead to the formation of various compounds, depending on the specific reactions and concentrations involved. These compounds could potentially form due to the presence of sulfur (S) in the environment. Sodium sulfate and potassium sulphate are salts that can crystallize under certain conditions, especially in high-temperature environments. But in this case, the temperature is not high so these phases are not formed. Sodium chloride (NaCl) and potassium chloride (KCl) are common salts that can also play a role in corrosion processes. These salts are hygroscopic, meaning they can absorb water vapor from the environment, creating localized areas of high concentration. This can lead to crevice corrosion or pitting corrosion, particularly in the presence of chlorides, which are known to accelerate corrosion processes. Also, the breakdown of KCl could release HCl, which is a corrosive product. This could lead to localized acidic environments that promote further corrosion reactions, possibly contributing to active oxidation mechanisms. If

the material is indeed a chromia-forming steel, the presence of alkali chlorides like KCl could potentially lead to the breakdown of the protective chromium oxide (Cr_2O_3) layer. This could occur through reactions that form compounds like K_2CrO_4. The breakdown of the protective oxide layer could expose the underlying material to more aggressive corrosion processes.

In Figure 4.4, we see an image of the pits across the failed edge of the blade, as well as SEM fractographs of the pit at 100x,300x,500x and a magnified view of the pits at 1000x,2000x and 4000x are shown in figures 4.5, 4.6 and 4.7. The EDS spectrum from the pit showed that it contained characteristic corrosive by-products (Figure 4.9). The elemental composition of the pit revealed that the deposits are a combination of sodium, magnesium, aluminium, silicon, sulphur, potassium, calcium, titanium, chromium, manganese, iron, and nickel oxides.

Table 4.1

EDX results of the eroded sample and original blade sample

	Original	**EDAX area of interest Region**			
Element	**(Weight%)**	**Weight%**	**Atomic%**	**Compd%**	**Oxides formed**
Na K	Added	**0.89**	**1.06**	**1.20**	**Na_2O**
Mg K	Added	**0.43**	**0.49**	**0.71**	**MgO**
Al K	Added	**4.45**	**4.53**	**8.41**	**Al_2O_3**
Si K	0.10-0.60	**11.51**	**11.25**	**24.62**	**SiO_2**
S K	≤0.02	**0.51**	**0.44**	**1.29**	**SO_3**
Cl K	Added	**0.55**	**0.43**	**0.00**	
K K	Added	**0.73**	**0.51**	**0.88**	**K_2O**
Ca K	Added	**1.20**	**0.82**	**1.68**	**CaO**
Ti K	Added	**0.34**	**0.19**	**0.56**	**TiO_2**
Cr K	12.50-14.0	**6.33**	**3.34**	**9.25**	**Cr_2O_3**
Mn K	0.30-0.80	**0.50**	**0.25**	**0.64**	**MnO**
Fe K	Added	**37.24**	**18.31**	**47.91**	**FeO**
Ni K	0.30-0.80	**1.79**	**0.84**	**2.28**	**NiO**
O	Added	**33.52**	**57.52**		
C	0.17-0.22	Lost			
P	≤0.03	Lost			
Totals		**100.00**			

Table 4.1 shows the difference in the chemical composition of the eroded area and original composition of blade material and the detail of oxides formed in the erosion pits.

4.4 Comments on the Metallographic Analysis of First Stage High Pressure Gas Turbine Blade

- The premature failure of a low-pressure steam turbine blade is investigated here. The blade had only been in service for 152241 hours. The findings indicate that blades with erosion and corrosion pits are more prone to fatigue cracks. For this reason, blades with erosion and corrosion pits should be inspected routinely.
- The metallurgical analysis showed that the fracture initiation locations were concentrated in erosion pits, which increased the local stresses. Corrosion deposits were discovered in the same area (erosion pits). As a result of these tests, we can say that erosion and corrosion can play a major role in both the onset and spread of blade fatigue failure.
- The study found that the water droplet erosion induced multiple pits on the surface of the X20Cr13 martensitic stainless steel, which eventually coalesced into a large void and the point of crack initiation. The failure was primarily attributed to the possible sites of fatigue crack initiation at erosion pits and the presence of non-metallic inclusions, such as oxides in the material.
- The microstructure analysis revealed that the material exhibited a typical martensitic microstructure with a high density of carbides and some retained austenite. The presence of carbides and retained austenite is known to have a significant effect on the mechanical properties of the material, including its toughness and fatigue strength.
- The chapter provides valuable insights into the degradation mechanisms of X20Cr13 under erosive conditions. Silicate and sodium oxides were found on the damaged surface. Because of this, corrosion pits form, and the corrosion attack occurs.
- SEM fractographs of the erosion pit at 100x,300x,500x and higher magnification at 1000x, 2000x, and 4000x were shown in the figures along with a picture of the pits across the edge of the blade. Electron dispersive spectroscopy analysis of the contents of the pit revealed the presence of corrosive compounds with specific spectral features. Element analysis of the deposits in the pits showed that they consisted of a mix of iron, chromium, and silicon oxides.
- It was concluded that the erosion of the chromium carbide results in the formation of chromium oxide, which in turn leaves pores in the blade.

- The fractographic examination revealed that the sizes of pits are 5µm,10µm, 50µm, and 100µm, 150µm and the reason is chemical erosion not mechanical.

4.5 Summary of Chapter

Water droplet erosion (WDE), which is brought on by the high-energy impact of liquid water droplets, is a serious problem for steam turbine blades. Nevertheless, rather than addressing the WDE of actual steam turbine blades, the majority of the published research on this issue uses laboratory test rigs. In this chapter, scanning electron microscopy and energy-dispersive X-ray analysis are used to examine how the surface of low-pressure steam turbine blades that had been in service eroded over time. The results of this study provide valuable insights into the microstructural features and elemental composition of X20Cr13 steel in steam turbine blades, as well as the factors that can contribute to damage and failure.

In the current study, erosion fatigue is identified as the primary cause of blade failure. Erosion fatigue occurs due to the repeated impact of particles on the blade surface, leading to material degradation over time. Unlike overheating or local melting, erosion fatigue is driven by mechanical impacts rather than thermal effects. Corrosion fatigue from pitting and crevice corrosion, previously mentioned in earlier investigations, may share some similarities with erosion fatigue, as both involve localized material degradation. However, the underlying mechanisms are distinct: corrosion fatigue is driven by cyclic corrosion processes, while erosion fatigue results from mechanical wear.

The next chapter will discuss the computational framework for fatigue life assessment of steam turbine blade. The static, transient and fatigue analysis have been performed to evaluate resultant stresses, strain and total life estimation of turbine blade.

CHAPTER 5

COMPUTATIONAL FRAMEWORK FOR LIFE ASSESSMENT OF SEVENTH STAGE LOW PRESSURE STEAM TURBINE BLADE

5.1 Introduction

Steam turbines serve as vital components in power generation systems, converting thermal energy into mechanical work and subsequently electrical power. The seventh stage, positioned in the low-pressure section of the turbine, plays a pivotal role in extracting energy from the steam with optimal efficiency. However, prolonged operation under high-temperature and high-stress conditions can lead to material degradation, potentially compromising the integrity and performance of turbine blades. To address these concerns, the development of a robust computational framework for life assessment becomes imperative. This framework integrates FEA techniques and computational fluid dynamics (CFD) simulations to predict the remaining useful life of low-pressure seventh stage steam turbine blades accurately.

Finite element analysis (FEA) is a computational technique used to anticipate the response of a product to various real-world factors, such as vibration, heat, fluid movement, and other physical phenomena. The method has been widely utilised in the field of structural mechanics and has also shown to be effective in solving several engineering problems, including heat conduction, fluid dynamics, seepage flow, and electric and magnetic fields. Software programmes like Ansys and Abaqus are utilised to do finite element modelling and analysis of components such as turbine blades, pistons, and connecting rods. Finite element analysis (FEA) is utilised to conduct static, dynamic/modal, harmonic, and fatigue analyses of structures. ANSYS® Inc. has validated finite element methods through the process of solving them.

In the realm of power generation, steam turbines stand as indispensable workhorses, converting thermal energy into mechanical power with remarkable efficiency. Among the critical components ensuring the smooth operation of these turbines, the blades hold a pivotal role. However, over time, the incessant forces of operation subject these blades to wear, fatigue, and potential failure, underscoring the importance of accurately assessing their remaining life.

In this chapter, the study delves into the intricate domain of remaining life assessment of steam turbine blades, leveraging the sophisticated capabilities of ANSYS software.

The chapter unfolds with an exploration into the methodology of evaluating the remaining life of steam turbine blades using ANSYS, a premier computational tool renowned for its prowess in engineering simulations. Through meticulous analysis, the study deciphers the underlying factors contributing to blade degradation, from stresses induced by cyclic operation to mechanical loading arising from rotational forces.

A central focus of this chapter lies in the calculation of fatigue life by a paramount consideration in ensuring the longevity and reliability of steam turbine blades. Employing fatigue analysis techniques available in ANSYS, fatigue damage accumulation is estimated. Furthermore, this chapter extends its purview to investigate the profound impact of varying rotating speed on blade life—a phenomenon of paramount significance in the context of turbine performance enhancement and operational optimization. Leveraging ANSYS's robust simulation capabilities, the study delves into the complexities of fluid-structure interaction, elucidating the interplay between rotational dynamics and blade integrity.

In essence, this chapter serves as a comprehensive guide to the remaining life assessment of steam turbine blades using ANSYS, encompassing fatigue life calculation and elucidating the ramifications of turbine operating cycle on blade integrity. Through rigorous analysis and simulation, the study may equip practitioners and researchers with the tools and knowledge requisite for safeguarding the longevity, reliability, and performance of steam turbine systems in the ever-evolving landscape of power generation.

5.2 Numerical Analysis of a Blade of seventh Stage low Pressure steam Turbine

Most of steam power plants operates a single-shaft turbine-generator that consists of one multi-stage HP turbine and three parallel multi-stage LP turbines, a main generator and an exciter. Each LP Turbine (low-pressure turbine) is usually double-flow reaction turbine with about 5-8 stages (with shrouded blades and with free-standing blades of last 3 stages). LP turbines produce approximately 60-70% of the gross power output of the power plant unit [80].

The nomenclature of a double flow LP turbine blade is shown in figure 5.1.

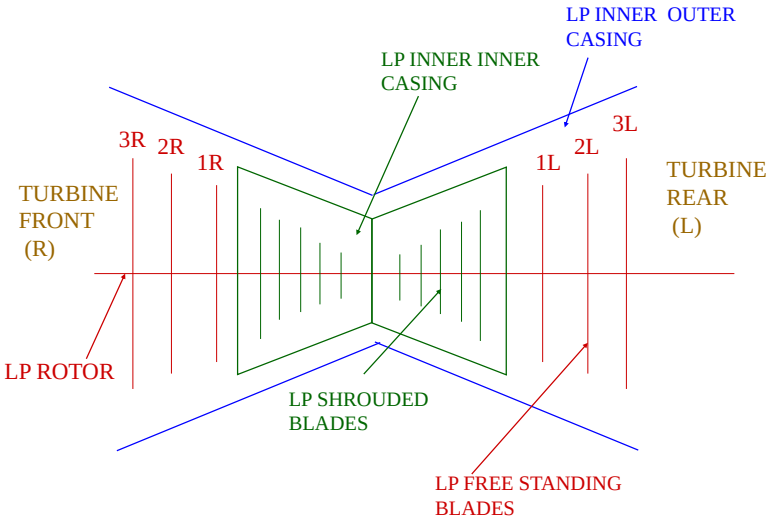

Figure 5.1 Double Flow LP Turbine Blade Nomenclature

A steam turbine goes through a typical operating cycle that includes start-up, steady state, load shift, shut down, and natural cooling. Creep wear occurs during steady-state operation, while fatigue damage is caused during transient phases [126]. This second last stage blade has completed 152241 hours of operation. A total of 379 start-ups have been performed on the turbine, comprising 118 hot start-ups, 205 warm start-ups, and 56 starts from cold state. The total no. of blades in stator and rotor row of seventh stage are 98 and 74 respectively.

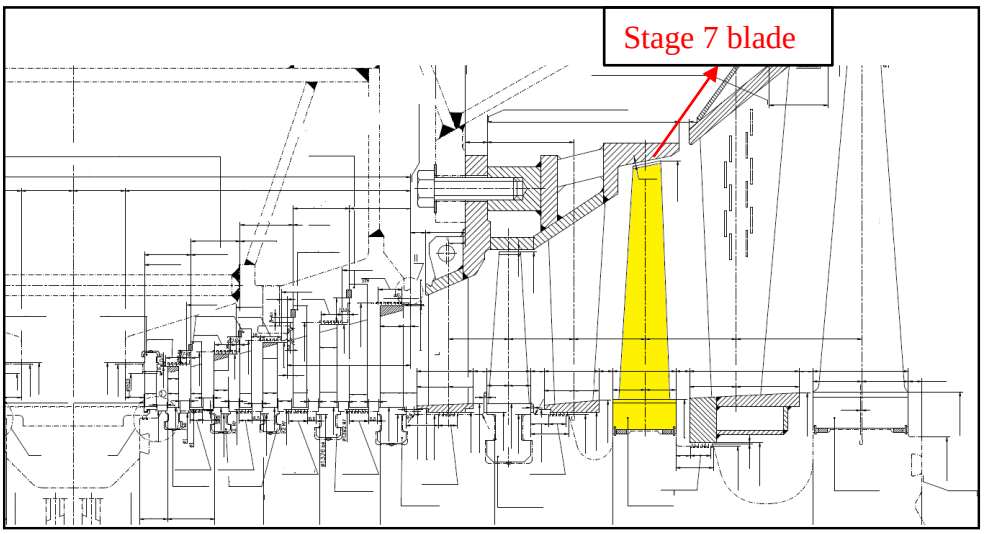

Figure 5.2 Longitudinal section of LP Cylinder

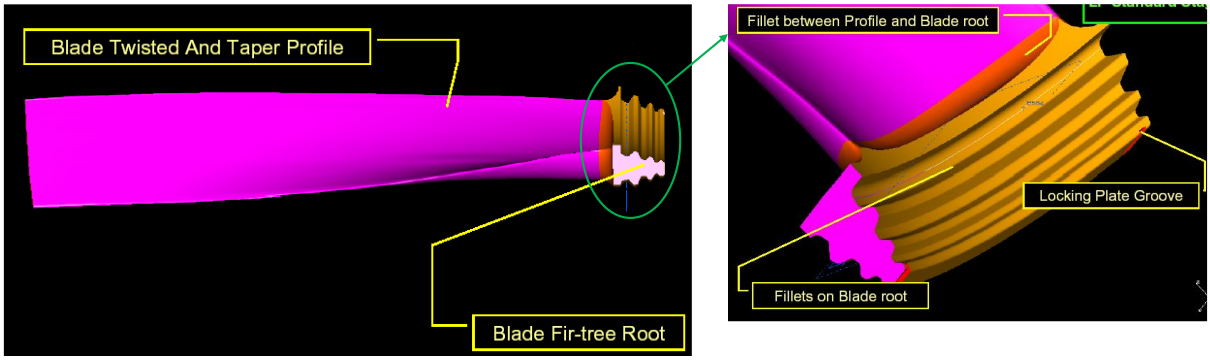

Figure 5.3 Profile of a typical LP turbine blade

The subject of this research is the life assessment of blade of the 7th stage of a 210 MW low-pressure steam turbine. A drawing of LP cylinder section is shown in figure 5.2 (the stage 7 blade selected for present study is highlighted in yellow colour). The geometric model of blade is generated in solid works according to the drawings provided, and the fluid passage of the blade is generated in ANSYS. In order to investigate the Fluid-Structure Interaction (FSI), ANSYS CFX and ANSYS Mechanical are utilized. A one-way connection was used to connect ANSYS CFX and ANSYS Mechanical, allowing pressure force calculations to be used from CFX in Mechanical for life estimation of blade. Figure 5.3 shows profile of a typical LP turbine blade and its root.

5.2.1 CFD modelling and meshing

CFD analyses of turbine blade using Fluent yield the temperature and pressure distribution at the blade surface. The fluid domain is characterized by the solution of the Reynolds-averaged Navier-Stokes (RANS) equations (of mass, momentum, and energy) and supplementary equations of the assumed turbulence model (k- SST). The turbine blade geometrical model and numerical mesh with the fluid domain is shown in figure 5.4. Turbogrid, a specialised mesh generating programme, creates the hexahedral mesh for the fluid domain. Ansys **TurboGrid** automates the production of high-quality hexahedral meshes needed for blade passages in rotating machinery. A hexahedral mesh gives some freedom to approximate curves or bends in flat surfaces by varying the angles between quadrilateral faces along the mesh.

Fluid domain mesh details are as follows:

For rotor fluid domain: no. of nodes=1155301 and no. of elements=1104300.

For stator fluid domain: no. of nodes=189596 and no. of elements=176128.

Skewness is directly related to the quality of mesh structure. Unlike other mesh metric options in ANSYS® Meshing, skewness directly shows how much the mesh structure is close to its ideal shape or form. The examples below show this situation for skewness value in

ANSYS® Meshing. Figure 5.5 depicts the Rotor blade Fluid domain mesh and mesh element quality.

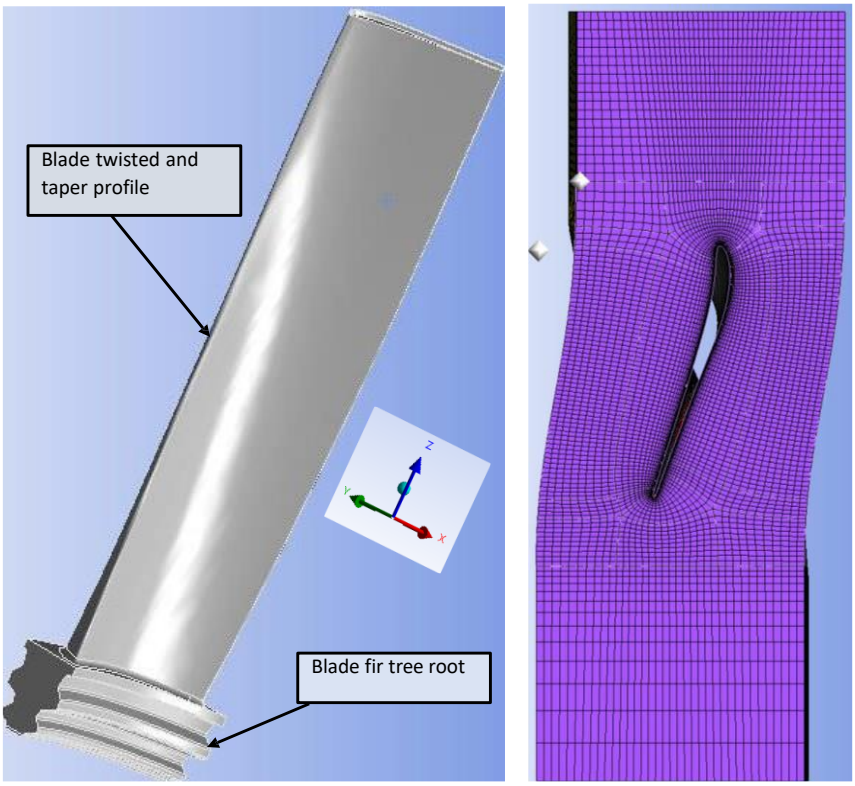

Figure 5.4 Blade Geometry and numerical mesh with fluid domain

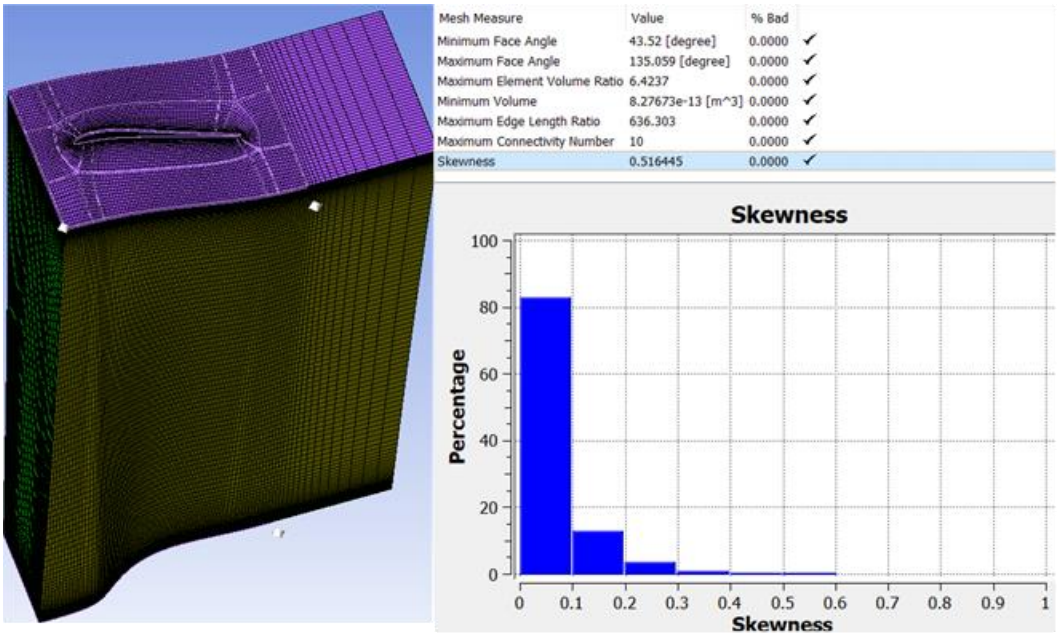

Figure 5.5 Rotor blade Fluid domain mesh and mesh element quality

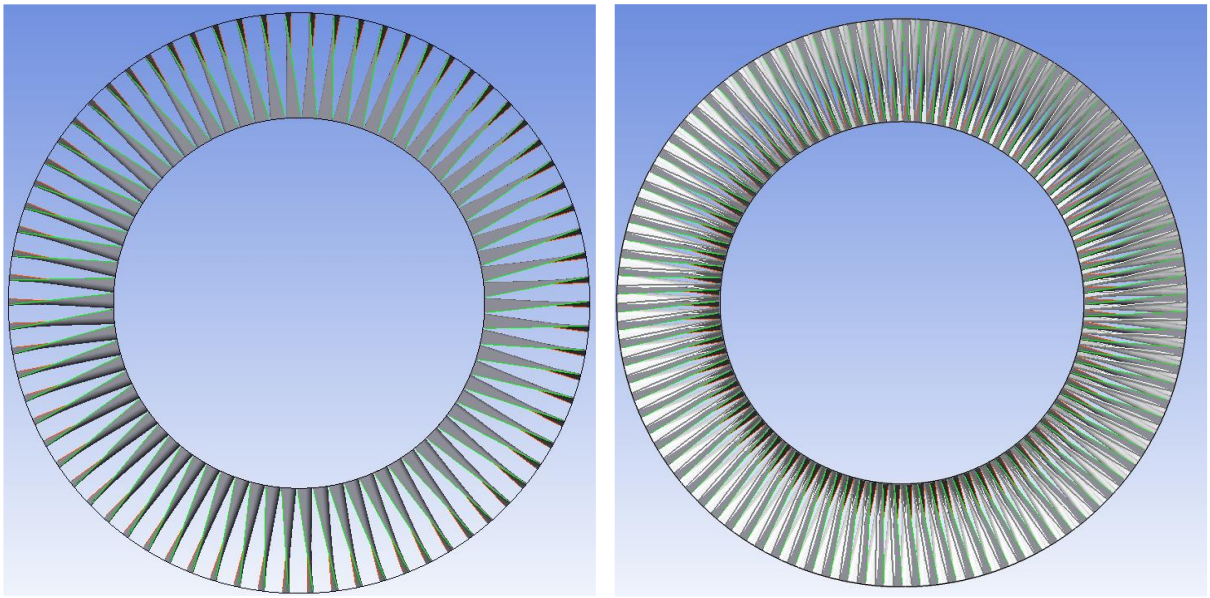

Figure 5.6 A full view of stator and rotor blades

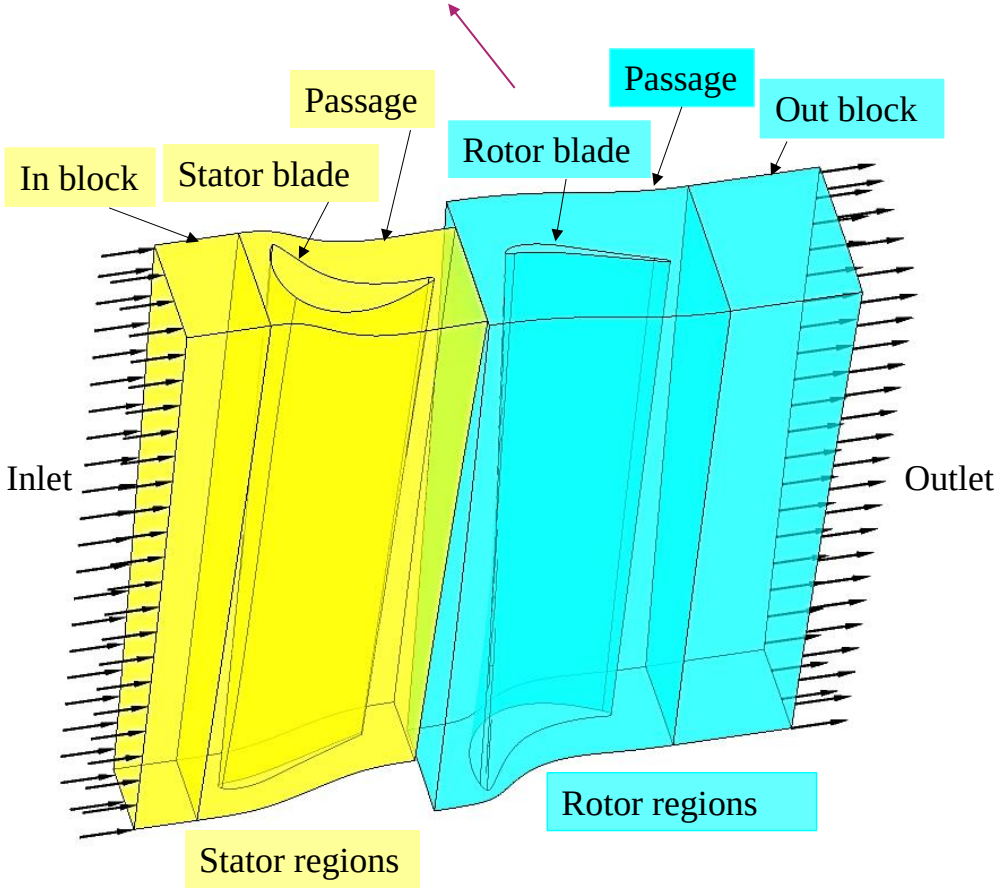

Figure 5.7 A detailed overview of stator and rotor region fluid domain

Figures 5.6 and 5.7 shows a full 3-D view of stator and rotor blades and a detailed overview of stator and rotor region fluid domain respectively.

5.2.1.1 Wet steam modelling

Wet steam modelling is essential for proper analysis of steam turbine blades. Increasing the wetness of the steam leaving the turbine can cause erosion of the low-pressure turbine blades and reduce aerodynamic efficiency in the wet steam area.

Wet steam flow is modelled using the Eulerian-Eulerian method in Ansys Fluent. The flow mixture is modelled by solving a system of compressible Navier-Stokes equations that include two transport equations for the mass fraction of the liquid phase and the density of liquid droplets per unit volume. The phase change model is based on the classical non-isothermal nucleation theory, which foretells the liquid-droplets formation in a homogeneous nonequilibrium condensation process [127], [128]. A turbine's last stage operates at a temperature of about 100°C [126]

5.2.1.2 Boundary conditions

Table 5.1 depicts the boundary conditions used in the numerical simulations, which include a mass flow inlet, a pressure outlet, a periodic boundary in the upstream and downstream areas of the blades, and no-slip and adiabatic walls on the pressure side and suction side, respectively.

Table 5.1

Boundary conditions applied in ANSYS CFD simulation

	Pressure [Pa]	**Total Temperature [°C]**	**Mass Flow Rate [kg/s]**	**Liquid Mass Fraction**
INLET	-	102.4	124.188	0
OUTLET	78660	-	-	0.1

Second order Discretization Scheme is used for this simulation. The minimum temperature limit is set to 323.15 °C. The convergence criterion for the governing equations is set to 10^{-6}.

5.2.2 Structural analysis

During a start-up and shut down cycle, centrifugal load and centrifugal stress are depicted in Figure 5.9. Therefore, a steam turbine's centrifugal load history across its operational lifetime can be expressed as a harmonic function [129], which takes into account the start-up and shutdown cycles. Tables 5.2,5.3 and 5.4, respectively, show the geometric dimensions, properties of the blade model and boundary conditions applied in structural analysis of turbine blade for structural analysis. The mesh element size is kept 0.05m (structural meshed model is shown in figure 5.8). Frictional support is applied at the mating surfaces of the blade root and

rotor groves to prevent movement in perpendicular directions. Fixed support is applied at that location of the blade root where locking plate groves are present in a real turbine blade. The blade rotated about a point that lies at a distance of 0.7 m, equal to the radial distance of the blade centroid from the rotor's centre.

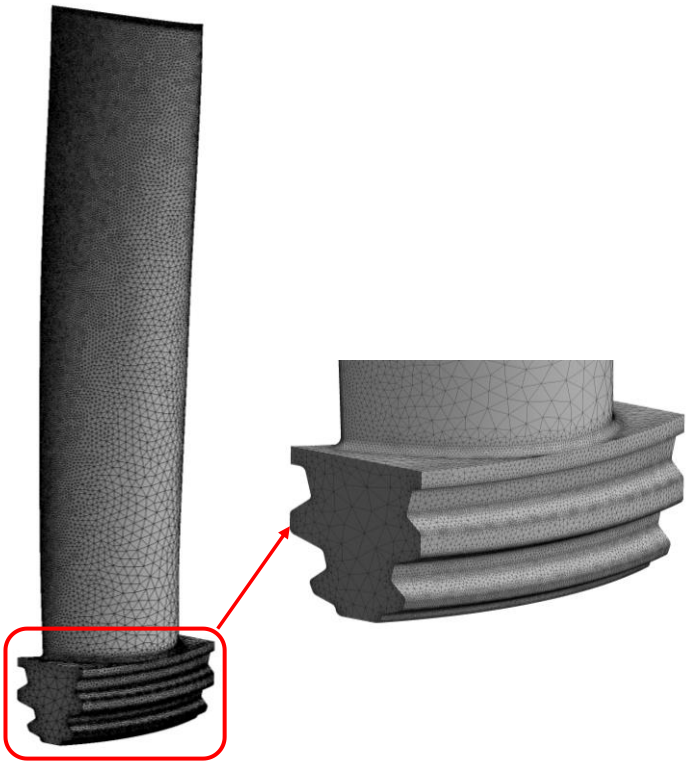

Figure 5.8 Structural meshed model of turbine blade

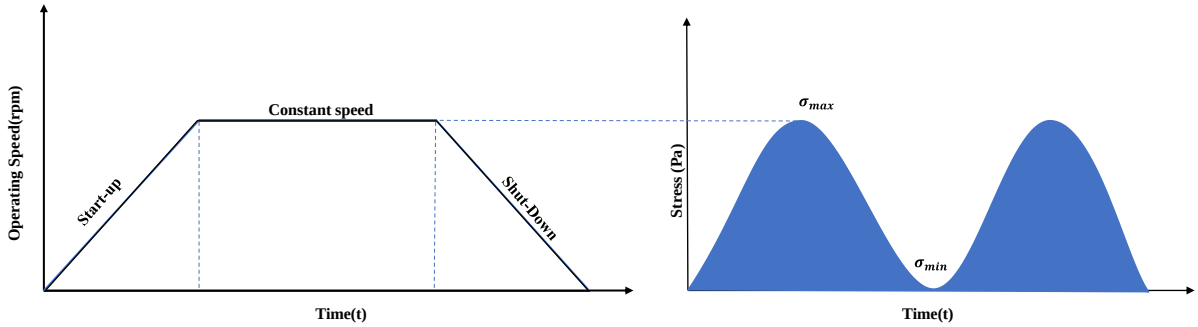

Figure 5.9 Steam turbine blade centrifugal force and stresses at start up and shutdown.

Table 5.2

Geometrical dimensions for the FEM-model of blade

Length X	Length Y	Length Z
0.116 m	8.6311e-002 m	0.49495

Table 5.3
Geometric properties of blade model

Mass (kg)	**Centroid (m)**			**Moment of Inertia (kg·m²)**		
	X	Y	Z	I_p1	I_p2	I_p3
5.2504	5.631e-005	-8.8725e-004	-0.27266	8.9129e-002	9.2492e-002	4.6108e-003

Table 5.4
Boundary conditions applied on a turbine blade in Ansys Mechanical

Fixed Support	At Blade Root (Upper flanks of fir tree root)
Frictional support	At Blade root (at locking pin clamping position)
Rotational velocity	At a distance of 0.7m from the blade root

5.2.2.1 Fatigue properties calculation

To calculate fatigue life, the material's fatigue properties should be calculated. Experimental fatigue testing is a costly and time-consuming procedure for determining a material's fatigue properties. All available estimation techniques for strain life fatigue properties were reviewed along with several ways for predicting fatigue characteristics from hardness by K.S. Lee *et al.* [130]. As a result, the methods for prediction of fatigue qualities based on more easily accessible material monotonic properties has continued to be of endless interest [131].

Table 5.5
Estimated fatigue properties of X20Cr13

Property	σ'_f **(MPa)**	**c**	**b**	ε'_f	**K'(MPa)**	**n'**
Magnitude	1399	-0.54	-0.09	0.845	1437.21	0.160

Based on the hardness method proposed by Zhao *et al.*[132], the fatigue properties have been estimated. The desired parameters for strain life analysis are approximated using the following equations (1,2,3,4) and the results are shown in table 5.5.

$$\sigma'_f = 3.98(\mathrm{HB}) + 285 \quad (1)$$

$$\varepsilon'_f = 1.5 \times 10^{-6}(\mathrm{HB})^{2.35} \quad (2)$$

$$b = -0.09 \quad (3)$$

$$c = -0.54 \quad (4)$$

5.2.2.2 Fatigue Damage Calculation

Palmgren-Miner Rule, Eq. (5) was used to determine the damage. This rule states that the ratio of operating cycles to the total cycles to failure at a particular stress value determines the proportion of damage at any given stress level.

$$D = \sum_{i=0}^{i} \frac{n_i}{n_{f,i}} \tag{5}$$

D = total damage, n_f = expected lifespan, and n_i = the number of loading cycles. D can be in the range of 0 (starting of cyclic loading) to 1 (failure) depending on the situation[133]. In order to assess fatigue damage, three techniques are employed: Strain-Life, Eq (6), Morrow equation (7) and the Smith-Watson-Topper (SWT) equation (8). When utilizing different approaches to assess fatigue damage, it is essential to have a comparing parameter. As a relative measure, $n_i = 10^9$ cycles are equivalent to an unlimited lifespan [134]–[136].

$$\frac{\Delta\varepsilon}{2} = \frac{\sigma'_f}{E}\left(2N_f\right)^b + \varepsilon'_f\left(2N_f\right)^c \tag{6}$$

$$\frac{\Delta\varepsilon}{2} = \frac{\sigma'_f - \sigma_m}{E}\left(2N_f\right)^b + \varepsilon'_f\left(2N_f\right)^c \tag{7}$$

$$\sigma_{max}\frac{\Delta\varepsilon}{2} = \frac{{\sigma'_f}^2}{E}\left(2N_f\right)^{2b} + \sigma'_f\varepsilon'_f\left(2N_f\right)^{b+c} \tag{8}$$

The current analysis of blade life estimation relies on the deformation-life equation, which can only be used if triaxial stresses are reduced. This condensing was accomplished with the help of Von Mises' theory. The parameters used in the Ansys® fatigue module are listed in table 5.6.

Table 5.6
Fatigue Tool Settings

Analysis Type	Stress component	Loading type	Mean stress correction
Strain life	Equivalent	Steam forces: R=0.9462	None
	(Von-Mises)	Centrifugal forces:	Morrow
		Zero Base	SWT

5.3 Stresses generated on steam turbine blade

The purpose of the study is to evaluate different approaches and select the one that will best determine the fatigue durability of the low-pressure turbine blade. The second objective is to find the fatigue life of low-pressure (LP) blade. Figure 5.10 is a flowchart depicting the process of estimating the fatigue life of a turbine blade.

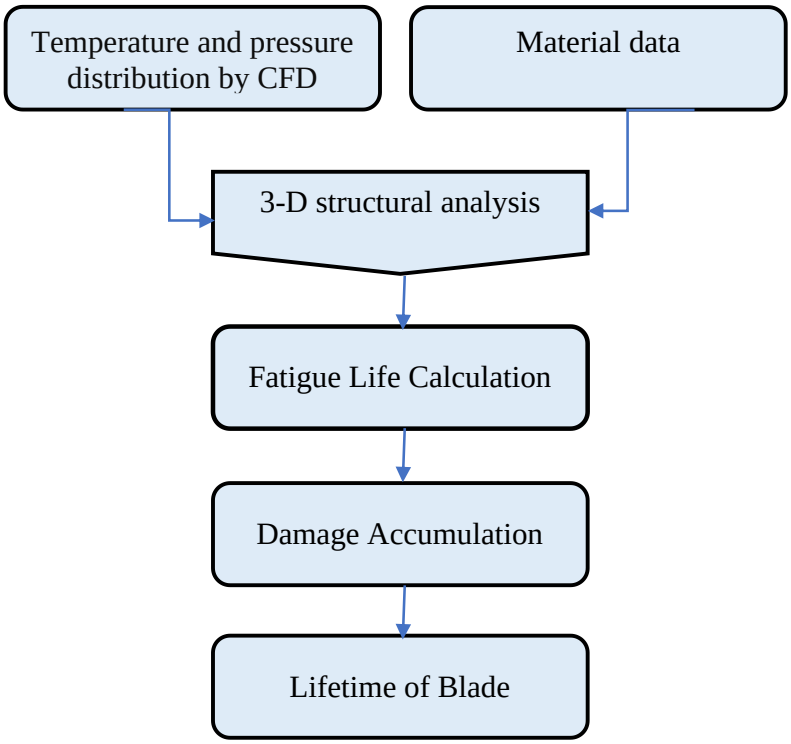

Figure 5.10 Fatigue Life estimation procedure flow chart

Solutions for the steady-state temperature and pressure distribution were obtained by applying the boundary conditions to the finite element model in ANSYS CFD analysis. The thermal loading in the model was the blade temperature distribution. The blade model was subjected to mechanical loading in the form of rotational body forces and steam pressure. A 2-D temperature and pressure distribution on the turbine blade are shown in figure 5.11.

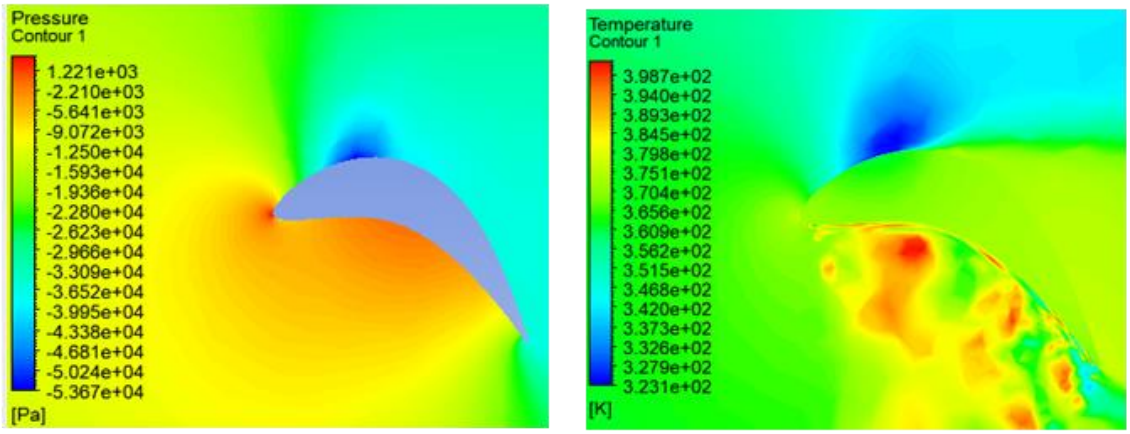

Figure 5.11 2-D temperature and pressure distribution on the turbine blade.

5.3.1 Stresses generated by steam forces

When the steam turbine functions normally, the forces exerted by the steam on the rotor blades fluctuate according to a harmonic pattern. Figure 5.12 shows the maximum stresses that occur at maximum steam loads. Maximum stresses occur close to the root of the blade. Compared to

the effect of a centrifugal load, these forces have lower stresses; yet, they can still be considered when estimating damage and usable life.

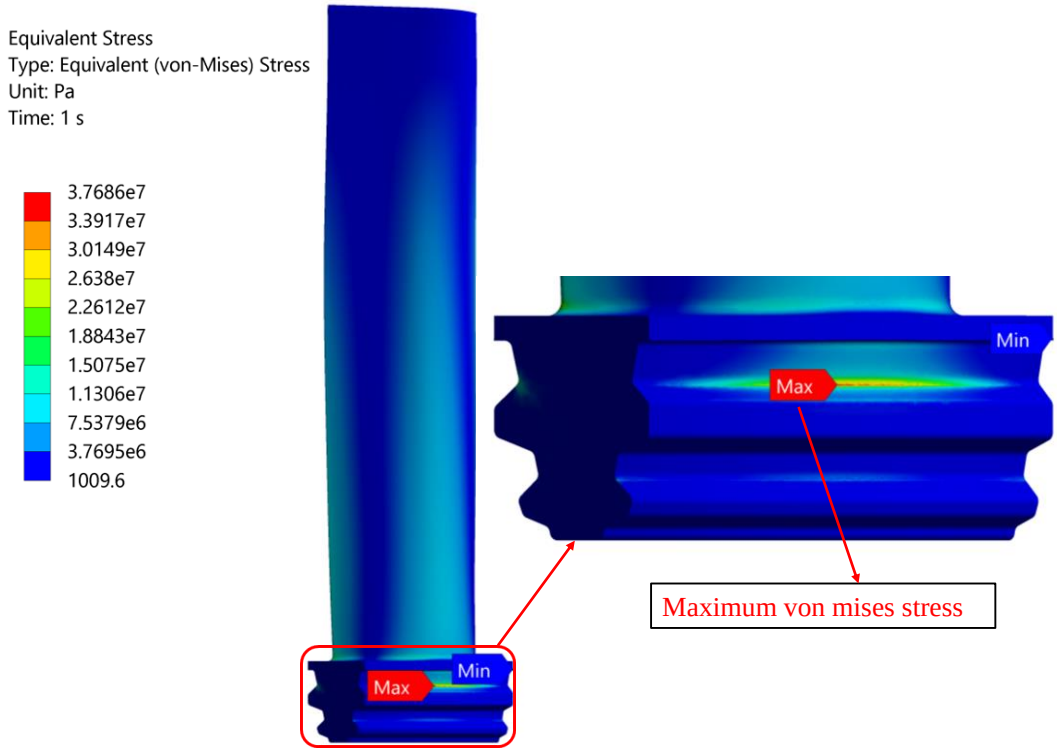

Figure 5.12 Maximum stress due to steam force

5.3.2 Steam forces effect on blade life

Table 5.7 displays the results of damage and useful life analysis performed on low-pressure stage blade using the Morrow, strain-life and SWT correction equations. Regardless of the situation, cycles are high and damage is minimal. Thus, steam forces have been calculated to have a minimal effect on the turbine blades.

Table 5.7

Estimated strain life and total damage cycles

Strain life		**SWT**		**Morrow**	
No. of cycles	Total damage	No. of cycles	Total damage	No. of cycles	Total damage
3.895×10^{39}	2.473×10^{-31}	2.0876×10^{30}	4.927×10^{-22}	3.276×10^{39}	3.234×10^{-31}

5.3.3 Stresses generated by centrifugal forces

Calculations of the centrifugal stresses at rotational speeds ranging from 500 to 3000 revolutions per minute are presented in table 5.8. Maximum centrifugal stresses were obtained at 3000 RPM under these conditions which is the operational speed of turbine. Figure 5.13

depicts the distribution of centrifugal stress within the blade. When the speed was increased to 3000 rotations per minute, the greatest centrifugal stress was found to be 555.7 MPa in the area around the fir tree roots on the suction side.

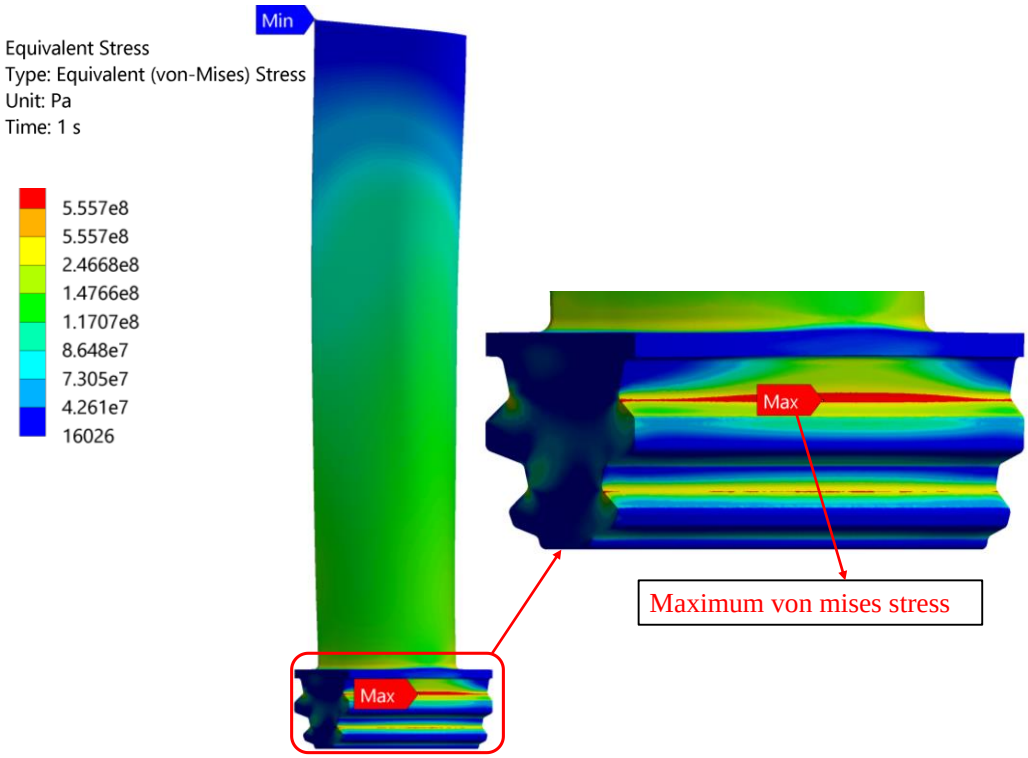

Figure 5.13 Stress due to centrifugal forces at 3000 RPM

Table 5.8

Maximum Von-mises Stresses at different operating speeds

Velocity (RPM)	**Maximum Von- Mises Stress (Pa)**
5×10^2	3.768×10^7
10^3	6.10575×10^7
15×10^2	1.37476×10^8
20×10^2	2.4423×10^8
25×10^2	3.8162×10^8
30×10^2	5.557×10^8

5.3.4 Centrifugal forces effect on blade life

The strain life with no stress correction, and Morrow's, and SWT correction were used to determine the impact of centrifugal force on N_f life, and the related damage was computed (table 5.9). As the RPM is raised, the damage is amplified and the lifespan is reduced. The SWT

correction calculated strain life of 62155 cycles and 16089 damage cycles at the same rotational velocity, while Morrow correction predicted life of 45765 cycles and 21851 damage cycles.

Table 5.9

Estimated strain life and total damage cycles at 3000 RPM

Strain life		**Morrow**		**SWT**	
No. of cycles	Total damage	No. of cycles	Total damage	No. of cycles	Total damage
6.23×10^{6}	1.89×10^{2}	2.33×10^{6}	7.86×10^{1}	6.22×10^{5}	1.61×10^{5}

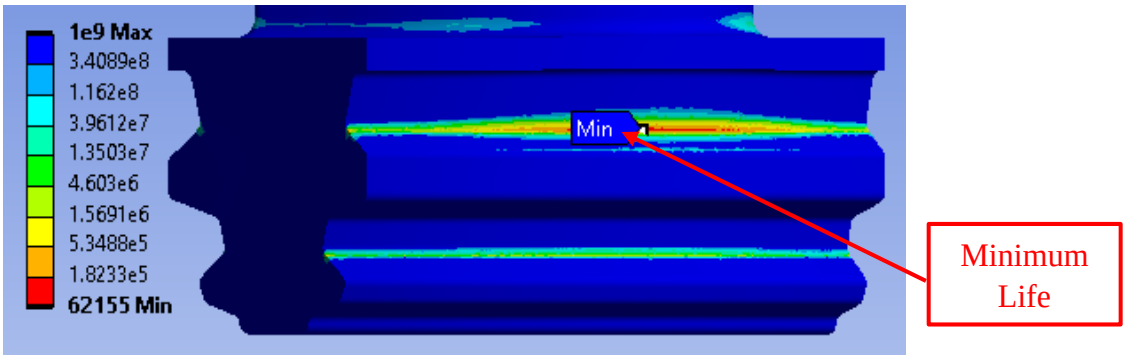

Figure 5.14 Strain life cycles at 3000 RPM in blade using SWT correlation.

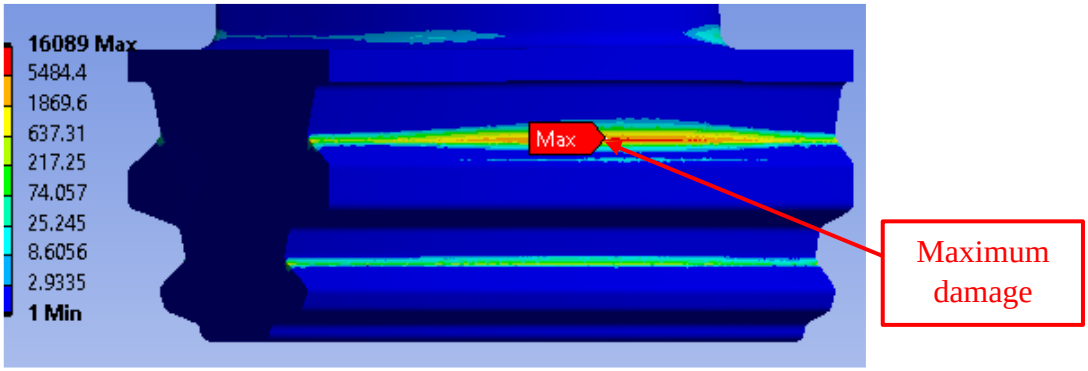

Figure 5.15 Damage cycles in blade at 3000 RPM using SWT correlation

Figures 5.14 and 5.15 depict the locations of the blades with the shortest life expectancy and the greatest amount of damage, respectively. The most vulnerable part of the blades is found in the vicinity of the blade root, where the damage is greatest. Since SWT includes more variables of analysis, it provides a more accurate prediction in steam turbine blades for damage detection. SWT damage parameter is recommended as being the most conservative in most cases according to previous research [126].

The author used Bhamu *et al.*'s and S. Cano *et al.*'s previously published work to verify her work [131][137] . In this chapter, the same strategy is employed.

5.4 Lifetime assessment of steam turbine blade

Historically, when components exhibit material degradation or damage during an overhaul, they are often discarded and replaced as a precautionary measure, even if they still have some remaining useful life. To prevent parts from being prematurely scrapped, remaining life evaluation provides a potential technique to determine the usable remaining lifetime. The utilisation of remaining life assessment is seen as a favourable approach for reducing costs and minimising periods of inactivity [138].

When it comes to power plant equipment, solving the issues of lifetime and reliability is crucial for two reasons: preventing components from failing before their design life is up, and keeping them in operation for as long as possible [139]. Any endeavour to increase the useful life of power turbo-sets must begin with an analysis of the current level of damage to its components [140].

Throughout the years, several researchers have attempted to tackle this problem. Using image recognition and machine learning, Zheyuan Zhang *et al.* [141] described a method for estimating the amount of time a turbine blade will continue to function reliably after being subjected to water droplet erosion (WDE). New mathematical models were presented to predict the service life of aircraft parts along with a literature survey on the life prediction in a creep-fatigue situations [142]. Methods for modelling probabilistic fatigue life are extensively explored in the literature. To deal with the unpredictable nature of fatigue damage, stochastic fatigue damage models have been implemented [143]–[146]. Creep-fatigue crack initiation and propagation processes have been studied by numerous researchers [121], [143], [154], [155], [146]–[153].

Xuefei Guana and Jingjing He [156] outlines a methodology for extending the lifespan of turbine rotating components considering risk constraints related to fatigue crack damage. They reviewed historical perspectives and current practices in lifetime extension, emphasizing the importance of evaluating fatigue life through ultrasonic inspection data and fracture mechanics. The study highlighted the significance of uncertainties, particularly in crack sizing, and proposed a method for scientifically quantifying and minimizing these uncertainties to extend component lifespan without compromising risk requirements, demonstrated through a realistic case study on a steam turbine rotor. David Dowson [72] has provided a summary of the steps involved in a metallurgical failure study. There are a number of case studies that show how the methods can be applied. A failure analysis can help to figure out why the components failed and then put measures in place to make sure that doesn't happen again. The creep behaviour of spinning components is analysed by Mariusz Banaszkiewicz [31] using a

characteristic strain model (CSM). There was a lot of nonuniform creep strain accumulating in the disc. There was a marked increase in the amount and pace of creep strain accumulation in the locations subjected to the highest elastic stresses. Therefore, areas with large stress concentrations may indicate that creep ductility has been depleted and that cracks may begin to form in the material. Mariusz Banaszkiewicz [22] also detailed the examination of fatigue cracking and non-stationary stresses in rotors of impulse steam turbines. Based on an examination of field experience with rotor cracking, the most prevalent crack spots were identified. Numerical calculations of an intermediate pressure rotor were presented, using mathematical models of heat transmission and material constitutive behaviour. Common transient occurrences, such as cold, warm, and hot start-ups and shutdowns, were modelled using the finite element approach. The thermal grooves of a balance piston, which frequently showed cracks during non-destructive testing, also had the highest stress and strain amplitudes. Y. Enomoto [157] presented an example of a steam turbine life evaluation and retrofitting plan. The reliability and efficiency of the retrofitted turbine will be higher than that of the original turbine because of use of modern technology and upgraded parts. The results of the integrity examination, data from operations, records of outages, and design information are the usual building blocks for a manufacturer's residual life evaluation of a steam turbine. This is used to develop a strategy for maintenance and retrofitting.

The existing literature on the lifetime assessment of low-pressure steam turbine blades primarily revolves around factors such as material properties, microstructure, and degradation mechanisms. Previous research has focused on methods for predicting blade lifespan, including fatigue analysis, creep behaviour modelling, and the effects of corrosion and erosion. However, there are several notable research gaps in this field. Firstly, while much attention has been paid to high-pressure turbine blades and turbine rotors, comparatively less emphasis has been placed on low-pressure turbine blades, despite their importance in overall turbine performance. Additionally, there is a need for further investigation into the specific degradation mechanisms affecting low-pressure turbine blades, as these may differ from those affecting high-pressure blades. Furthermore, there is a lack of standardized methodologies for assessing the remaining useful life of low-pressure turbine blades. Research is needed to develop comprehensive assessment frameworks that account for these factors and provide accurate predictions of blade lifespan.

With the help of deterministic damage calculation, fracture mechanics, and probabilistic simulations, this section aims to give a methodology for assessing the lifetime of steam turbine blades. When making predictions of lifetime based on limited material property data, this

approach has the benefit of being able to estimate the probability of crack initiation due to creep and fatigue. This method is widely used in the field of engineering, and it is typically very cautious. In addition to the creep-fatigue calculations, the technique also takes into account the likelihood of crack initiation and microstructural damage, allowing for a more accurate evaluation of damage and prediction of remaining life. Deterministic and probabilistic lifetime estimates for a low-pressure steam turbine blade are shown.

5.5 Lifetime Assessment Methodology

The term "remaining life assessment" has frequently been incorrectly labelled as "life extension". This examination will not effectively prolong the lifespan of the components. The assessment is limited to determining the remaining useful lifespan, which is determined by metallurgical tests and theoretical calculations using fracture mechanics principles. If these evaluations show that major repairs and renovations are required, life extension might not be a practical choice. In addition to this objective, life assessment technology serves various other functions. It facilitates the establishment of appropriate inspection schedules, maintenance processes, and operating procedures. Thus, it should be seen right once that the advancement of methods for assessing remaining life has a wider and more lasting significance than only extending plant life. For example, based on evaluations from fracture mechanics calculations, it has been feasible to increase the inspection interval for current rotors from six to 10 years, leading to significant cost savings [158].

A schematic representation of the standard procedure for performing a lifespan evaluation is shown in figure 5.16 as outlined in [33]. The procedure begins with two almost independent steps: theoretical computations and material testing.

Theoretical calculations are conducted to assess the creep-fatigue damage by considering the lowest possible material characteristics. The failure probability is then determined by calculating the damage using a deterministic model and accounting for the dispersion in material property data. Material testing is conducted to detect both surface and volumetric cracks, as well as to assess micro-structural damage. This is achieved through the use of replica or microscopic tests. Crack presence testing is conducted on all available surfaces of the component, whereas microstructure damage and volumetric crack tests are specifically carried out at the most significant sites determined through numerical analysis. Damage calculations serve the purpose of identifying essential regions for testing and providing crucial information regarding the following aspects: - The dominant damage mechanism at a certain location. - The

extent of damage for the most unfavourable material properties. - The rate at which damage accumulates.

In cases when no cracks are discovered, the remaining useful life of the component is estimated using damage calculation, failure probability, and microstructure damage. If cracks are discovered in the part, an evaluation by fracture mechanics can find how much time can pass while the crack continues to spread without compromising the integrity of the part. Depending on the nature of the damage and the component, it is not always feasible to make such an evaluation. Whenever the failure is not controlled by crack propagation, fracture mechanics models are not useful [153].

When time to initiate a crack is much longer than the time needed to grow a crack up to critical size, traditional non-destructive examination techniques and fracture mechanics analyses are of no use in determining the likelihood of initiation-controlled failures. If a macroscopic crack is found in such a situation, it is usually an indication that the component has reached the end of its useful life and must be either repaired or retired. That's why it's crucial to conduct an analysis through calculation and material analysis to find out if failure is controlled by crack initiation or propagation, and to correctly assess the critical size of crack.

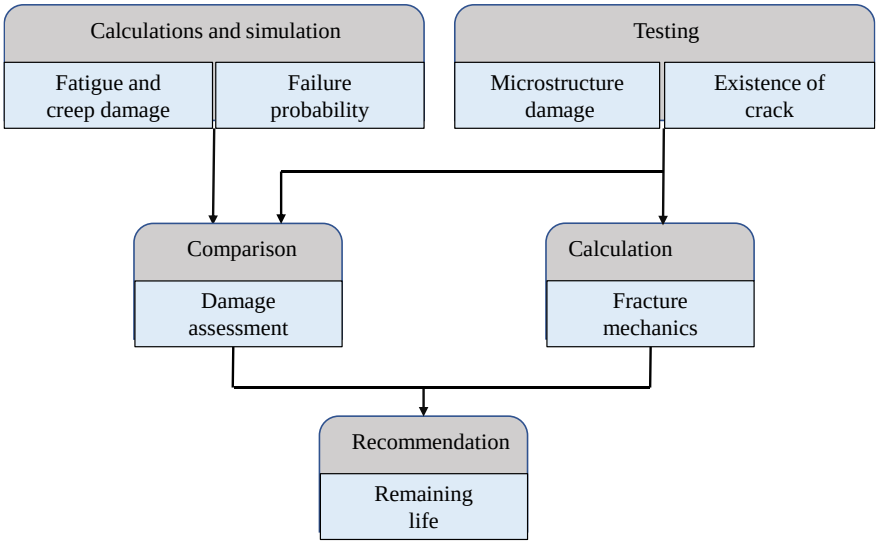

Figure 5.16 General flowchart of the lifespan evaluation procedure.

Cracks are not always deemed as a perilous form of damage for component safety, as the rate at which cracks expand can diminish as the crack size increases, and crack propagation can stop. This occurrence is referred to as crack arrest and can happen, for instance, in turbine casings where thermal fatigue cracking takes place. Skelton and Nix [159] presented experimental proof of this phenomenon, whereas Meshii and Watanabe [160], [161] extensively examined the underlying theory.

5.5.1 Total Damage Calculation by Deterministic Approach

How long and under what circumstances can a turbine be safely operated after its design lifetime? To answer this question, we need to analyse the turbine's operational history and assessment of the life expenditure because the material condition of the component after 100,000 to 200,000 operating hours relies on the operation mode firstly. This requires conducting stress studies on the turbine parts to find material damage theoretically (computational). Damage estimation based on operating time alone is insufficient if fatigue damage, which varies with the number of starts from different starting thermal conditions, is not taken into consideration. For assessing the remaining life of a turbine component, three kinds of information are needed [162]:

- The current degree of damage,
- Degree of damage causing failure, and
- Damage accumulation rate.

Creep and fatigue damage are calculated theoretically using the lifespan fractions summation technique. The linear formula of damage summation represents a linear model of damage commonly used in steam turbine practice. Total damage is the sum of creep and fatigue damage as per modified Miner and Palmgren's rule, and this rule can be expressed as [142].

$$Z = Z_B + Z_N \tag{9}$$

Here Z_N represents fatigue damage and Z_B represents creep damage.

Time-dependent creep damage accumulation is summed linearly, as predicted by Robinson's theory. The following algorithm can estimate the creep damage for a given temperature and stress combination under steady-state conditions [163].

$$Z_B = \sum_{i=1}^{r} \frac{T_i}{T_{Bi}} \tag{10}$$

where T is no. of operating hours at a steady state temp. of t(°C), and operating stresses and T_B is time to creep rupture corresponding to temp t (°C) and operating stresses. The minimal creep curve provides the basis for the calculation of T_B. Here r represents the count of temperature conditions.

The total fatigue damage depends on the number of load cycles and the damage magnitude in each loading cycle, where N_A is the number of crack initiation cycles. Its value is derived from (Low cycle fatigue) LCF curve. A summation is done in a proportional manner to the number of cycles, as stated by the linear fatigue damage accumulation rule (Palmgren's

Miners' hypothesis). The fatigue damage is determined using the following formula [164] under a stress spectrum, which in actual turbine operating conditions consists of warm, cold and hot starts, and load changes.

$$Z_N = \sum_{i=1}^{q} \frac{N_i}{N_{Ai}} \tag{11}$$

where, N represents actual number of warm, cold and hot starts, load and temperature fluctuations and N_A shows number of these starts, load and temperature fluctuations to crack initiation. Colombo [165] confirmed the linear rule of damage summation for 1CrMoV rotor steels by thermal fatigue experiments. These tests were conducted on uniaxial and component feature specimens, simulating service-like circumstances.

When the cumulative damage Z equals one, the computational lifetime is at an end, theoretically [133]. In fatigue cycles, this crucial value indicates the initiation of cracking due to fatigue. A greater probability of failure is related with continuing operations past the instant of crack initiation up to the ultimate rupture. Components of steam turbines where creep and fatigue processes occur simultaneously are expected to have a critical value of Z equals to 0.75 [152]. When this critical value D is reached, there is a greater chance of cracking and a greater chance of failure; as a result, the turbine is run with a steadily decreasing safety margin. Theoretical service life expiration is a warning indicator that the operated component needs to be subject to longer supervision and the need to begin a systematic testing programme.

5.5.2 Probabilistic Method of Lifetime Assessment

The findings of the laboratory tests form the basis of the lifetime assessment's probabilistic technique. The log-normal distribution is used to characterise the scatter of turbine steels' creep and fatigue parameters. According to the data in ALSTOM's material database, It can infered that the minimum and average values of the creep rupture strength (R_m) and strain amplitude (ε_a) are connected by a constant factor (f_{Rm} and f_ε) as shown in Figure 4a and b. The following are the appropriate relationships:

$R_m(P = 50\%) = f_{Rm}\, R_m(P = p_{\min})$,

$\varepsilon(P = 50\%) = f_\varepsilon \varepsilon(P = p_{\min})$,

The given probabilistic assessment of steam turbine lifetime [150], [166] is useful because it provides an alternative to deterministic studies and can be used to create a useful tool for engineering simulations. It can be expressed as follows using the deterministic approach's linear law of damage accumulation [167]:

$$z = \frac{t}{t_B(P=p_{\min})} + \frac{n}{N(P=p_{\min})} = 1 \tag{12}$$

P_{min}, the minimal value of the probability distribution. Degree of damage Z=1 for a failure probability p can be expressed as:

$$z(P) = \frac{t}{t_B(P=p)} + \frac{n}{N(P=p)} = 1 \quad (13)$$

Considering that the allowable limit D_N for fatigue damage is distinct from the creep damage limit D_B, we can reformulate Eq. (13) as:

$$z(P) = \frac{1}{D_B}\frac{t}{t_B(P=p_{\min})} + \frac{1}{D_N}\frac{n}{N(P=p_{\min})} = 1 \quad (14)$$

It is possible to express the time to failure for operational time t_{op} and no. of start-ups n_{op} as:

$$\left[\frac{t}{D_B t_B(P=p)} + \left(\frac{n_{op}}{t_{op}}\right)\frac{n}{D_N N(P=p)}\right] \quad (15)$$

Considering

$$Z_B = \frac{t_{op}}{t_B(P=p_{\min})} \quad (16)$$

$$Z_N = \frac{n_{op}}{t_B(P=p_{\min})} \quad (17)$$

and differentiating between cold, warm, and hot cycles, the following formula was derived to describes operating time t spent operating before the failure probability *p* is reached.

$$t = \frac{t_B(P=p_{\min})}{\left[\frac{t_B(P=p_{\min})}{t_B(P=p)}\cdot\frac{1}{D_B} + \sum_{i=Z,C,G}\left(\frac{Z_{N,i}}{Z_t}\cdot\frac{N(P=p_{\min})}{N(P=p)}\cdot\frac{1}{D_N}\right)\right]} \quad (18)$$

The start of fatigue cracks or tertiary creep represents failure here.

5.5.3 Fracture Mechanics for Crack Analysis

Damage from fatigue & creep is capped at a critical value, where macroscopic fatigue or creep crack initiation is presumed to begin. In some cases, the interval between the onset of a fracture and its eventual failure may be long enough to allow a cracked component to continue functioning during periodic inspections while still providing an adequate margin of safety.

Necessary information required to complete the remaining lifespan assessment study of components with cracks are [168]:

- Initial crack size
- Critical crack size
- Crack growth rate

Using traditional non-destructive testing methods macroscopic cracks can be located and measured. The analysis can then be expanded upon to assess the growth rate of crack utilising

fracture mechanics techniques. The following steps are part of the approach for crack growth analysis for steam turbine parts:

- Time-independent fatigue
- Creep-fatigue interactions
- Time-dependent creep crack growth

At low temperatures, fatigue alone controls crack formation because creep mechanisms are either negligible or insignificant. The expansion of a fatigue fracture can be characterised by the Paris law [169].

$$\frac{da}{dn} = C\Delta K^m \tag{19}$$

Where C&m are material constants, a=crack size, and ΔK is the stress intensity factor range defined as $K_{max} - K_{min}$.

5.6 Life assessment of seventh stage low pressure steam turbine blade

A low-pressure stage blade of a 210 MW turbine is subjected to the above-described method of applying the theory of probability to lifespan studies. No cracks are detected in non-destructive testing of the blade as already discussed by the author in chapter 3 and 4. Temperature and stress computations by finite element method are conducted to provide a deterministic estimate of the blade damage. Steady state and transient temperature distribution are found by applying the boundary conditions to the finite element model. The structural model was subjected to thermal loading based on the temperature distribution of the blade. The blade model is subjected to steam pressures and spinning body forces to simulate real-world mechanical conditions.

The linear-elastic material model was employed in transient evaluations that simulated power-ups and shut-downs. By using Neuber's correction method to von Mises stress amplitudes, we are able to determine the equivalent strain amplitudes needed for assessing fatigue damage caused by start-up and shut-down cycles.

$$\varepsilon_a = \frac{{\sigma_a}^2}{\sigma_y E} \tag{20}$$

where ε_a– strain amplitude, E – Young modulus, σ_y– cyclic yield stress, σ_a –Von-Mises stress amplitude.

The linear elastic-plastic material model is utilised when calculating the expected lifetime of new components [170].

Blades used in LP turbines typically run at temperatures near 100 degrees Celsius. So, there shouldn't be any creep yielding [126]. However, as indicated in the literature [171], the blade's expected operating life can be shortened even at temperatures below 400 degrees Celsius. However, simulation on the material is conducted at a temperature of 102.4 degrees Celsius. This means that temperature has been factored into forecasts all along. The viscoelastic material model is used to calculate steady-state creep for the creep damage estimate. Bolton's characteristic strain model is used to determine creep strain, which is expressed as follows [172]:

$$\varepsilon_c = \frac{\varepsilon_x}{\sigma_R/\sigma - 1} \tag{21}$$

where σ is the current stress, ε_c is the creep strain, σ_R is the creep rupture strength, ε_x is a material constant (known as characteristic creep strain). The strain hardening rule is used for changing stress. The model was effectively applied to analyse rotating [173] as well as stationary [174], [175] components.

Finite element analysis was performed to provide a deterministic estimate of the level of damage to the blade material. As a result, temperature and stress distributions in steady-state conditions and for different start-up conditions are obtained. Based on this, the most highly stressed zones are identified. Finite element method temperature and stress evaluations with automatically generated input files including thermal and mechanical boundary conditions form the basis for lifetime estimations. Equivalent Von mises stress and Equivalent total strains for cold, warm and hot startups are shown in figures 5.17, 5.18 and 5.19 respectively. It is evident that the maximum stress and strain is generated during cold startup. Figure 5.20 depicts stress distributions at crucial blade locations during cold start-up where critical locations for crack initiation are marked.

Compared to the blade position 1, position 2 experiences more transient stress because it is directly heated by the steam, which results in higher metal temperature value. The calculation of fatigue damage is based on transient temperature and stress fluctuations, whereas the calculation of damage due to creep is based on steady-state temperature and stress distributions.

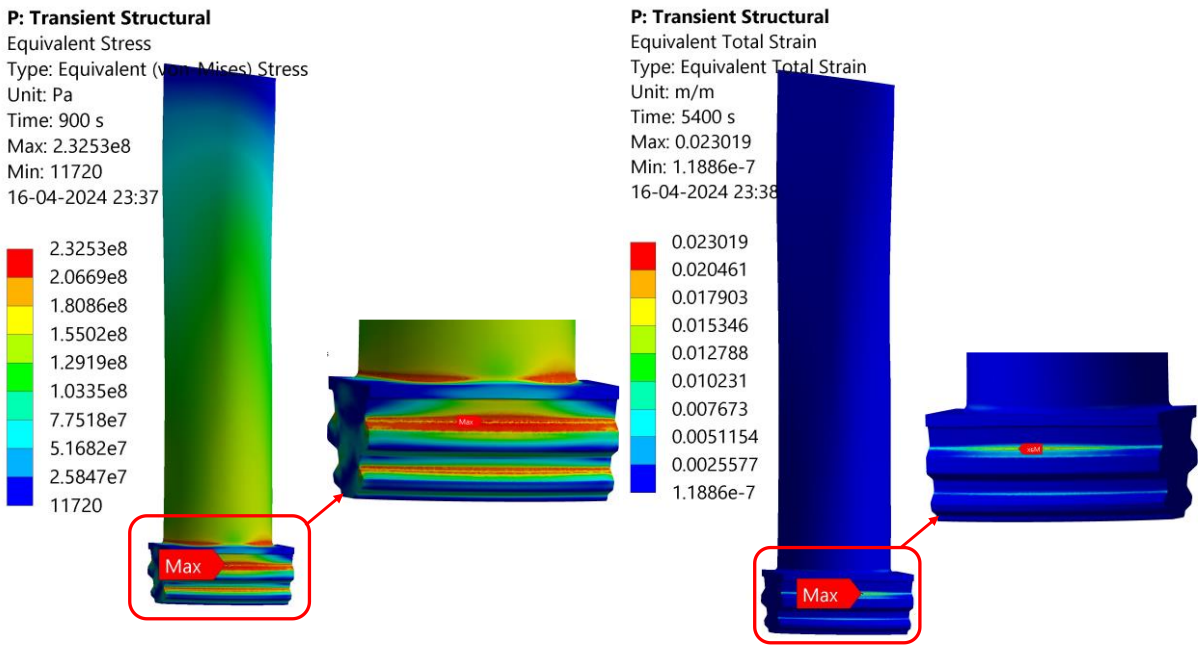

Figure 5.17 Equivalent (von-mises) Stress generated and equivalent total strain on steam turbine blade during hot startup

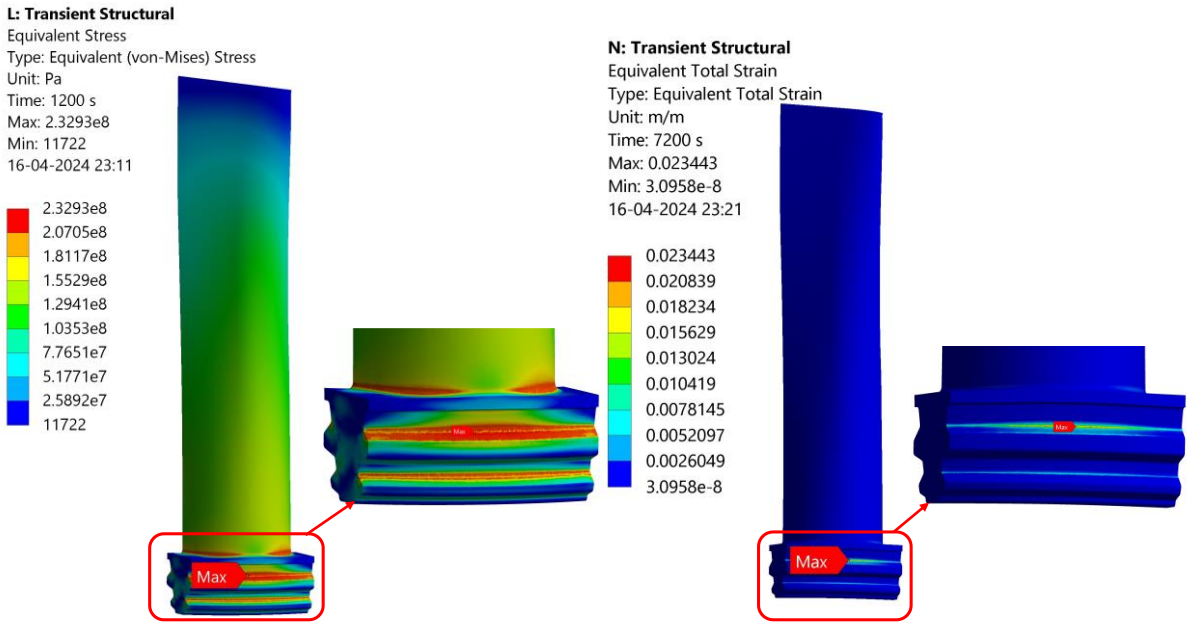

Figure 5.18 Equivalent (von-mises) Stress generated and equivalent total strain on steam turbine blade during warm startup

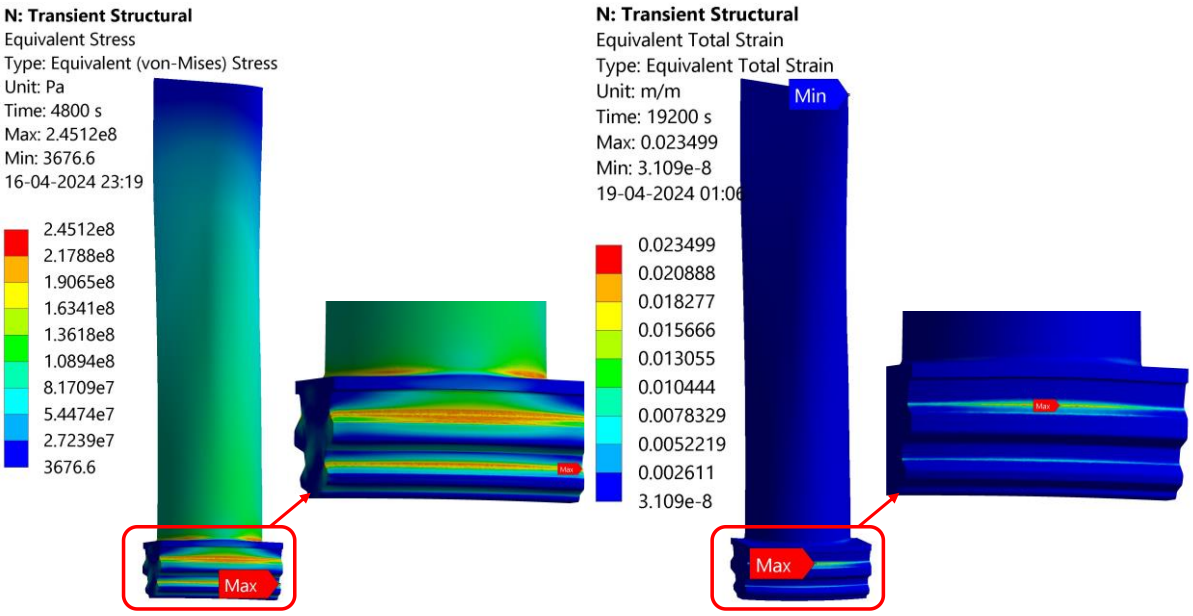

Figure 5.19 Equivalent (von-mises) Stress generated and equivalent total strain on steam turbine blade during cold startup

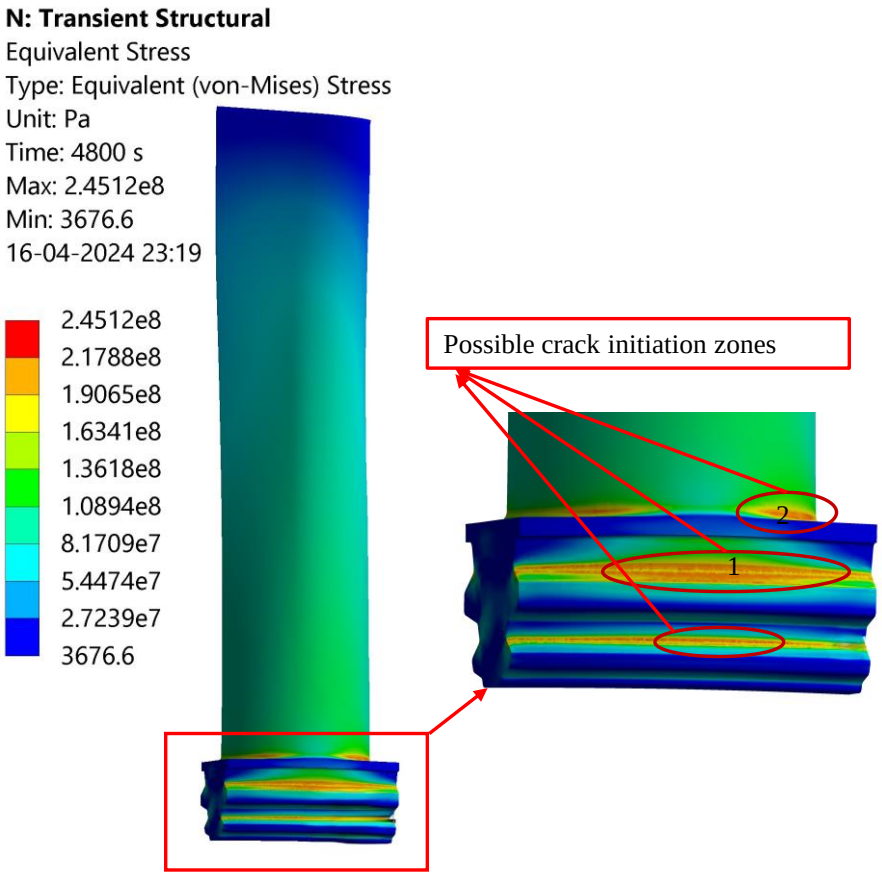

Figure 5.20 Von Mises equivalent stress distribution on blade after 4800 seconds of cold start

The following operating statistics are taken into consideration for the lifetime calculations:

For creep life damage evaluation

Based on the loading data available from the site, it has been assumed that the unit has been run with the following load conditions under steady-state operation.

- 100% load for 60% of total time 1,52, 241 hours
- 90% load for 20% of total time 1,52, 241 hours
- 80% load for 10% of total time 1,52, 241 hours
- < 80% load for 10% of total time 1,52, 241 hours

For life consumption due to Fatigue

210 MW unit was commissioned in April 1994. And the blade considered for study has clocked 1,52, 241 hours.) The estimated data for the total start-up of the turbine since commissioning are 379 till Dec. 2017. As per the data from the site for the limited period of operation of the blade, the following data has been estimated for Fatigue calculations as mentioned:

- No. of Cold starts -56
- No. of Hot starts- 118
- No. of Warm starts -205
- Total No. of starts- 379

Using the method outlined above in Section 5.5.1 and the operational data provided here, the lifetime expense is calculated. Table 5.10 provides an overview of the computations' findings. As can be seen from the table 5.10, location 1 has experienced a substantial accumulation of creep and fatigue damage, which together only leaves the blade with a very limited life expectancy of 60238 hours. Fatigue damage is dominant and creep damage is negligible. Non-destructive tests and metallurgical analyses were carried out as part of the blade lifetime evaluation [125]. While metallurgical investigations included hardness tests, tensile test and microstructure inspections, non-destructive exams included visual and dye penetration test. The findings show greatest damage to the blade’s surfaces is at location 1, because it has the minimum hardness value and the largest grains of medium-sized carbides and bulky carbides indicating the highest microstructure damage. Figure 5.21 displays a picture of the microscopic test's substructure.

Table 5.10

Life assessment of the blade

Location	Fatigue damage			Creep damage	Total damage	Remaining life
	Cold	Warm	Hot			
1	0.718	0.012	0.019	0.019	0.768	60238 hrs
2	0.304	0.023	0.024	0.032	0.383	159,926 hrs

The failure probability is 0.05% at position 1, where the total damage value is approx. 0.7676 which is very near to critical damage, and 0.005% at place 2, where the damage is equal to 0.383**.**

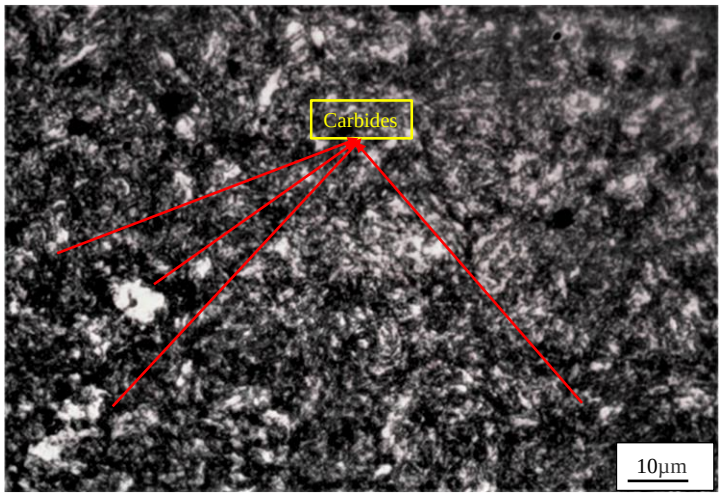

Figure 5.21 Material microstructure at location 1 at 100x

The absence of creep-fatigue cracking on the blade surface is consistent with forecasts of theoretical damage. Based on the simulation results (table 5.10), the crack initiation probability in the blade was calculated according to the procedure outlined in Section 5.5.2. Figures 5.22 and 5.23 show the calculated findings.

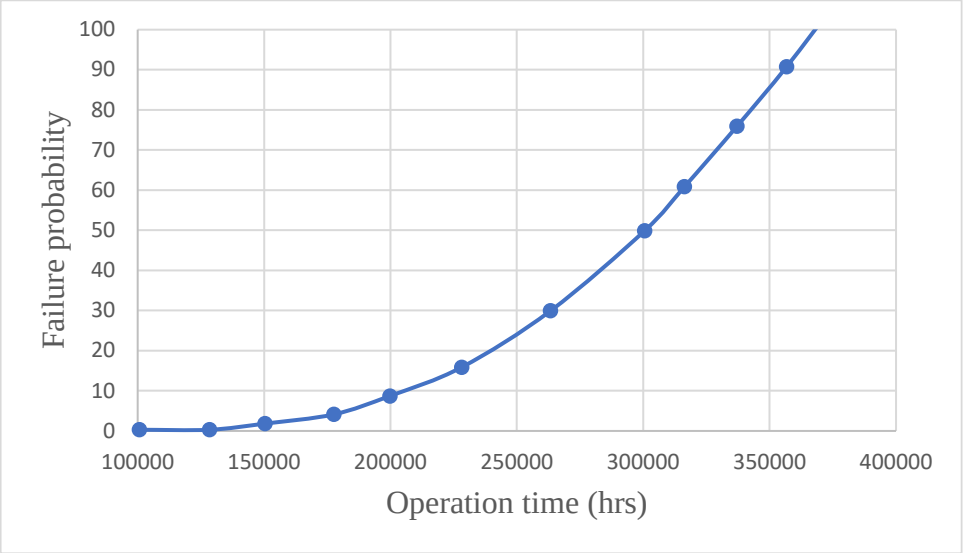

Figure 5.22 Failure probability at location 1

The probability of failure is 0.05% at location 1, where the damage level is currently around 0.7, which is very near to the critical value.

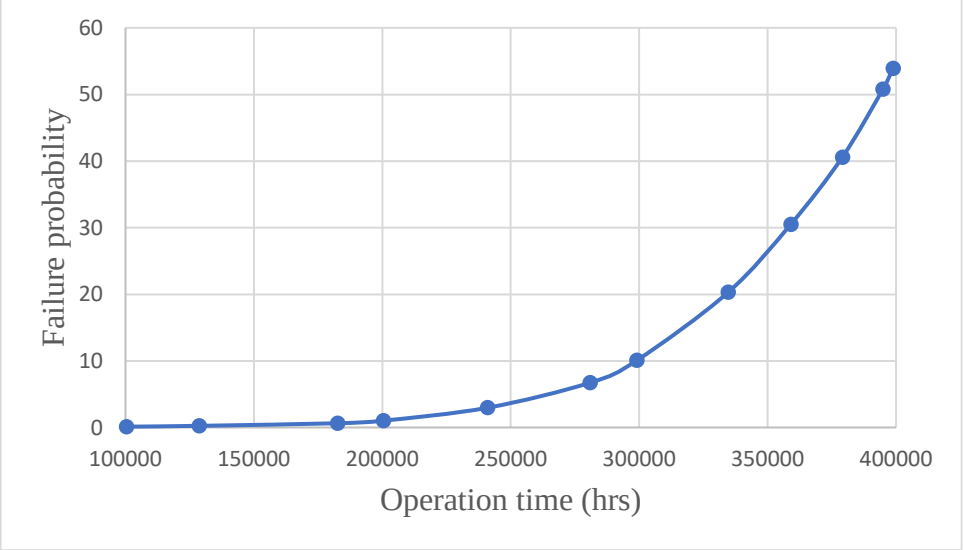

Figure 5.23 Failure probability at location 2

Here failure, rather than total rupture, is characterised as the beginning of a crack due to fatigue or the onset of tertiary creep. Regular inspections can track the development of fatigue cracks on the blade surface, however monitoring tertiary creep operation is extremely dangerous. It should be emphasised that failure probability does not just depend on the passage of time and the extent of damage. Instead, the failure probability will depend on how much creep and fatigue damage are involved, and the suggested method takes this into account.

5.7 Fracture mechanics' approach

The surface of the blade at position 1 is the most heavily worn, and it has the most likelihood of crack getting initiated. Furthermore, because the stress intensity factor (SIF) is greatest in this location, the crack is likely to propagates faster here. SIF is defined by the maximum level of stress for determined stress and temperature distributions throughout startup and steady-state operation, Paris' law can be used to analyse crack propagation owing to fatigue.

Since transient stresses are greatest during the cold start-shutdown cycle, that is when cracks spread the quickest. In order to learn more about the current safety margin and additional safe operation time, it is helpful to compare the actual crack size to its critical value.

Critical crack length

Assume the available non-destructive technique can detect all cracks of size greater than 0.5 mm. So initial crack size on blade surface can be taken as 0.5 mm, with SIF being given by $K_I = \beta\left(\sigma\sqrt{\pi a}\right)$, where β is configuration factor assumed to be 1.13.

Combined peak thermal and centrifugal stress value is 556 MPa. Assuming fracture toughness of X20Cr13 blade material lies in the range 50-80 MPa$\sqrt{m}$, the lower value of fracture toughness 50 MPa$\sqrt{m}$ is considered for finding the no. of cycles required to propagate the crack to critical size. The critical crack size corresponding to the above data is 2 mm.

Crack propagation rate

Crack grows according to Paris' law given by

$$\frac{da}{dn} = C\Delta K^m$$

For martensitic stainless steel, $C = 2.02 \times 10^{-11}$and $m = 2.66$ [96]where ΔK is given in MPa$\sqrt{m}$. ΔK is stress intensity factor range.

The number of cycles until the crack propagates to failure is given by

$$N_f = \int_{a_0}^{a_f} \frac{da}{C(\Delta\sigma\sqrt{\pi a}\beta)^m}$$

Where a_0 is initial crack length equal to 0.5 mm and a_f is critical crack length equal to 2mm. The estimated number of cycles for failure is 6481. The blade has undergone only 379 startup and shutdown cycles over 152,241 hours of operation. So, according to fracture mechanics approach, the blade can still be used.

Maximum stress due to steam pressure on blade surface is seen to be about 38 MPa. The value of threshold stress intensity factor for the turbine blade material is 4.5 MPa$\sqrt{m}$ [36]. The crack size corresponding to 38 MPa applied stress required to achieve SIF of 4.5 MPa$\sqrt{m}$

is 3 mm. Since crack size assumed in the blade is below 2 mm, the crack will not grow due to the bending stress caused by steam forces which are causing alternating stresses for every rotation of the rotor shaft.

The methodology for lifetime assessment outlined in this study for assessing the lifetime of steam turbine components is of significant practical importance. Starting with deterministic damage assessment, it progresses to probabilistic and fracture mechanics methods, providing valuable insights for damage assessment and remaining life estimations. Widely used by lifetime assessment engineers and validated through numerous studies, this methodology is integrated into engineering tools. M. Banaszkiewicz [33] exemplified this method through a practical application to a steam turbine rotor & Mariusz Banaszkiewicz and Ralf Gerdes [150] applied to an 200 MW turbine HP stop valve manufactured by ALSTOM Power Elblag.

5.8 Comments on numerical simulation of seventh stage LP blade

- This chapter provides a prediction of the maximum damage and minimum life of the low-pressure stage blade of a 210 MW steam turbine under LCF circumstances. Using finite element analysis, the minimum life and maximum damage of a blade containing a fir-tree root region are estimated subjected to centrifugal loads and steam pressure.
- From the FE-based numerical analysis, the Von Mises stresses have been extracted, and the minimum life and maximum damage of the blade were computed using the Morrow, strain life, and SWT approaches, respectively. Since SWT includes more analysis variables, it provides a more accurate prediction in steam turbine blades for damage detection. The fatigue life of the blades of a steam turbine isn’t compromised by high stresses produced by steam forces to seriously threaten the steam turbine blades' ability to withstand pressure. The results of this study, however, suggested that the beginning and growth of cracks may be influenced by centrifugal stresses.
- The findings revealed that the area closest to the blade's root had the most damage. Previous investigations [119], [176]–[178] revealed that damage was greatest at the root and fir-tree zone of the blade roots. Therefore, cracks are anticipated to emerge there.
- By combining FSI and elastic-plastic analysis techniques, the chapter aims to provide a comprehensive understanding of the strength performance of the last stage blade, accounting for both fluid dynamics and structural response. This approach can lead to more accurate predictions and insights into the blade's behaviour, which is essential for optimizing its design and ensuring its structural integrity.

- This chapter also presents a useful way for estimating the lifetime of steam turbine parts. This method is a multi-tiered strategy that utilises cutting-edge techniques and software for temperature, stress, and damage estimates. Theoretical investigations typically begin with a deterministic damage estimate as a foundational level. Probabilistic and fracture mechanics-based supplementary analyses add valuable insight to component damage assessments and remaining life estimations.
- For both estimating how long a turbine will last under current operating conditions and discovering how changes in service will affect its lifespan, a thorough understanding of the existing damage state is essential.
- Damage calculations are used to designate high-risk areas for testing, but they also provide crucial details such as: - the predominance of a certain mechanism that led to damage at a given place; - the level of damage for the worst possible properties of material; and damage accumulation rate. This data can be used to define suggestions for fixing broken parts, increasing inspection intervals, or shifting the way the machine is used. From a failure probability standpoint, the combined effect of fatigue-creep damage is also crucial. The probability of failure is affected by the relative contributions of creep and fatigue damage to the total damage [33].
- We calculated a damage of amount 0.7676 and 0.383 at location 1 and 2 respectively. By probabilistic approach, failure probability is 0.05% at position 1 and 0.005% at position 2.
- According to Fracture Mechanics' approach, the blade still has useful remaining life.
- Overall, steam turbine blade life assessment methodology based on deterministic damage calculation, fracture mechanics consideration and probabilistic simulation is a comprehensive approach that can help to ensure the safe and efficient operation of steam turbines.

5.9 Summary of chapter

The assessment of remaining life in steam turbine blades is a critical endeavor in the field of mechanical engineering, particularly in the realm of power generation. As steam turbines serve as the workhorses of many industrial processes, ensuring their continued reliability and efficiency is paramount. Among the various components of a steam turbine, the blades are particularly vulnerable to degradation over time due to factors such as cyclic loading, high temperatures, and erosion.

The theoretical framework for evaluating the lifespan of steam turbines, as outlined in this study, holds significant practical significance. It serves as a valuable complement to deterministic analysis and can be utilised in the development of practical tool engineering simulations. There are several advantages associated with the probabilistic technique in comparison to the deterministic approach.

Probabilistic analysis places significant focus on the input data, such as the fatigue and creep characteristics that are examined in the study. For conducting a lifetime consumption analysis, it is necessary to provide not only the average or lowest values of a specific quantity, but also a description of its uncertainty, typically in the form of a probability distribution.

Furthermore, the outcomes of probabilistic calculations are especially crucial for periods of operation when the damage surpasses the critical threshold. Once this threshold is reached, as per the deterministic model, it becomes impossible to monitor the operation using computational methods due to the unknown risk of failure. Currently, probabilistic approaches are assuming a prominent role as they yield a distribution of failure probabilities throughout ongoing operation. Hence, it serves as a complementary approach to deterministic analysis and expands the scope of theoretical lifetime research.

Furthermore, the probabilistic approach offers a robust foundation for making decisions regarding running or retiring. The ultimate determination of retirement is contingent upon the evaluation of the trade-off between the potential risks and benefits associated with ongoing operation.

CHAPTER 6

CONCLUSIONS AND FUTURE SCOPE

6.1 Conclusions

The primary aim of this research is to assess the remaining life of a turbine blade used in a steam thermal power plant. Chapter 2 explores various approaches for diagnosing the underlying reasons of turbine blade failure. Chapter 3 proposes various remedial measures to mitigate future failures and enhance the longevity of a low-pressure steam turbine blade. The primary objective of the thesis is to examine the factors that contributed to failure of the low-pressure seventh stage steam turbine blade. This blade was rejected after being in operation for a total of 1,52,241 hours.

Various fractographic and metallographic techniques have been used to identify the causes of failure in low pressure seventh stage steam turbine blade. The turbine blade underwent experimental analysis using visual examination, chemical analysis, dye penetration testing, and metallurgical testing: optical microscopy, scanning electron microscopy (SEM), Energy-dispersive X-ray (EDAX) analysis. The results of this inquiry are as follows:

- This blade has completed over 100000 hours of operation and some pits and dent marks were observed in the profile of blade. That is the reason for blade rejection.
- The premature failure of a low-pressure steam turbine blade is investigated here. The blade had only been in service for 152241 hours. The literature indicates that blades with erosion and corrosion pits are more prone to fatigue cracks. For this reason, blades with erosion and corrosion pits should be inspected routinely.
- No crack or any other defect like appearance was noticed on the surface in visual inspection of a turbine blade. However, considerable erosion damage was observed on edge sections of Blade.
- It was determined that the blade material was not faulty based on chemical analysis and mechanical testing.
- The turbine blade under inquiry did not fail due to a material flaw, according to the dye penetration testing and microstructure study.

- The defective sections were carefully analyzed in order to determine the causes of failure, and it was found that water droplet erosion was the cause of blade damage. Identifying the deteriorating mode in advance allows us to replace and repair turbine parts at the best possible moment, reducing the need for unneeded replacement and preventing unscheduled outages.
- The metallurgical analysis showed that the fracture initiation locations were concentrated in erosion pits, which increased the local stresses. Corrosion deposits were discovered in the same area (erosion pits). As a result of these tests, it can be said that erosion and corrosion can play a major role in both the onset and spread of blade failure.
- This study found that the water droplet erosion induced multiple pits on the surface of the X20Cr13 martensitic stainless-steel blade, which eventually coalesced into a large void and it can lead to crack initiation that may cause the turbine blade to fail. The failure was primarily attributed to the possible sites of fatigue crack initiation at erosion pits and the presence of non-metallic inclusions, such as oxides in the material.
- The microstructure analysis revealed that the material exhibited a typical martensitic microstructure with a high density of carbides and some retained austenite. The presence of carbides and retained austenite is known to have a significant effect on the mechanical properties of the material, including its toughness and fatigue strength.
- The investigation also provides valuable insights into the degradation mechanisms of X20Cr13 under erosive conditions. Silicate and sodium oxides were found on the damaged surface. Because of this, corrosion pits form, and the corrosion attack occurs.
- SEM fracstographs of the erosion pit at 100x,300x,500x and higher magnification at 1000x, 2000x, and 4000x were shown in the Figures along with a picture of the pits across the edge of the blade. Electron dispersive spectroscopy analysis of the contents of the pit revealed the presence of corrosive compounds with specific spectral features. Element analysis of the deposits in the pits showed that they consisted of a mix of iron, chromium, and silicon oxides.
- It is also concluded that the oxidation of the chromium carbide results in the formation of chromium oxide, which in turn leaves pores on the blade.
- The fractographic examination revealed that the sizes of pits are 5µm,10µm, 50µm, and 100µm,150µm and the reason is chemical erosion not mechanical.

Through the application of advanced analytical tools such as finite element analysis (FEA) and computational fluid dynamics (CFD), this study has elucidated the complex

interplay between mechanical loading, and aerodynamic forces, enabling a more nuanced understanding of fatigue mechanisms in turbine blades. The stress and strains generated on turbine blade at different operational speeds has been also evaluated. The findings of FEA analysis are as follows:

- This analysis provides a prediction of the maximum damage and minimum life of the low-pressure stage blade of a 210 MW steam turbine under LCF circumstances. Using finite element analysis, the minimum life and maximum damage of a blade containing a fir-tree root region are estimated subjected to centrifugal loads and steam pressure.
- From this numerical analysis, the Von Mises stresses have been extracted, and the minimum life and maximum damage of the blade were computed using the Morrow, strain life, and SWT approaches, respectively. Since SWT includes more analysis variables, it provides a more accurate prediction in steam turbine blades for damage detection.
- For the Strain life method, the estimated number of cycles to failure of the steam turbine blade at 3000 RPM is approximately 6.23×10^{6} cycles, with total damage cycle being 1.89×10^{2}. Using the Morrow method, the blade is expected to fail after approximately 2.33×10^{6} cycles, with total damage cycles of 7.86×10^{1}. Finally, applying the SWT method predicts a fatigue life of approximately 6.22×10^{5} cycles, with corresponding damage cycles of 1.61×10^{5}. A total damage value of 1 signifies complete failure of the steam turbine blade. Comparing the total damage values obtained from the different fatigue life estimation methods to this threshold, it can be observed that none of the methods indicate complete failure at 3000 RPM. However, the Morrow method suggests the lowest total damage, followed by the SWT method and the Strain life method, indicating varying levels of fatigue damage accumulation under the given operating conditions.
- The fatigue life of the blades of last stages of low-pressure steam turbine isn’t compromised by high stresses produced by steam forces to seriously threaten the steam turbine blades' ability to withstand pressure. The results of this study, however, suggested that the beginning and growth of cracks may be influenced by centrifugal stresses.
- The findings revealed that the area closest to the blade's root had the most damage. Previous investigations [119], [176]–[178] revealed that damage was greatest at the

root and fir-tree zone of the blade roots. Therefore, cracks are anticipated to emerge there.

- By combining FSI and elastic-plastic analysis techniques, the analysis aims to provide a comprehensive understanding of the strength performance of the last stage blade, accounting for both fluid dynamics and structural response. This approach can lead to more accurate predictions and insights into the blade's behaviour, which is essential for optimizing its design and ensuring its structural integrity.

Furthermore, the calculation of remaining life in steam turbine blades has emerged as a crucial endeavour for ensuring the continued reliability and performance of these components throughout their operational lifespan. By integrating theoretical models with empirical data and predictive simulations, methodologies have been developed for estimating remaining life based on factors such as fatigue damage accumulation, material degradation, and operating conditions. Through the utilization of advanced software platforms such as ANSYS, the feasibility of conducting detailed remaining life assessments has been demonstrated, providing actionable insights for maintenance scheduling, component replacement, and operational optimization.

- This methodology presents a useful way for estimating the lifetime of steam turbine parts. This method is a multi-tiered strategy that utilises cutting-edge techniques and software for temperature, stress, and damage estimates. Theoretical investigations typically begin with a deterministic damage estimate as a foundational level. Probabilistic and fracture mechanics-based supplementary analyses add valuable insight to component damage assessments and remaining life estimations.
- For both estimating how long a turbine will last under current operating conditions and discovering how changes in service will affect its lifespan, a thorough understanding of the existing damage state is essential.
- Damage calculations are used to designate high-risk areas for testing, but they also provide crucial details such as: - the predominance of a certain mechanism that led to damage at a given place; - the level of damage for the worst possible properties of material; and damage accumulation rate. This data can be used to make suggestions for fixing broken parts, increasing inspection intervals, or shifting the way the machine is used. From a failure probability standpoint, the combined effect of fatigue-creep damage is also crucial. The probability of failure is affected by the relative contributions of creep and fatigue damage to the total damage [33].

- A damage of amount 0.7676 and 0.383 at location 1 and 2 respectively were calculated. By probabilistic approach, failure probability is 0.05% at position 1 and 0.005% at position 2.
- According to Fracture Mechanics' approach, the blade still has useful remaining life.
- Overall, steam turbine blade life assessment methodology based on deterministic damage calculation, fracture mechanics consideration and probabilistic simulation is a comprehensive approach that can help to ensure the safe and efficient operation of steam turbines.

6.2 Recommendations regarding the component repair, inspection intervals or modification of operating conditions based on above conclusions

- The thermal power plant has a life span of 30-35 years. However, life of a blade depends upon the operational history as well as maintenance activities. There is no hard and fast time frame for the replacement of blade. Blades are recommended for check-up after 100000 hours of operation.
- General inspection of the blades can be done while they are mounted on the rotor. However, in case of any visible defect or higher vibration or after completing 1 lakh hours of operation, blades are dismounted and MPI is done on profile as well as on the root of blades to decide for its further operation.

To avoid water droplet induced erosion and pitting of the last stage of LP blade, following measures can be used:

- Moisture removal from steam in the last stage hollow guide blade by having slits on profile part.
- Supply of hot steam inside hollow guide blade.
- Flame hardening/ laser hardening of inlet edge of last stage moving blade (shown in figure 6.1).

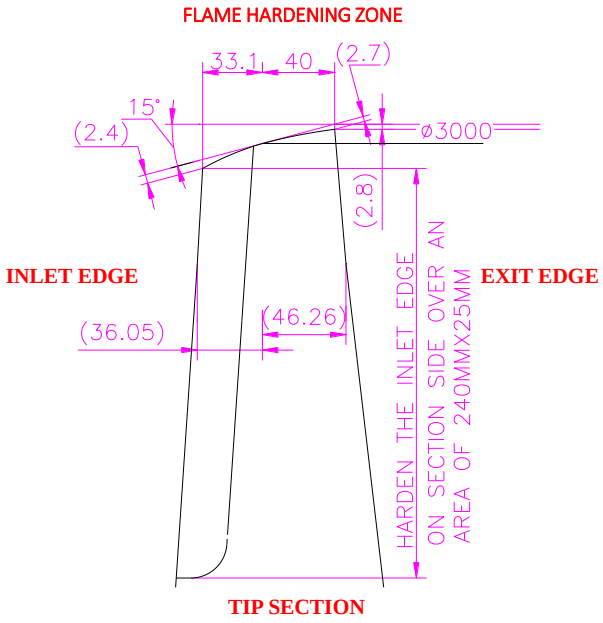

Figure 6.1 Flame hardening zone of LP blade

The evolution of maintenance strategies for steam turbine components has shifted towards condition-oriented approaches, aiming to optimize plant reliability and availability while reducing maintenance costs. Original Equipment Manufacturers (OEMs) have developed sophisticated plant data management systems that leverage real-time operation and condition data, expert analysis, and diagnostic modules to support operators in daily operations, maintenance scheduling, and outage management.

- These systems facilitate the implementation of spot-on maintenance programs tailored to individual plant needs, enabling operators to extend service intervals by operating units in gentle modes while ensuring the utilization of critical components' actual lifetimes. The emphasis is on condition-oriented maintenance, allowing for longer intervals between major overhaul outages while prioritizing maintenance tasks towards areas of highest risk within the steam turbine.
- For the low-pressure (LP) turbine blade, recommendations for component repair, inspection intervals, or modifications of operating conditions should align with this condition-oriented approach. Inspection intervals should be informed by real-time monitoring and diagnostic reports, focusing on detecting hidden or developing problems that could lead to blade failures. Additionally, modifications to operating conditions should be considered to mitigate risks such as overspeed, water induction, loss of lube oil, or corrosive steam, all of which pose significant threats to turbine integrity and reliability.

- In summary, the key recommendation is to adopt a proactive and data-driven approach to LP turbine blade maintenance, prioritizing tasks and frequencies based on risk assessment and real-time condition monitoring. By doing so, operators can enhance plant reliability, extend service intervals, and minimize the risk of forced outages due to turbine damage.

6.3 Future directions

This work does not explicitly discuss the sensitivity of the results to various input parameters. Conducting a sensitivity analysis could help identify the most influential parameters on fatigue life predictions and guide efforts to improve accuracy and robustness.

The thesis focuses on fatigue life evaluation, but it may be worthwhile to also investigate other failure modes like creep. Future research could explore the integration of more advanced fatigue models, such as multiaxial fatigue criteria or damage accumulation models, to capture the complex stress states experienced by turbine blades and provide more accurate fatigue life predictions.

Bibliography

[1] S. Kumar, B. Bhattacharyya, and V. K. Gupta, “Present and Future Energy Scenario in India,” *J. Inst. Eng. Ser. B*, vol. 95, no. 3, pp. 247–254, Sep. 2014, doi: 10.1007/S40031-014-0099-7/TABLES/3.

[2] HLEC, “Report of the High Level Empowered Committee to Address the issues of Stressed Thermal Power Projects.,” 2018.

[3] M. Heidari and K. Amini, “Structural modification of a steam turbine blade,” *IOP Conf. Ser. Mater. Sci. Eng.*, vol. 203, no. 1, 2017, doi: 10.1088/1757-899X/203/1/012007.

[4] S. Senoo, D. Ph, and G. Lee, “Titanium 50 - inch and 60 - inch Last-stage Blades for Steam Turbines,” vol. 62, no. 1, pp. 23–30, 2013.

[5] “The twin problems that India’s thermal power sector must overcome,” *The Economic Times*, p. 51056423, Feb. 2017.

[6] D. Dowson and D. Bauer, “Remaining Life Assessment of Steam Turbine and Hot Gas Expander Components,” *Asia Turbomachinery & Pump Symposium*, USA, Feb. 2016.

[7] M. Banaszkiewicz, “Steam turbines start-ups,” *Trans. Inst. Fluid-Flow Mach.*, vol. 14, no. 126, pp. 169–198, 2014, [Online]. Available: https://www.imp.gda.pl/files/transactions/126/126_12_.pdf.

[8] M. Banaszkiewicz, “Numerical Modeling of Cyclic Creep-Fatigue Damage Development for Lifetime Assessment of Steam Turbine Components,” *Therm. Power Plants - New Trends Recent Dev.*, 2018, doi: 10.5772/intechopen.73186.

[9] P. D. Murari P. Singh and P. George M. Lucas, “Blade Design and Analysis for Steam Turbines,” in *McGraw-Hill Education*, vol. 6, no. August, McGraw-Hill Education, 2011, p. 128.

[10] C. R. F. Azevedo and A. Sinátora, “Erosion-fatigue of steam turbine blades,” *Eng. Fail. Anal.*, vol. 16, no. 7, pp. 2290–2303, 2009, doi: 10.1016/j.engfailanal.2009.03.007.

[11] D. Yu *et al.*, “A LCF Life Assessment Method for Steam Turbine Long Blade Based on Elastoplastic Analysis and Local Strain Approach,” *Proc. ASME Turbo Expo*, vol. 8, Aug. 2015, doi: 10.1115/GT2015-43955.

[12] T. Tanuma, “Development of last-stage long blades for steam turbines,” in *Advances in Steam Turbines for Modern Power Plants*, Tadashi Tanuma, Ed. Japan: Woodhead Publishing, Elsevier, 2017, pp. 279–305.

[13] K. A. Soady, “Reducing conservatism in life assessment approaches: Industrial steam turbine blade to disc interfaces and the shot peening process,” *Proc. Int. Jt. Conf. Biometrics*, 2013.

[14] “NPTEL.” https://nptel.ac.in/courses/112108150 (accessed Sep. 26, 2023).

[15] K. B. Syariah and G. Ilmu, *Advances in Steam Turbines for Modern Power Plants*, no. september 2016. Woodhead Publishing, Elsevier, 2017.

[16] S. K. Giri, M. Krishnan, and U. Ramamurty, “Enhancement of fatigue life of Ni-Ti-Fe shape memory alloys by thermal cycling,” *Mater. Sci. Eng. A*, vol. 528, no. 1, pp. 363–370, 2010, doi: 10.1016/j.msea.2010.09.006.

[17] S. Suresh, “Total-Life Approaches,” *Fatigue of Materials*. 1998.

[18] S. P. Zhu, Q. Liu, W. Peng, and X. C. Zhang, “Computational-experimental approaches for fatigue reliability assessment of turbine bladed disks,” *Int. J. Mech. Sci.*, vol. 142–143, pp. 502–517, Jul. 2018, doi: 10.1016/J.IJMECSCI.2018.04.050.

[19] D. Tulsidas, M. Shantharaja, and V. G. Bharath, “Life Estimation of a Steam Turbine Blade Using Low Cycle Fatigue Analysis,” *Procedia Mater. Sci.*, vol. 5, pp. 2392–2401, Jan. 2014, doi: 10.1016/J.MSPRO.2014.07.484.

[20] R. Citarella, M. A. Lepore, M. Shlyannikov, and Yarullin R, “Fatigue Crack Growth by FEM-DBEM Approach in a Steam Turbine Blade ‘Advanced Numerical Approaches for Crack Growth Simulation’ View project,” *Ind Eng Manag.*, vol. 4, no. 2, 2015, doi: 10.4172/2169-0316.1000160.

[21] V. N. Shlyannikov, R. R. Yarullin, and A. P. Zakharov, “Fatigue of Steam Turbine Blades With Damage on the Leading Edge,” *Procedia Mater. Sci.*, vol. 3, pp. 1792–1797, Jan. 2014, doi: 10.1016/J.MSPRO.2014.06.289.

[22] M. Banaszkiewicz, “Numerical investigations of crack initiation in impulse steam turbine rotors subject to thermo-mechanical fatigue,” *Appl. Therm. Eng.*, vol. 138, pp. 761–773, Jun. 2018, doi: 10.1016/J.APPLTHERMALENG.2018.04.099.

[23] M. Banaszkiewicz and A. Rehmus-Forc, “Stress corrosion cracking of a 60 MW steam turbine rotor,” *Eng. Fail. Anal.*, vol. 51, pp. 55–68, May 2015, doi: 10.1016/J.ENGFAILANAL.2015.02.015.

[24] A. L. Tejeda, J. A. Rodríguez, J. M. Rodríguez, J. C. García, and M. A. Basurto-Pensado, “Failure Analysis to Blades of Steam Turbines at Normal Conditions of Operations and Resonance,” *Adv. Mater. Res.*, vol. 891–892, pp. 54–59, 2014, doi: 10.4028/WWW.SCIENTIFIC.NET/AMR.891-892.54.

[25] R. N. Salzman, N. F. Rieger, and L. Wang, “Turbine Blade Fatigue Crack Growth,” *Am. Soc. Mech. Eng. Power Div. PWR*, vol. 35, pp. 333–339, Nov. 2008, doi: 10.1115/POWER2004-52138.

[26] Z. Mazur, R. García-Illescas, and A. Hernández-Rossette, “Steam Turbine Low Pressure Blades Fatigue Failures Caused by Operational and External Conditions,” *Proc. ASME Turbo Expo*, vol. 6, no. PART A, pp. 93–106, Feb. 2010, doi: 10.1115/GT2009-59040.

[27] B. M. Schönbauer *et al.*, “Fatigue life estimation of pitted 12% Cr steam turbine blade steel in different environments and at different stress ratios,” *Int. J. Fatigue*, vol. 65, pp. 33–43, 2014, doi: 10.1016/j.ijfatigue.2013.10.003.

[28] M. Shakeel, M. Anis, M. Ali, S. F. Hasan, and H. A. Saeed, “Fatigue Analysis of Low-Pressure Steam Turbine Blades during Startup Using Probabilistic Concepts . Fatigue

Analysis of Low-Pressure Steam Turbine Blades during Start- up using Probabilistic Concepts," in *International Conference on Advances in Mechanical Engineering (ICAME), Pakistan*, 2022, no. March.

[29] A. Roy, "A Take Stock of Turbine Blades Failure Phenomenon," *J. Inst. Eng. Ser. C*, vol. 99, no. 1, pp. 97–103, 2018, doi: 10.1007/s40032-017-0375-9.

[30] S. M. S. Kumar, Manju.M, and Raghavendra.S, "Creep life prediction of steam turbine blade using finite element method," *Int. J. Adv. Eng. Res. Stud.*, vol. 1, no. 2, pp. 95–98, 2012.

[31] M. Banaszkiewicz, "Analysis of Rotating Components Based on a Characteristic Strain Model of Creep," *J. Eng. Mater. Technol. Trans. ASME*, vol. 138, no. 3, pp. 1–11, 2016, doi: 10.1115/1.4032661.

[32] M. Banaszkiewicz, "Materials at High Temperatures Creep life assessment method for online monitoring of steam turbine rotors," *Mater. High Temp.*, vol. 00, no. 00, pp. 1–14, 2019, doi: 10.1080/09603409.2019.1570701.

[33] M. Banaszkiewicz, "Multilevel approach to lifetime assessment of steam turbines," *Int. J. Fatigue*, vol. 73, pp. 39–47, 2015, doi: 10.1016/j.ijfatigue.2014.10.009.

[34] J. S. Rao, "Turbine blade life estimation," *Alpha Sci. Int'l Ltd*, 2000.

[35] J. A. Segura, L. Castro, I. Rosales, J. A. Rodriguez, G. Urquiza, and J. M. Rodriguez, "Diagnostic and failure analysis in blades of a 300 MW steam turbine," *Eng. Fail. Anal.*, vol. 82, no. April, pp. 631–641, 2017, doi: 10.1016/j.engfailanal.2017.04.039.

[36] E. Plesiutschnig, P. Fritzl, N. Enzinger, and C. Sommitsch, "Fracture analysis of a low pressure steam turbine blade," *Case Stud. Eng. Fail. Anal.*, vol. 5–6, pp. 39–50, 2016, doi: 10.1016/j.csefa.2016.02.001.

[37] N. S. Vyas and J. S. Rao, ""Fatigue Life Estimation Procedure for a Turbine Blade Under Transient Loads.," *ASME. J. Eng. Gas Turbines Power*, vol. 1, no. 116, pp. 198–206, 1994, doi: https://doi.org/10.1115/1.2906792.

[38] S. Holdsworth, "Creep-fatigue failure diagnosis," *Materials (Basel).*, vol. 8, no. 11, pp. 7757–7769, Nov. 2015, doi: 10.3390/ma8115418.

[39] D. Saidi, B. Zaid, N. Souami, M. Negache, and A. S. Ahmed, "Microstructure and fracture mode of a martensitic stainless steel steam turbine blade characterized via scanning auger microscopy and potentiodynamic polarization," *IOP Conf. Ser. Mater. Sci. Eng.*, vol. 60, no. International Symposium on Advanced Materials (ISAM 2013) 23–27 September 2013, Islamabad, Pakistan, pp. 1–9, 2014, doi: 10.1088/1757-899X/60/1/012004.

[40] A. Shukla and S. P. Harsha, "An Experimental and FEM Modal Analysis of Cracked and Normal Steam Turbine Blade," *Mater. Today Proc.*, vol. 2, no. 4–5, pp. 2056–2063, 2015, doi: 10.1016/j.matpr.2015.07.191.

[41] A. Shukla and S. P. Harsha, "Vibration Response Analysis of Last Stage LP Turbine Blades for Variable Size of Crack in Root," *Procedia Technol.*, vol. 23, pp. 232–239, 2016, doi: 10.1016/j.protcy.2016.03.022.

[42] J. Pereira, L. A. M Torres, T. S. Energia Florianópolis, B. E. da Rosa, H. Bindewald, and M. Eng, "A Low Cycle Fatigue Analysis on a Steam Turbine Bladed Disk-Case

Study," *12 th IFToMM World Congr*.

[43] N. Vyas, J. R.-M. and machine theory, and undefined 1997, "Dynamic stress analysis and a fracture mechanics approach to life prediction of turbine blades," *Elsevier*, Accessed: Oct. 03, 2023. [Online]. Available: https://www.sciencedirect.com/science/article/pii/S0094114X96000675.

[44] Britannica, "The Editors of Encyclopaedia. 'Sir Charles Algernon Parsons'. Encyclopedia Britannica, 7 Feb. 2024, https://www.britannica.com/biography/Charles-Algernon-Parsons. Accessed 30 March 2024.," 2024. .

[45] Nick Connor, "What is Steam Turbine – Description and Characteristics– Definition," 2019. https://www.thermal-engineering.org/what-is-steam-turbine-description-and-characteristics-definition/.

[46] Kenneth S. Krane., *Introductory Nuclear Physics*, 3rd Editio. Wiley, 1987.

[47] S. Glasstone and A. Sesonske, *Nuclear Reactor Engineering: Reactor Systems Engineering*, 4th ed. Springer, 1994.

[48] "https://www.nuclear-power.com/nuclear-power-plant/turbine-generator-power-conversion- system/what-is-steam-turbine-description-and-characteristics/." info@nuclear-power.com.

[49] P. D. Murari P. Singh and P. George M. Lucas, *Blade Design and Analysis for Steam Turbines*, no. august. New York: McGraw-Hill Education, 2011.

[50] D. Maxell, "The History of the Steam Turbine," *Pacific Turbines*, no. 1629, 1996.

[51] N. P. Plant, R. Physics, and R. Protection, "LP Turbine - Low-pressure Steam Turbine | nuclear-power.com," pp. 1–6, [Online]. Available: https://www.nuclear-power.com/nuclear-power-plant/turbine-generator-power-conversion-system/what-is-steam-turbine-description-and-characteristics/lp-turbine-low-pressure-steam-turbine/.

[52] M. Benedetti, V. Fontanari, and B. Monelli, "Numerical simulation of residual stress relaxation in shot peened high-strength aluminum alloys under reverse bending fatigue," 2010, Accessed: Sep. 23, 2023. [Online]. Available: https://asmedigitalcollection.asme.org/materialstechnology/article-abstract/132/1/011012/403588.

[53] M. Benedetti, V. Fontanari, C. Santus, and M. Bandini, "Notch fatigue behaviour of shot peened high-strength aluminium alloys: Experiments and predictions using a critical distance method," *Int. J. Fatigue*, vol. 32, no. 10, pp. 1600–1611, 2010, doi: 10.1016/j.ijfatigue.2010.02.012.

[54] X. Song *et al.*, "An eigenstrain-based finite element model and the evolution of shot peening residual stresses during fatigue of GW103 magnesium alloy," *Int. J. Fatigue*, vol. 42, pp. 284–295, 2012, doi: 10.1016/j.ijfatigue.2012.01.019.

[55] P. J. Budden, J. K. Sharples, and A. R. Dowling, "The R6 procedure: Recent developments and comparison with alternative approaches," *Int. J. Press. Vessel. Pip.*, vol. 77, no. 14–15, pp. 895–903, 2001, doi: 10.1016/S0308-0161(01)00012-6.

[56] R. A. Ainsworth and D. G. Hooton, "R6 and R5 procedures: The way forward," *Int. J. Press. Vessel. Pip.*, vol. 85, no. 3, pp. 175–182, 2008, doi: 10.1016/j.ijpvp.2007.10.003.

[57] M. Achintha and D. Nowell, “Eigenstrain modelling of residual stresses generated by laser shock peening,” *J. Mater. Process. Technol.*, vol. 211, no. 6, pp. 1091–1101, 2011, doi: 10.1016/j.jmatprotec.2011.01.011.

[58] M. N. James, M. Newby, D. G. Hattingh, and A. Steuwer, “Shot-peening of steam turbine blades: Residual stresses and their modification by fatigue cycling,” *Procedia Eng.*, vol. 2, no. 1, pp. 441–451, 2010, doi: 10.1016/j.proeng.2010.03.048.

[59] “EN_10088-3-stainless-steel.” .

[60] R. Dewey and N. Rieger, “Survey of steam turbine blade failures.,” United States, 1985. doi: EPRI-CS-3891 ON: TI85920554.

[61] E. R. Reinhart, “In-service inspection of steam turbine blades without disassembly,” *Am. Nucl. Soc. Int. Meet. Nucl. power plant Oper. Chicago, IL, USA*, vol. 54, 1987, Accessed: Sep. 24, 2023. [Online]. Available: https://www.osti.gov/biblio/5579556.

[62] M. Jobbins, “Fractography,” *Forensics, Materials Science*. https://www.nanoscience.com/applications/materials-science/fractography/.

[63] I. Le May, “Microstructural Analysis and Fractography BT - Microstructural Analysis: Tools and Techniques,” J. L. McCall and W. M. Mueller, Eds. Boston, MA: Springer US, 1973, pp. 153–168.

[64] L. Tian, Y. Hai, Z. Qingyue, and Y. Qin, “Non-destructive testing Techniques based on Failure Analysis of Steam Turbine Blade,” *IOP Conf. Ser. Mater. Sci. Eng.*, vol. 576, no. 1, 2019, doi: 10.1088/1757-899X/576/1/012038.

[65] K. Mondal and V. Verma, “Physical Metallurgy Lab Manual 2015-2016,” pp. 1–19, 2016.

[66] A. Molodtsov, A. Dedov, I. Klevtsov, L. Kommel, T. Lausmaa, and V. Mikli, “Investigation of steam turbine blades damage and reliability in a power plant,” *Key Eng. Mater.*, vol. 799 KEM, pp. 89–94, 2019, doi: 10.4028/www.scientific.net/KEM.799.89.

[67] W. Z. Wang, F. Z. Xuan, K. L. Zhu, and S. T. Tu, “Failure analysis of the final stage blade in steam turbine,” *Eng. Fail. Anal.*, vol. 14, no. 4, pp. 632–641, 2007, doi: 10.1016/j.engfailanal.2006.03.004.

[68] G. I. Ilieva, “Erosion failure mechanisms in turbine stage with twisted rotor blade,” *Eng. Fail. Anal.*, vol. 70, pp. 90–104, 2016, doi: 10.1016/j.engfailanal.2016.07.008.

[69] N. K. Mukhopadhyay, S. Ghosh Chowdhury, G. Das, I. Chattoraj, S. K. Das, and D. K. Bhattacharya, “an Investigation of the Failure of Low Pressure Steam Turbine Blades,” *Fail. Anal. Case Stud. II*, vol. 5, no. 3, pp. 211–223, 2001, doi: 10.1016/b978-0-08-043959-4.50021-3.

[70] M. C. Antony Harison, M. Swamy, A. H. V. Pavan, and G. Jayaraman, “Root Cause Analysis of Steam Turbine Blade Failure,” *Trans. Indian Inst. Met.*, vol. 69, no. 2, pp. 659–663, 2016, doi: 10.1007/s12666-015-0750-2.

[71] C. R. F. Azevedo and A. Sinátora, “Erosion-fatigue of steam turbine blades,” *Eng. Fail. Anal.*, vol. 16, no. 7, pp. 2290–2303, 2009, doi: 10.1016/j.engfailanal.2009.03.007.

[72] D. Dowson, “Metallurgical Failure Analysis of Steam Turbine, Compressor, and Hot Gas Expander Components,” SINGAPORE, 2018. [Online]. Available: https://hdl.handle.net/1969.1/172544.

[73] M. Sameezadeh, S. Hasanlou, H. Zafari, and M. Vaseghi, “Numerical simulation and experimental investigation on a steam turbine blade fractured from the lacing hole,” *Eng. Fail. Anal.*, vol. 117, no. July, p. 104809, 2020, doi: 10.1016/j.engfailanal.2020.104809.

[74] P. Puspitasari, A. Andoko, and P. Kurniawan, “Failure analysis of a gas turbine blade: A review,” *IOP Conf. Ser. Mater. Sci. Eng.*, vol. 1034, no. 1, p. 012156, 2021, doi: 10.1088/1757-899x/1034/1/012156.

[75] H. S. Kirols, D. Kevorkov, A. Uihlein, and M. Medraj, “Water droplet erosion of stainless steel steam turbine blades,” *Mater. Res. Express*, vol. 4, no. 8, 2017, doi: 10.1088/2053-1591/aa7c70.

[76] L. K. Bhagi, P. Gupta, and V. Rastogi, “Fractographic investigations of the failure of L-1 low pressure steam turbine blade,” *Case Stud. Eng. Fail. Anal.*, vol. 1, no. 2, pp. 72–78, 2013, doi: 10.1016/j.csefa.2013.04.007.

[77] Rivaz, S. H. Mousavi Anijdan, M. Moazami-Goudarzi, A. N. Ghohroudi, and H. R. Jafarian, “Damage causes and failure analysis of a steam turbine blade made of martensitic stainless steel after 72,000 h of working,” *Eng. Fail. Anal.*, vol. 131, no. October 2021, p. 105801, 2022, doi: 10.1016/j.engfailanal.2021.105801.

[78] A. Rivaz, S. H. Mousavi Anijdan, and M. Moazami-Goudarzi, “Failure analysis and damage causes of a steam turbine blade of 410 martensitic stainless steel after 165,000 h of working,” *Eng. Fail. Anal.*, vol. 113, no. April, p. 104557, 2020, doi: 10.1016/j.engfailanal.2020.104557.

[79] J. Latcovich, T. Astrom, P. Frankhuizen, S. Fukushima, H. HAmberg, and S. Keller, “Maintenance and Overhaul of Steam Turbines HMN,” *Int. Assoc. Eng. Insur. 38th Annu. Conf.*, vol. 42, no. 05, p. 46, 2005, [Online]. Available: http://www.steamforum.com/pictures/wgp4205 Turbine.pdf.

[80] N. Connor, “What is LP Turbine - Low-pressure Steam Turbine - Definition,” 2019, [Online]. Available: https://www.thermal-engineering.org/what-is-lp-turbine-low-pressure-steam-turbine-definition/.

[81] M. Ahmad, M. Casey, and N. Sürken, “Experimental assessment of droplet impact erosion resistance of steam turbine blade materials,” *Wear*, vol. 267, no. 9–10, pp. 1605–1618, 2009, doi: 10.1016/j.wear.2009.06.012.

[82] A. Specification, “Standard Test Method For Liquid Penetrant Examination,” *Se-165*, vol. 165, 2001.

[83] A. A.-751 ASTM A-751 E-23, “ASTM A-751. Standard Test Methods, Practices, and Terminology for Chemical Analysis of Steel Products.,” *Astm E-23*, vol. ASTM A-751, pp. 1–6, 2011.

[84] G. F. Vander Voort, G. M. Lucas, and E. P. Manilova, “Metallography and Microstructures of Stainless Steels and Maraging Steels,” *Metallogr. Microstruct.*, vol. 9, no. c, pp. 670–700, 2018, doi: 10.31399/asm.hb.v09.a0003767.

[85] ASTM A370, “Standard Test Methods and Definitions for Mechanical Testing of Steel

Products," *ASTM Int.*, vol. 01.03, no. Rapproved, pp. 1–48, 2004, doi: 10.1520/A0370-16.2.

[86] H. Law and V. Koutsos, "Leading edge erosion of wind turbines: Effect of solid airborne particles and rain on operational wind farms," *Wind Energy*, vol. 23, no. 10, pp. 1955–1965, 2020, doi: 10.1002/we.2540.

[87] G. F. Vander Voort and G. M. Lucas, "Metallography and Microstructures of Stainless Steels and Maraging Steels," vol. 9, no. c, 2004, doi: 10.1361/asmhba0003767.

[88] J. A. Pineault, M. Belassel, and M. E. Brauss, "X-Ray Diffraction Residual Stress Measurement in Failure Analysis," *Failure Analysis and Prevention*, vol. 11. ASM International, p. 0, Jan. 01, 2002, doi: 10.31399/asm.hb.v11.a0003528.

[89] W. A. Theiner, "Micromagnetic techniques," *Struct. Residual Stress Anal. by Nondestruct. Methods*, pp. 564–589, 1997, doi: 10.1016/b978-044482476-9/50019-0.

[90] Noyan, I. C., and J. B. Cohen., "Residual stress: measurement by diffraction and interpretation.," *Springer*, p. 2013, 2013.

[91] B. D. Cullity, "Elements of X-ray Diffraction." Addison-Wesley Publishing.

[92] P. M. L. J.A Pineault, M. Belassel, and M.E. Brauss, "X-Ray Diffraction Residual-Stress.pdf." ASM Handbook, Volume 11, 2021, doi: 10.31399/asm.hb.v11.a0006768.

[93] Y. Kawamura, T., Baba, M., Ozawa, N., & Sugiyama, "A Residual Stress Measurement Technique for Turbine Blade Dovetails," in *Proceedings of ASME Turbo Expo 2011 GT2011 June 6-10, 2011, Vancouver, British Columbia, Canada*, 2017, vol. 54662, pp. 69–76.

[94] "Barkhausen Noise Analysis," *Cond-M*. Hill Engineering, 2004, [Online]. Available: https://hill-engineering.com/barkhausen-noise analysis/.

[95] M. O. Speidel and A. Atrens, "Corrosion in power generating equipment," 1984, doi: Corpus ID: 109096209.

[96] M. S. Khan and C. Sasikumar, "A water droplet erosion-induced fatigue crack propagation and failure in X20Cr13 martensitic stainless-steel turbines working at low pressure," *Eng. Fail. Anal.*, vol. 139, no. June, p. 106491, 2022, doi: 10.1016/j.engfailanal.2022.106491.

[97] X. Guo *et al.*, "Evaluation of microstructural degradation in a failed gas turbine blade due to overheating," *Eng. Fail. Anal.*, vol. 103, no. December 2018, pp. 308–318, 2019, doi: 10.1016/j.engfailanal.2019.04.021.

[98] H. Kim, "Crack evaluation of the fourth stage blade in a low-pressure steam turbine," *Eng. Fail. Anal.*, vol. 18, no. 3, pp. 907–913, 2011, doi: 10.1016/j.engfailanal.2010.11.004.

[99] G. Das, S. Ghosh Chowdhury, A. Kumar Ray, S. Kumar Das, and D. Kumar Bhattacharya, "Turbine blade failure in a thermal power plant," *Eng. Fail. Anal.*, vol. 10, no. 1, pp. 85–91, 2003, doi: 10.1016/S1350-6307(02)00022-5.

[100] M. Ananda Rao, M. V. Pavan Kumar, T. S. N. Sankara Narayanan, S. Subba Rao, and N. Narasaiah, "Failure Analysis of a Low-Pressure Turbine Blade in a Coal-Based Thermal Power Plant," *J. Fail. Anal. Prev.*, vol. 15, no. 5, pp. 750–757, 2015, doi:

10.1007/s11668-015-0013-x.

[101] S. Prifiharni, H. Perdana, T. B. Romijarso, B. Adjiantoro, A. Juniarsih, and E. Mabruri, "The Hardness and Microstructure of The Modified 13Cr Steam Turbine Blade Steel in Tempered Conditions," *Int. J. Eng. Technol.*, vol. 8, no. 6, pp. 2672–2675, 2016, doi: 10.21817/ijet/2016/v8i6/160806224.

[102] I. A. Channa, A. A. Shah, S. H. Abro, and M. Ali, "Vol 2 No 1," *Sukkur IBA J. Emerg. Technol.*, vol. 2, no. 1, 2019, doi: 10.30537/sjet.v2i1.

[103] P. Novak, R. Yuan, B. P. Somerday, P. Sofronis, and R. O. Ritchie, "A statistical, physical-based, micro-mechanical model of hydrogen-induced intergranular fracture in steel," *J. Mech. Phys. Solids*, vol. 58, no. 2, pp. 206–226, 2010, doi: 10.1016/j.jmps.2009.10.005.

[104] W. Maktouf and K. Saï, "An investigation of premature fatigue failures of gas turbine blade," *Eng. Fail. Anal.*, vol. 47, no. PA, pp. 89–101, 2015, doi: 10.1016/j.engfailanal.2014.09.015.

[105] M. R. Khajavi and M. H. Shariat, "Failure of first stage gas turbine blades," *Eng. Fail. Anal.*, vol. 11, no. 4, pp. 589–597, 2004, doi: 10.1016/j.engfailanal.2003.08.010.

[106] S. Wang, A. Ditta, Y. Xu, and Z. Zhang, "Effect of microstructures restoration on high temperature fatigue behavior of DZ125 superalloy," *Prog. Nat. Sci. Mater. Int.*, vol. 31, no. 4, pp. 633–640, 2021, doi: 10.1016/j.pnsc.2021.07.005.

[107] S. Qu, C. M. Fu, C. Dong, J. F. Tian, and Z. F. Zhang, "Failure analysis of the 1st stage blades in gas turbine engine," *Eng. Fail. Anal.*, vol. 32, pp. 292–303, 2013, doi: 10.1016/j.engfailanal.2013.03.017.

[108] S. Kumari, D. V. V. Satyanarayana, and M. Srinivas, "Failure analysis of gas turbine rotor blades," *Eng. Fail. Anal.*, vol. 45, pp. 234–244, 2014, doi: 10.1016/j.engfailanal.2014.06.003.

[109] J. Kanesund, H. Brodin, and S. Johansson, "Hot corrosion influence on deformation and damage mechanisms in turbine blades made of IN-792 during service," *Eng. Fail. Anal.*, vol. 96, no. November 2016, pp. 118–129, 2019, doi: 10.1016/j.engfailanal.2018.10.004.

[110] L. K. Bhagi, V. Rastogi, P. Gupta, and S. Pradhan, "Dynamic Stress Analysis of L-1 Low Pressure Steam Turbine Blade: Mathematical Modelling and Finite Element Method," *Mater. Today Proc.*, vol. 5, no. 14, pp. 28117–28126, 2018, doi: 10.1016/j.matpr.2018.10.053.

[111] P. Rani and A. K. Agrawal, "Natural Frequency Evaluation of Low-Pressure Stage Blade of a 210 MW Steam Turbine," *IOP Conf. Ser. Mater. Sci. Eng.*, vol. 1248, no. 1, p. 012032, 2022, doi: 10.1088/1757-899x/1248/1/012032.

[112] Z. Mazur, R. García-Illescas, and J. Porcayo-Calderón, "Last stage blades failure analysis of a 28 MW geothermal turbine," *Eng. Fail. Anal.*, vol. 16, no. 4, pp. 1020–1032, 2009, doi: 10.1016/j.engfailanal.2008.05.012.

[113] L. K. Bhagi, R. Vikas, and P. Gupta, "Residual Stress Influences on L-1 Low Pressure Steam Turbine Blade," no. January, 2018.

[114] A. T. Patel, "Steam Turbine Blade," no. 19. 1994.

[115] K. Chandler, A. White, and J. Young, “Non-equilibrium wet-steam calculations of unsteady low-pressure turbine flows,” *Proc. Inst. Mech. Eng. Part A J. Power Energy*, vol. 228, no. 2, pp. 143–152, 2014, doi: 10.1177/0957650913511802.

[116] M. Sarim Khan and C. Sasikumar, “Failure analysis of AISI 420 steel turbine blade operating at low-pressure,” *Mater. Today Proc.*, vol. 66, pp. 3804–3808, 2022, doi: 10.1016/j.matpr.2022.06.197.

[117] T. Molale, N. Ahmed, and M. Bhamjee, “Numerical Analysis of Flow Induced Vibrations of a Low-Pressure Steam Turbine Rotating Blade,” *J. Phys. Conf. Ser.*, vol. 1378, no. 3, 2019, doi: 10.1088/1742-6596/1378/3/032059.

[118] J. Kubiak Sz., G. Urquiza B., J. García C., and F. Sierra E., “Failure analysis of steam turbine last stage blade tenon and shroud,” *Eng. Fail. Anal.*, vol. 14, no. 8 SPEC. ISS., pp. 1476–1487, 2007, doi: 10.1016/j.engfailanal.2007.01.012.

[119] S. J. Kubiak, G. R. Gonzalez, D. R. Juarez, J. G. Nebradt, and F. E. Sierra, “An investigation on the failure of an L-O steam turbine blade,” *J. Fail. Anal. Prev.*, vol. 4, no. 3, pp. 47–51, 2004, doi: 10.1361/15477020419811.

[120] A. Al-Taie, “Stress Evaluation of Low Pressure Turbine Rotor Blade and Design of Reduced Stress Blade,” *Eng.Tech*, vol. 26, no. 2, 2008.

[121] C. Booysen, P. S. Heyns, M. P. Hindley, and R. Scheepers, “Fatigue life assessment of a low pressure steam turbine blade during transient resonant conditions using a probabilistic approach,” *Int. J. Fatigue*, vol. 73, pp. 17–26, 2015, doi: 10.1016/j.ijfatigue.2014.11.007.

[122] M. Zhu, “Design and analysis of steam turbine blades,” 2019, doi: 10.1088/1742-6596/1300/1/012056.

[123] R. Dewey and T. Lam, “Steam Turbine Blade Failure Root Cause Analysis Guide,” 2008.

[124] M. D. Hayes, D. B. Edwards, and A. R. Shah, “Fractography as a Failure Analysis Tool,” *Fractography Fail. Anal. Polym.*, pp. 6–22, 2015, doi: 10.1016/b978-0-323-24272-1.00002-7.

[125] P. Rani and A. K. Agrawal, “Failure Analysis of a low-pressure stage steam turbine blade,” *Nondestruct. Test. Eval. GNTE*, 2022, doi: 10.1111/jipb.13407.

[126] P. Měšt´ Anek, “Low cycle fatigue analysis of a last stage steam turbine blade,” *Appl. Comput. Mech.*, vol. 2, pp. 71–82, 2008.

[127] ANSYS FLUENT 13 User’s Guide, “Ansys Fluent Theory Guide,” *ANSYS Inc., USA*, vol. 15317, no. November, pp. 724–746, 2013.

[128] Ansys Inc., “Ansys Fluent User’s Guide 14.0,” vol. 15317, no. November, p. 2498, 2011, [Online]. Available: http://cdlab2.fluid.tuwien.ac.at/LEHRE/TURB/Fluent.Inc/v140/flu_ug.pdf.

[129] S. Cano *et al.*, “Detection of damage in steam turbine blades caused by low cycle and strain cycling fatigue,” *Eng. Fail. Anal.*, vol. 97, no. August 2018, pp. 579–588, 2019, doi: 10.1016/j.engfailanal.2019.01.015.

[130] K. S. Lee and J. H. Song, “Estimation methods for strain-life fatigue properties from

hardness," *Int. J. Fatigue*, vol. 28, no. 4, pp. 386–400, 2006, doi: 10.1016/j.ijfatigue.2005.07.037.

[131] R. K. Bhamu, A. Shukla, S. C. Sharma, and S. P. Harsha, "Low-Cycle Fatigue Life Prediction of LP Steam Turbine Blade for Various Blade–Rotor Fixity Conditions," *J. Fail. Anal. Prev.*, vol. 21, no. 6, pp. 2256–2277, 2021, doi: 10.1007/s11668-021-01282-9.

[132] E. Zhao, Q. Zhou, W. Qu, and W. Wang, "Fatigue Properties Estimation and Life Prediction for Steels under Axial, Torsional, and In-Phase Loading," *Adv. Mater. Sci. Eng.*, vol. 2020, 2020, doi: 10.1155/2020/8186159.

[133] A. Fatemi and L. Yang, "Cumulative fatigue damage and life prediction theories," *Int. J. Fatigue*, vol. 20, no. I, pp. 9–34, 1998, [Online]. Available: http://dx.doi.org/10.1016/S0142-1123(97)00081-9.

[134] N. E. Dowling, "Mean stress effects in strain-life fatigue," *Fatigue Fract. Eng. Mater. Struct.*, vol. 32, no. 12, pp. 1004–1019, 2009, doi: 10.1111/j.1460-2695.2009.01404.x.

[135] A. Ince and G. Glinka, "A modification of Morrow and Smith-Watson-Topper mean stress correction models," *Fatigue Fract. Eng. Mater. Struct.*, vol. 34, no. 11, pp. 854–867, 2011, doi: 10.1111/j.1460-2695.2011.01577.x.

[136] S. Jhons, "Ansys® (Version R2) [Software]," 2022.

[137] S. Cano *et al.*, "Detection of damage in steam turbine blades caused by low cycle and strain cycling fatigue," *Eng. Fail. Anal.*, vol. 97, no. August 2018, pp. 579–588, 2019, doi: 10.1016/j.engfailanal.2019.01.015.

[138] R. Viswanathan, "Life-assessment technology for fossil power plants," *Sadhana*, vol. 20, no. 1, pp. 301–329, 1995, doi: 10.1007/BF02747295.

[139] R. Viswanathan and R. I. Jaffee, "Metallurgical factors affecting the reliability of fossil steam turbine rotors," *J. Eng. Gas Turbines Power*, vol. 107, no. 3, pp. 642–651, 1985, doi: 10.1115/1.3239784.

[140] R. J. In Becker, W. T., In Shipley, *Failure Analysis and Prevention*. ASM International, 2002.

[141] Z. Zhang, T. Liu, D. Zhang, and Y. Xie, "Water droplet erosion life prediction method for steam turbine blade materials based on image recognition and machine learning," *J. Eng. Gas Turbines Power*, vol. 143, no. 3, pp. 1–9, 2021, doi: 10.1115/1.4049768.

[142] M. H. Sabour and R. B. Bhat, "Lifetime prediction in creep-fatigue environment," *Mater. Sci. Pol.*, vol. 26, no. 3, pp. 563–584, 2008.

[143] D. Zhang, J. Hong, Y. Ma, and L. Chen, "A probability method for prediction on High Cycle Fatigue of blades caused by aerodynamic loads," *Adv. Eng. Softw.*, vol. 42, no. 12, pp. 1059–1073, 2011, doi: 10.1016/j.advengsoft.2011.07.010.

[144] Y. Liu and S. Mahadevan, "Stochastic fatigue damage modeling under variable amplitude loading," *Int. J. Fatigue*, vol. 29, no. 6, pp. 1149–1161, 2007, doi: 10.1016/j.ijfatigue.2006.09.009.

[145] M. H. H. Shen, "Reliability assessment of high cycle fatigue design of gas turbine blades using the probabilistic Goodman diagram," *Int. J. Fatigue*, vol. 21, no. 7, pp.

699–708, 1999, doi: 10.1016/S0142-1123(99)00033-X.

[146] H. Shen, J. Lin, and E. Mu, “Probabilistic model on stochastic fatigue damage,” *Int. J. Fatigue*, vol. 22, no. 7, pp. 569–572, 2000, doi: 10.1016/S0142-1123(00)00030-X.

[147] K. Sadananda and P. Shahinian, “Elastic-Plastic Fracture Mechanics for High-Temperature Fatigue Crack Growth,” in *ASTM International.*, vol. STP700-EB, P. C. Paris, Ed. ASTM International, 1980, pp. 365–390.

[148] S. Marie and C. Delaval, “Fatigue and creep-fatigue crack growth in 316 stainless steel cracked plates at 650°C,” *Int. J. Press. Vessel. Pip.*, vol. 78, no. 11–12, pp. 847–857, 2001, doi: 10.1016/S0308-0161(01)00099-0.

[149] S. P. SADANANDA K., “Creep-Fatigue Crack Growth,” *Appl. Sci. Publ London*, pp. 109– 195, 1981.

[150] MARIUSZ BANASZKIEWICZ and RALF GERDES, “probabilistic approach to lifetime assessment of steam turbines,” *Trans. Inst. Mach. FLUID-FLOW*, vol. 113, no. No. 113, pp. 95–106, 2003.

[151] M. T. K Maile, A Klenk, J Granacher, G Schellenberg, “Creep and creep fatigue crack behavior of 1Cr-and 9Cr-steels.,” in *Key Engineering Materials*, vol. 171–174, Switzerland: Trans Tech Publications Ltd, 1999, pp. 85–98.

[152] K. Mazur-Buyko, “‘Computational methods of lifetime determination of steam turbine casings and rotors.,’” *1st Sci. Tech. Sess. “Lifetime steam turbine components methods its Predict.*, pp. 42–53, 1986.

[153] Ramaswamy Viswanathan, *Damage Mechanisms and Life Assessment of High Temperature Components*. 1989.

[154] R. Rzadkowski, R., Drewczynski, M., Rao, J. S., Ranjith, M. C., Piechowski, L., & Szczepanik, “Crack initiation and propagation of compressor blade of aircraft engine.,” *J. Vib. Eng. Technol.*, vol. 2, no. 4, pp. 371–384, 2014.

[155] M. F. Geng, “An idea for predicting crack growth time to fracture under creep-fatigue conditions,” *Mater. Sci. Eng. A*, vol. 257, no. 2, pp. 250–255, 1998, doi: 10.1016/S0921-5093(98)00849-1.

[156] X. Guan and J. He, “Life time extension of turbine rotating components under risk constraints : A state-of-the-art review and case study,” *Int. J. Fatigue*, vol. 129, no. April 2018, p. 104799, 2019, doi: 10.1016/j.ijfatigue.2018.08.003.

[157] Y. Enomoto, *Steam turbine retrofitting for the life extension of power plants*. Elsevier Ltd, 2017.

[158] R. Viswanathan and S. M. Gehl, “Life-Assessment Technology for Power-Plant Components,” no. February, 1992.

[159] R. P. Skelton and K. J. Nix, “Crack growth behaviour in austenitic and ferritic steels during thermal quenching from 550°C,” *High Temp. Technol.*, vol. 5, no. 1, pp. 3–12, 1987, doi: 10.1080/02619180.1987.11753335.

[160] T. Meshii, M. Iiosoda, and K. Watanabe, “Crack arrest depth under cyclic thermal shock for an inner-surface circumferential crack in a cylinder,” *Nihon Kikai Gakkai Ronbunshu, A Hen/Transactions Japan Soc. Mech. Eng. Part A*, vol. 67, no. 661, pp.

1535–1541, 2001, doi: 10.1299/kikaia.67.1535.

[161] T. Meshii and K. Watanabe, “Analytical approach to crack arrest tendency under cyclic thermal stress for an inner-surface circumferential crack in a finite-length cylinder,” *J. Press. Vessel Technol. Trans. ASME*, vol. 123, no. 2, pp. 220–225, 2001, doi: 10.1115/1.1358840.

[162] R. J. In Becker, W. T., In Shipley, “Failure Analysis and Prevention,” *Fail. Anal. Prev.*, p. 2002, 2002, doi: 10.31399/asm.hb.v11.9781627081801.

[163] Webster, G. A., and R. A. Ainsworth, “High temperature component life assessment,” *Springer Science & Business Media*, 2013.

[164] Ramu naik maloth, “Advanced lifetime assessment of steam turbines,” *ALSTOM design instruction*, 2007. .

[165] F. Colombo, “Service-like thermo-mechanical fatigue characteristics of 1CrMoV rotor steel,” Swiss Federal Institute of Technology, 2007.

[166] B. E. Gooley, T. A., Leisenring, W., Crowley, J., & Storer, “Estimation of failure probabilities in the presence of competing risks: new representations of old estimators,” *Stat. Med.*, vol. 18, no. 6, pp. 695–706, 1999, doi: https://doi.org/10.1002/(SICI)1097-0258(19990330)18:6<695::AID-SIM60>3.0.CO;2-O.

[167] G. B. and R. GERDES, “probabilistic approach to lifetime assessment of steam turbines,” *Trans. Inst. Mach. FLUID-FLOW*, vol. 113, no. No. 113, pp. 95–106, 2003.

[168] A. F. Liu, *Structural life assessment methods*. ASM international, 1998.

[169] P. C. Paris, M. P. Gomez, and W. E. Anderson., “A rational analytic theory of fatigue.,” *Trend Eng.*, vol. 13, no. 9, pp. 9–14, 1960.

[170] Ramu naik maloth, “Advanced lifetime assessment of steam turbines,” *ALSTOM design instruction*, 2007. .

[171] M. Ruzicka, M. Hanke, and M. Rost., “"Dynamická pevnost a zivotnost,” *Czech Tech. Univ. Prag, Prag*, 1989.

[172] J. Bolton, “A ‘characteristic-strain’ model for creep,” *Mater. High Temp.*, vol. 25, no. 3, pp. 197–204, 2008, doi: 10.3184/096034008X357573.

[173] M. Banaszkiewicz, “Analysis of Rotating Components Based on a Characteristic Strain Model of Creep,” *J. Eng. Mater. Technol.*, vol. 138, no. 3, Mar. 2016, doi: 10.1115/1.4032661.

[174] J. T. Boyle, “The behavior of structures based on the characteristic strain model of creep,” *Int. J. Press. Vessel. Pip.*, vol. 88, no. 11–12, pp. 473–481, 2011, doi: 10.1016/j.ijpvp.2011.08.002.

[175] J. Bolton, “Analysis of structures based on a characteristic-strain model of creep,” *Int. J. Press. Vessel. Pip.*, vol. 85, no. 1–2, pp. 108–116, 2008, doi: 10.1016/j.ijpvp.2007.06.013.

[176] J. A. Rodríguez, Y. El Hamzaoui, J. A. Hernández, J. C. García, J. E. Flores, and A. L. Tejeda, “The use of artificial neural network (ANN) for modeling the useful life of the failure assessment in blades of steam turbines,” *Eng. Fail. Anal.*, vol. 35, pp. 562–575,

2013, doi: 10.1016/j.engfailanal.2013.05.002.

[177] J. A. Rodríguez, J. C. Garcia, E. Alonso, Y. El Hamzaoui, J. M. Rodríguez, and G. Urquiza, “Failure probability estimation of steam turbine blades by enhanced Monte Carlo Method,” *Eng. Fail. Anal.*, vol. 56, pp. 80–88, 2015, doi: 10.1016/j.engfailanal.2015.04.009.

[178] Y. El Hamzaoui, J. A. Rodríguez, J. A. Hernández, and V. Salazar, “Optimization of operating conditions for steam turbine using an artificial neural network inverse,” *Appl. Therm. Eng.*, vol. 75, pp. 648–657, 2015, doi: 10.1016/j.applthermaleng.2014.09.065.